Chapter 2
The Charge Conduction Process at Poly(o-aminophenol) Film Electrodes

2.1 Introduction

Electroactive polymers contain electron donor and acceptor sites that usually consist of up to hundreds of molecular layers. Oxidation and reduction of fixed sites introduce charged sites into the polymer, which, to achieve charge neutrality, require the ingress of counter-ions from the contacting electrolyte solution and, according to the Donnan relation, the egress of co-ions. Electron hopping is believed to be the mechanism for electron transport, but it is also possible that ion motions may partially or totally control the rate of charge transport. Thus, the charge-transport rate in electroactive polymer films is quantitatively characterised by a heterogeneous constant of charge transfer and an effective (or apparent) diffusion coefficient for charge transport across the film. The factors governing the magnitude of these parameters are not well understood. Furthermore, in general, these transport parameters depend on different variables such as degree of oxidation of the polymer, polymer film thickness, type of electrolyte, ionic strength and *pH* of the solution in contact with the polymer film. A combination of different techniques was employed to determine the rates of the charge-transfer and charge-transport processes in electroactive polymers, such as Cyclic Voltammetry (CV), Rotating Disc Electrode Voltammetry (RDEV), Normal Pulse Voltammetry (NPV), Potential Step Chronoamperometry (PSCA), Potential Step Chronocoulometry (PSCC), EQCM measurements, Electron Spin Resonance (ESR), Probe Bean Deflection (PBD), Surface Resistance (SR) and Electrochemical Impedance Spectroscopy (EIS).

The electropolymerization of *o*-AP in acid medium yields a conducting polymer. The electroactivity of POAP was explained by a redox mechanism that involves an addition/elimination of protons coupled with a reversible electron transfer. However, POAP shows a relatively low conductivity as compared with other conjugated polymers. The charge-transport process at poly(o-aminophenol) (POAP) films was found to depend not only on the medium used for the electrosynthesis, but also on the polymer oxidation state, the polymer film thickness and *pH* and type of ions of the external solution in contact with the polymer.

R. Tucceri, *Poly(o-aminophenol) Film Electrodes*, Engineering Materials,
DOI: 10.1007/978-3-319-02114-0_2, © Springer International Publishing Switzerland 2013

Particularly, the electro-oxidation of *o*-AP in neutral buffer solutions leads to the formation of a non-conducting and permselective thin film of POAP. The permselectivity of a non-conducting POAP film synthesized at *pH* values over 3 was found to be suitable to reduce the effect of interferents in amperometric determinations of different biologically important substances. In this chapter of this book concerns charge-transfer and charge-transport processes occurring in the curse of redox reactions of POAP film electrodes. This chapter first deals with the case where the solutions contacting POAP films only contain ions that do not possess a redox activity ("background electrolyte"). Thus, the counter-ion is able to cross the film|solution interface to retain the bulk film electroneutrality. Then, the transport properties of POAP films contacting redox active solutions are treated. In this last case, redox species inside the electrolyte solution participate in an interfacial electron exchange with the polymer at the polymer|solution boundary. In practical applications of POAP is necessary to maintain the conducting properties of the polymer unaltered. However, in some of them the polymer is subjected to extreme conditions that can cause its partial deactivation. In this regard, it seems to be important to know the fundamental nature of the charge propagation in poly(o-aminophenol) film electrodes.

2.2 The Charge Conduction Process at Poly(o-aminophenol) (POAP) Film Electrodes in Contact with Inactive Electrolytes

A study about the electrochemical properties of POAP, determining its thermodynamical properties and some of the kinetic and charge transport parameters, is reported in Ref. [1]. A mechanism of charge transport for the charging and discharging process of POAP is also proposed [1]. POAP was obtained [1] by electrooxidation of the monomer on platinum and glassy carbon (GC) electrodes in aqueous solution. The electrochemical behavior of POAP films was studied by cyclic voltammetry (CV) under different experimental conditions. On both, platinum and GC, the POAP response is highly asymmetric (see Fig. 1.2 of Chap. 1). It presents anodic and cathodic peak potential separations ($E_{pa} - E_{pc}$) independent of the sweep rate (v) for values of v between 1 and 100 mV s^{-1}(0.1 M $HClO_4$ + 0.4 M $NaClO_4$ solution). However, at $v > 100$ mV s^{-1} E_{pc} shifts to more negative values, indicating a non-ideal behavior. Since the presence of the film does not inhibit the proton reduction, the negative potential limit for the film depends on the base electrode, being about −0.5 V (SCE) over Pt and Au and −1.0 V (SCE) over GC. On the other hand, the positive potential limit is about 1.0 V and independent of the bare electrode. Beyond these limits irreversible modifications with formation of electroinactive films are produced. The anodic peak, as well its E_{pa}, does not vary with v or with *pH* in the range 1–3. On the other hand, the cathodic peak shape and E_{pc} show variations with these variables, which indicate additional

kinetic effects in the reduction cycle. The effect of the scan rate on the maximum current of the anodic voltammetric peak current (i_{pa}) was also studied [1]. A plot of ln i_{pa} versus ln v (where i_{pa} is the anodic peak current and v is the potential scan rate) showed, for values of v less than 0.5 V s^{-1}, a slope that approaches unity as predicted theoretically for an adsorbed species of film-modified electrodes with thin-layer behaviour. For v values greater than 2.5 V s^{-1}, the slope was 0.5, which indicates semi-infinite diffusion behaviour. The intermediate zone, between 0.5 and 2.5 V s^{-1}, was shown to correspond to finite diffusion behaviour. Similar results were obtained for the cathodic peak but with the difference that the thin-layer behaviour was restricted to values of v lower than 0.3 V s^{-1}, revealing that the cathodic process is slower than the anodic one. Plots of i_{pa} versus $v^{1/2}$ were linear for values of v as high as 10 V s^{-1}. By assuming that these plots follow the Randles–Sevcik or the equivalent Nicholson and Shain equation [2], the slope was proportional to $cD^{1/2}$. The concentration of active sites, c, was calculated for a homogeneous film considering the film thickness known from ellipsometric data [3] and employing Eq. (2.1):

$$Q_T = nFAc\,d \tag{2.1}$$

where $n = 1$ is the number of exchanged electrons during the redox reaction of the polymer and d is the film thickness. Q_T is either the anodic or the cathodic charge corresponding to voltammograms obtained at $v < 0.10$ V s^{-1} in order to ensure the completion of the redox process in the film. Besides, F is the Faraday constant and A the electrode area in Eq. (2.1). A value of $c = 4.7$ M was obtained in [1]. Then, an apparent diffusion coefficient for the anodic process D was calculated from the $cD^{1/2}$ slope. A D value of 4.0×10^{-11} $cm^2 s^{-1}$ was obtained in [1]. The close fit to the i_{pa} versus $v^{1/2}$ plot with the Randles–Sevcik equation suggested that the anodic charge transport within the film might be by electron hopping with the necessarily charge-compensating counter-ion motion [4]. Since the reduction peak was affected by kinetic effects, this invalidates the previous calculation on the basis of CV in the reduction process. A value of the conductivity of POAP by using the formalism of Nicholson [5] was also calculated in Ref. [1]. The obtained value, with the assumption of fast charge transfer at the electrode/film and film|solution interfaces, was 1.34×10^{-4} S cm^{-1}. However, as the proton diffusion at POAP-coated electrodes depends on the base electrode, then, it was considered to be possible that both D and the film conductivity are affected by proton transport. As the proton diffusion process seems to occur, allowing them to reach the metal electrode surface, this fact was explained [1] considering that protons reach the electrode surface by permeation through pores in the film. However, these pores should be very small since other cations do not diffuse [1]. Another reasonable explanation given in Ref. [1] was to consider a fast assisted Grotthus-like diffusion of protons through the polymer matrix.

As the POAP film behaves as a thin-layer cell in equilibrium, at sweep rates lower than 0.10 V s^{-1} [1], then its electrochemical behavior should obey to the

Nernst's law [2]. For an n-electron redox reaction involving reversible charge transfer, Nernst's equation for the POAP cathodic process was written in Ref. [1] as:

$$a_O/a_R = \gamma_O c_O/\gamma_R c_R = \exp\left[nF\left(E - E^0\right)/RT\right] \tag{2.2}$$

where a_i and γ_j are the activity and activity coefficient of the species, respectively, and E^0 is the standard potential of the redox reaction. To a first approximation the activity coefficients were considered independent of the concentration and equal to unity [1]. With this assumption [1], the relationship between i_p and v was written as:

$$i_{pa} = i_{pc} = nFQv/4RT \tag{2.3}$$

where Q (= $nFcAd$) is obtained by integration of the voltammetric peak, A is the film area and $c = c_O + c_R$ (where c_O and c_R are the concentration of oxidized and reduced redox sites, respectively). As can be seen from Fig. 2.1, the values of i_{pa} and i_{pc}, although linear with v, the slopes are not equal to values predicted by Eq. (2.3). This fact confirms a non-ideal behavior of POAP suggested in [1], which is actually expected considering the rather high concentration of active sites on the film ($c = 4.7$ M). The deviation from the ideal behavior was explained [1] considering that the redox process produces notable physical and probably structural changes in the polymer matrix. To account for the non-ideal behavior of POAP, interaction between active sites in the film was assumed in Ref. [1]. Thus, to evaluate such interaction quantitatively, the activity coefficients were defined, following the Frumkin's isotherm, as:

$$\gamma_O = \exp\left[-(r_{OO}c_O + r_{OR}c_R)\right] \tag{2.4}$$

$$\gamma_R = \exp\left[-(r_{RR}c_R + r_{RO}c_O)\right] \tag{2.5}$$

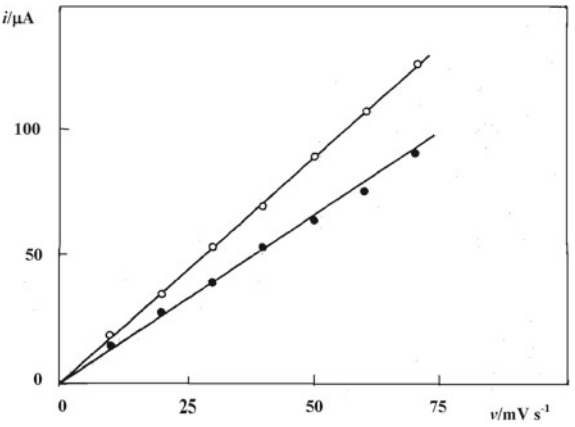

Fig. 2.1 Plots of i_p versus v for a POAP-modified electrode on Pt. $A = 0.159$ cm^2. (•) anodic; (o) cathodic. Film thickness, $d = 38$ nm [1]

where r_{ij} and r_{ji} are the interaction parameters, which describe the mutual interaction between sites *i* and *i* and *i* and j, respectively. The corresponding expression for non-ideal behavior deduced for the i_p–v relationship was expressed as Ref. [1]:

$$i_p = nFQv/(4 - 2cr)RT \tag{2.6}$$

where $r = (r_O + r_R)$, $r_O = (r_{OO} + r_{RO})$ and $r_R = (r_{RR} + r_{OR})$ assuming that $r_{RO} = r_{OR}$.

From data of the type shown in Fig. 2.1 and using Eq. (2.6), the parameters cr_a and cr_c, for the anodic and cathodic response, respectively, were calculated for various films in [1]. Different values of the interaction coefficients, r_a and r_c were obtained in Ref. [1]. Both are negative, thus involving a repulsive energy of interaction. However, while for the cathodic process a value of r_c around $-0.13\ M^{-1}$ was obtained, for the anodic process r_a resulted about $-0.5\ M^{-1}$. Other measurements, peak width, charge needed to oxidize or reduce the film at a given potential, directly related to the interaction parameters were also performed in Ref. [1], and the corresponding interaction parameters were calculated. Then, it was concluded in Ref. [1] that POAP films exhibit a Nernstian behavior with interaction between the active redox sites.

Temperature and *pH* effects on the POAP charge conduction process were also analyzed in Ref. [1]. With regard to temperature effects, it was observed that in the tin-layer domain, both i_{pa} and i_{pc} increase with increasing the temperature. Considering the ideal behavior (Eq. (2.3)) an opposite effect should be expected. Thus, the observed POAP response with temperature was attributed to the effects of temperature on the interaction parameters. To quantify these effects a current function was calculated for each temperature. It was found that interaction parameters become more negative (more repulsive) when the temperature decreases. Concerning *pH* effects, the POAP response is highly dependent on the *pH*, being optimal at *pH* 3. At $pH > 7$ no response was observed. The *pH* effect was considered as an indication that protons and electrons take part in the electrode reaction of POAP. The redox response of thin POAP films ($d < 30$ nm) at different *pH* in $HClO_4$ solutions of variable concentration and 0.4 M $NaClO_4$ was studied in Ref. [1]. All measurements were performed at $v < 0.1\ V\ s^{-1}$ to ensure thin-layer behavior. As the *pH* is increased the voltammetric peaks maintain the shape, but the peak current decreases, particularly the cathodic peak. At *pH* close to 5, the cathodic response disappears completely, while this occurs for the anodic peak at *pH* 7. Although a response of POAP is not observed at $pH > 7$, the film is not destroyed and recovers its original response when *pH* is restored to 1. The behavior of E_{pa} and E_{pc} at low *pH* values is shown in Fig. 2.2. As can be observed, E_{pa} does not vary with *pH* until a value of 2.3 is reached. However, E_{pc} varies significantly in the same *pH* range and the plot of gives straight lines with different slopes. This complicated behavior was not explained in Ref. [1]. An attempt to quantify the observed *pH* effects was made in [1]. In this respect, the change of the formal potential ($E^{0\prime}$) with the *pH*, was measured. On the assumption that the redox process of POAP can be represented by reaction (2.7) [1]:

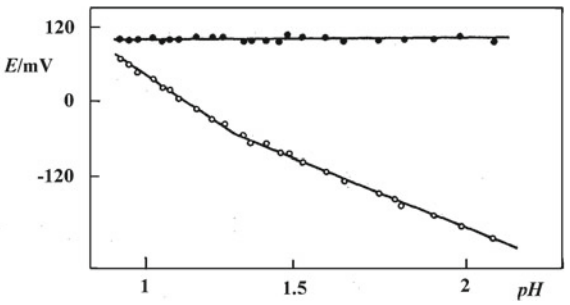

Fig. 2.2 Plot of E_p versus *pH* of a POAP-modified electrode on GC. $A = 0.071$ cm^2. (•) anodic; (o) cathodic. $v = 100$ mV/s [1]

$$R_pH_x \Leftrightarrow O_p + xH^+ + ne \tag{2.7}$$

The relation between $E^{0\prime}$ and *pH* was written as:

$$E^{0\prime} = E^0 + 2.303\,(RT/nF)\,\log\left\{\left[\,O_p\right]/\left[\,R_pH_x\right]\right\} - 2.303\,(RT\,x/nF)pH \tag{2.8}$$

As the concept of $E^{0\prime}$ is not easily applicable in the case of POAP, an operational formal potential ($E^{\#\prime}$) was adopted in [1], defined and measured as the equilibrium potential of a film-modified electrode when half of the charge required for total film conversion, has been passed. Using this assumption, the dependence of $E^{\#\prime}$ on the *pH* was measured in the range 1–6. At *pH* between 1 and 2.3, no variation of $E^{\#\prime}$ was observed. At $pH > 2.3$ the film showed a variation of $E^{\#\prime}$ with *pH* with a slope around 50 mV/decade. The latter is close to the theoretical slope for a reaction in which protons and electrons take part in the electrode reaction in the film in a 1:1 ratio ($n = x$ in Eq. (2.8)). The breakpoint (*pH* 2.3) was considered to correspond to the apparent pK_a of the film (Fig. 2.2).

Kinetic effects on the reduction process of POAP were also studied in Ref. [1]. Kinetic effects are shown in Fig. 2.3, where it is observed that while E_{pa} is independent of v, E_{pc} depends on v.

This behaviour was explained by assuming a chemical reaction coupled with the charge transfer. The theoretical model available for EC processes in surface

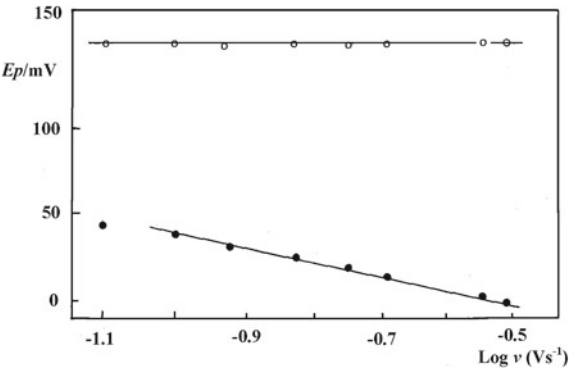

Fig. 2.3 Plot of the peak potential versus log$v$ for a POAP-modified electrode on GC. $A = 0.071$ cm^2. (•) cathodic peak; (O) anodic peak [1]

reactions proposed by Laviron [6] was employed in Ref. [1] to explain the linear relation of E_{pc} with log v observed in Fig. 2.3. This model leads to the peak potential versus potential scan rate dependence represented by Eq. (2.9) [6]:

$$E_p = E^{0\prime} + 2.303\,(RT/nF)\,\log\,(RT\,k/nFv) \tag{2.9}$$

where k is the pseudo-first-order rate constant for the coupled chemical reaction. However, the experimental slope obtained in [1] is higher than that predicted by Eq. (2.9). This discrepancy was attributed to repulsive interactions, which affect the reduction wave. The coupled chemical reaction with the charge transfer process was considered to be the protonation of the oxidized film [1]. The protonation reaction of POAP was considered as the rate-controlling step due to the constrains of H^+ diffusion through the film matrix. Some experiments were also performed in Ref. [1] varying the ClO_4^- concentration between 0.1 and 1.7 M. While the anodic peak was not affected, the cathodic peak showed a positive variation. Also, it was observed that i_{pc} increases when the concentration of proton is increased. It is indicated that the high concentration of perchlorate produces the same effect as a high proton concentration, making POAP more easily reducible. However, no noticeable changes were observed for other species, such as SO_4^{2-}, PO_4^{3-} and Cl^- or cations such as Li^+, K^+ and Cs^+.

A redox mechanism of POAP films was proposed in Ref. [1] (Fig. 2.4). In this mechanism the redox reaction of POAP involves a process of addition/elimination of protons coupled with a reversible electron transfer. As there is no influence of the nature of cation in the electrolyte solution, it was concluded that the proto-electronic oxidation reaction (I ↔ II ↔ III) is fast and reversible. On the other hand, the kinetic and strong *pH* effects observed in the reduction process seem to indicate that the protonation and corresponding counter-ion motion (III ↔ IV) could be rate-determining. As it is observed in Ref. [1], these processes are favoured by high proton and/or counter-ion concentrations. Also, the protonation reaction is considered to require a demanding polymeric matrix reorganization in the reduction process.

A comparative study of the conduction properties of polyaminoarene films was performed in Ref. [4]. The charge transport in the case of POAP is diffusion-limited and a linear dependence of peak current on the square root of the sweep rate $\left(i_p - v^{1/2}\right)$ was observed. The dependence was explained on the basis of Eq. (2.10):

$$i_p = 2.69\,10^5 n^{3/2} A D_{ef}^{1/2} v^{1/2} c \tag{2.10}$$

with c given by Eq. (2.11):

$$c = Q/nFAd \tag{2.11}$$

where n is the number of electrons participating in the redox process, A the area of the film in cm^2, c is the concentration of active centers in the film (mol cm^{-3}), Q the total charge calculated by the integration of the anodic or cathodic cyclic

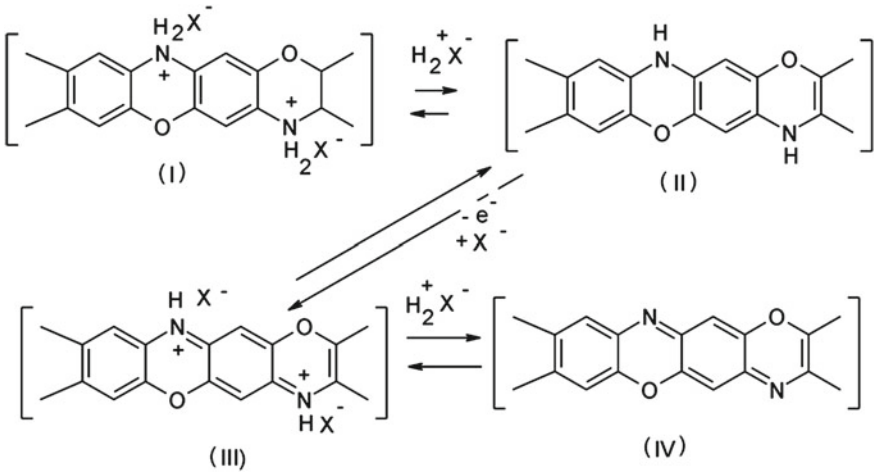

Fig. 2.4 Redox mechanism of POAP [1]

voltammetric currents at slow sweep rate, d is the film thickness and F is the Faraday's constant. From this feature the authors of Ref. [7] calculated an effective diffusion coefficient, D_{ef}, using a model of semi-infinite diffusion developed in Ref. [8]. The calculated D_{ef} values for polyaminophenol films in acid electrolytes are listed in Table 2.1. These parameters of charge transport correlate with the absolute mobility of anions [9]. For the rigid ladder polymer structure of POAP the values of D_{ef} are 2–3 orders of magnitude lower as compared with PANI, indicating a low rate of charge transport in POAP films. The strong difference between diffusion coefficient values of polyaminophenols and PANI films was attributed to the different molecular structure and segment mobility of polymer chains. The presence of electron-donor substituents in the benzene rings was considered to cause some loss of conductivity and electron-transport rate [10].

The effect of the electrolyte composition on the conduction properties of POAP film electrodes was studied by CV in [11]. Measurements were performed in $LiClO_4$ and $HClO_4$ solutions at different pH values and constant ionic strength (1 M). It was assumed that CV curves for POAP films result from two different processes. The former corresponds to a background film conduction, similar to that observed for the unmodified base electrode, while the latter is determined only by redox activity of the film. In order to separate the contributions of such processes from the total CV trace, subtraction of a base current $I_f(E)$, from the total one $I(E)$, was performed in Ref. [11]. Anodic and cathodic peak currents ($I^{(p)}$), as computed by the background subtraction, were found not to be proportional to $v^{1/2}$. Also, the slope of ln $I^{(p)}$ versus ln v was 0.9. This result was attributed to the fact that injection of one or two types of charge carriers into the film is the limiting step of the total charge-transfer process under the conditions of the CV measurements.

Table 2.1 Absolute mobilities of anions (u_c) and effective diffusion coefficients (D_{ef}) of polyaminoarene films in acid solutions [7]

Polyaminoarene film, area and thickness	Electrolyte	u_c, $m^2/V\ s$	$D_{ef}\ 10^{10}$, $cm^2\ s^{-1}$
Poly-*o*-aminophenol	CH_3COOH (1 M)	3.7	0.08 ± 0.02
A = 3.4 cm^2, d = 0.25 μm	HCl (1 M)	6.8	0.15 ± 0.02
	H_2SO_4 (0.5 M)	7.1	0.23 ± 0.04
Poly-*m*-aminophenol	HCl (1 M)	6.8	1.17 ± 0.07
A = 4.0 cm^2, d = 0.28 μm	H_2SO_4 (0.5 M)	7.1	1.56 ± 0.07
	CH_3COOH (1 M)	3.7	40.2 ± 0.5
Polyaniline	$HClO_4$ (1 M)	6.7	73.7 ± 0.5
A = 4.0 cm^2, d = 0.28 μm	H_2SO_4 (0.5 M)	7.1	90.2 ± 0.5

D_{ef} values extracted from the method reported in Ref. [8]. A and d represent the electrode area and film thickness, respectively

Kinetic and charge transport parameters for POAP (the standard rate constant, k^0, the transfer coefficient, α, and the apparent diffusion coefficient, D_{app}) were obtained in [12] by employing different electrochemical techniques, such as CV, PSCA (potential-step chronoamperometry), PSCC (potential-step chronocoulometry) and NPV (normal pulse voltammetry). Anodic and cathodic peak currents of the voltammetric response were found to scale linearly with the square root of the potential scan rate within the range 5–200 mV s^{-1}. Thus, both anodic and cathodic charge-transport processes within POAP films were considered to be diffusion-controlled [12]. Potential Step Chronoamperometric and Chronocoulometric responses for the oxidation and reduction of POAP films were employed in Ref. [12] to obtain Cottrell plots ($i - t^{-0.5}$ (Eq. (2.12)) and $Q - t^{0.5}$ (Eq. (2.13)). These plots were found to be linear for POAP, indicating that, in agreement with CV results, the charge-transport processes within POAP films follow Fickian diffusion laws [2].

$$i = nFA\, D_{app}^{Ox} C\pi^{-0.5} \cdot t^{-0.5} \tag{2.12}$$

$$Q = Q_{dl} + (2nFA\, D_{app}^{Ox} C\pi^{-0.5} t^{-0.5}) \tag{2.13}$$

Equations (2.12) and (2.13) are expressed for the oxidation process. D_{app}^{ox} is the apparent diffusion coefficient for the oxidation process, n is the number of electrons involved in the heterogeneous electron transfer reaction, F is the Faraday constant and A is the electrode area. C is the volume concentration of the redox sites and Q_{dl} represents the charge corresponding to the double layer. The slopes of the linear chronoamperometric and chronocoulometric Cottrell plots give the D_{app} values for the diffusion-like charge transport process within POAP films. The D_{app} values obtained in [12] are summarized in Table 2.2. With regard to NPV, normal pulse voltammograms for the oxidation and reduction of a POAP film were recorded at various sampling times. Plots of the cathodic and anodic limiting currents (i_{lim}) of normal pulse voltammograms against the inverse of the square root of the sampling time (τ) were found to be linear, as expected for a diffusion-

Table 2.2 Apparent diffusion coefficient values for the homogeneous charge transport within POAP films and kinetic parameters for the heterogeneous electron transfer at the electrode|POAP film interface [12]

Method[a]	$10^{10} D_{app}^{ox} (D_{app}^{red})^{a}$ cm^2 s^{-1}	10^4 k^o cm^2 s^{-1}	α^b
PSCA	4.0 ± 0.5 (A)		
	5.8 ± 0.6 (C)		
PSCC	3.3 ± 0.4 (A)		
	5.2 ± 0.6 (C)	1.1 ± 0.3	0.75 ± 0.02 (A)
NPV	1.3 ± 0.2 (A)		
	2.6 ± 0.3 (C)		0.21 ± 0.03 (C)

The measurements were carried out in 0.2 M $NaClO_4$ aqueous solution (pH 1) where the $E'_{1/2}$ values of the POAP film were estimated to be 0.044 V versus SSCE from the average of the anodic and cathodic peak potentials of the cyclic voltammograms for the oxidation–reduction reaction of the POAP film. Other parameters are: the thickness (0.60 ± 0.06) μm and the concentration of electroactive site (4.5 ± 0.04) M for POAP deposited on BPG electrode [12]

[a] *PSCA*, Potential-step chronoamperometry; *PSCC*, Potential-step chronocoulometry; *NPV*, Normal pulse voltammetry

[b] "A" and "C" are used for the anodic and cathodic processes, respectively

controlled limiting current. Thus, D_{app} values were also obtained from the slope of i_{lim} versus $\tau^{-0.5}$ plots by using the normal pulse voltammetric Cottrell equation (Table 2.2). The kinetic parameters (k^0 and α) of the heterogeneous electron-transfer reaction were extracted from the rising part of the normal pulse voltammograms [2] (Table 2.2).

At this point it is interesting to compare results reported in Refs. [11, 12]. In this regard, transient currents for POAP-modified electrodes as a function of the reciprocal of the square root of time were also recorded in Ref. [11].

Authors of Ref. [11] remark that current relaxation for POAP films does not satisfy the Cottrell equation. It is indicated that the main part of the recorded current responses well fits a two-exponential time dependence, which most likely indicates a limiting influence of the charge carrier injection processes at both interfaces of POAP films. Thus, results reported in Ref. [11] seem to indicate that charge transfer through POAP films is complicated by irreversible injection processes at the film interfaces.

Electrochemical Impedance Spectroscopy (EIS) was employed in Ref. [13] to obtain transfer and transport parameters of POAP films of different thickness in contact with a 0.1 M HCO_4 + 0.4 M $NaClO_4$ ($pH1$) solution. Impedance measurements were made within the potential range $0.125 < E < 0.7$ V (vs. NHE). Impedance diagrams were interpreted through a simple charge-transfer resistance in parallel with a constant capacity at high frequencies and the redox capacity (C_{lf}) in series with the film resistance at low frequencies. The electrochemical rate constant ($k_{s,\,h}$), the concentration of redox centres (c), the film conductivity (σ_{lf}) and the diffusion coefficient of electrons (D_e) for POAP were obtained in Ref. [13]. The charge transfer resistance, R_c, was obtained by fitting experimental data to a semicircle, and it was expressed by Eq. (2.14):

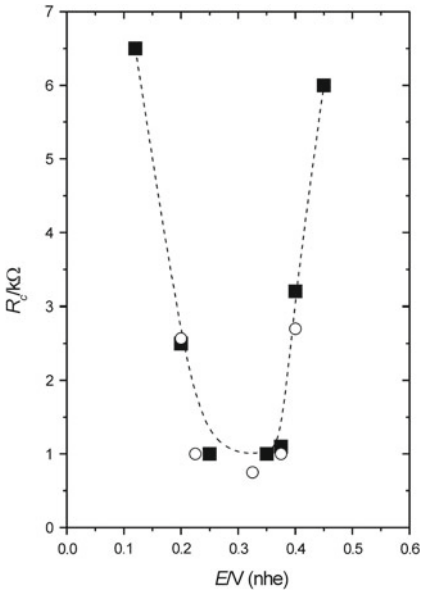

Fig. 2.5 Potential dependence of R_c: (o) $d = 30$ nm, (■) 300 nm [13]

$$R_c = 2RT(e^{\beta\phi} + e^{-\alpha\phi})/An^2F^2k_{s,\,h}c_T \tag{2.14}$$

α and β are the charge transfer coefficients for the anodic and cathodic partial processes, respectively, A the electrode area, $k_{s,\,h}$ the standard rate constant for the charge transfer process (cm s^{-1}), $c_T = C_O + C_R$ the sum of the concentrations of the oxidized and reduced forms, respectively, and $\phi = nF(E - E_0)/RT$ where E_0 is the standard potential of the redox couple. A plot of R_c versus E is shown in Fig. 2.5. No thickness dependence of the semicircle radius was observed in Ref. [13]. With c_T values extracted from a previous work [1] and assuming $\alpha = \beta = 0.5$, a $k_{s,\,h}$ value about 2.3×10^6 cm s^{-1} was obtained from Eq. (2.14). A high-frequency capacitance (C_{dl}) value about 8×10^{-6} F cm^2 was obtained in Ref. [13] and it was roughly independent of E and d. The redox capacity (C_{lf}) was obtained from $-Z''$ versus ω^{-1} plots at sufficiently low frequencies. C_{lf} versus potential dependence exhibits a maximum value around $E = 0.3$ V (Fig. 2.6). As can be seen from Fig. 2.6, C_{lf} increases with the film thickness, d. The low-frequency resistance, R_{lf} versus E dependence obtained in [13] is shown in Fig. 2.7. As R_{lf} is related to the conductivity (σ_{lf}) through:

$$\sigma_{lf} = d/(R_{lf}A) \tag{2.15}$$

a σ_{lf} value of $(4.55 \pm 0.2) \times 10^{-7}$ ohm^{-1} cm^{-1} was obtained at E_0. In this connection, authors of [13] remark that POAP exhibits a lower conductivity as compared with PANI. An electron-diffusion coefficient value D_e of about 1.3×10^{-11} cm^2 s^{-1} was also obtained by employing the formalism of Chidsey and Murray [14]:

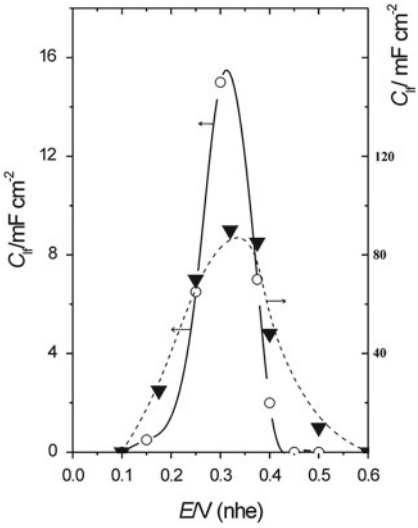

Fig. 2.6 C_{lf} versus E for (o) $d = 30$ nm and (▼) 300 nm [11]

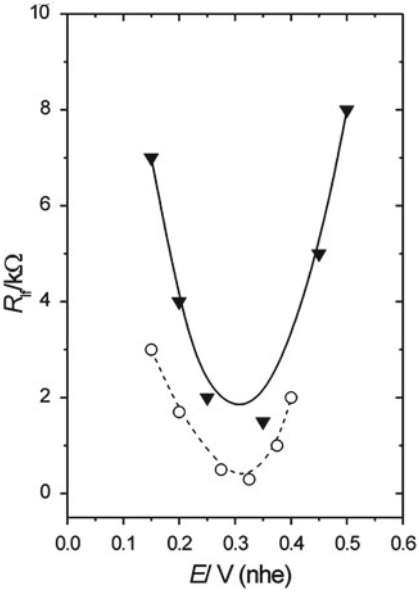

Fig. 2.7 The R_{lf} versus E dependence for POAP at different thickness: (o) $d = 30$ nm and (▼) 300 nm [13]

$$D_e = \sigma_{lf}/C_{lf} \tag{2.16}$$

D_e results nearly independent of E (Fig. 2.8).

Impedance measurements were performed in Ref. [15] to obtain charge transport parameters of POAP films and their dependence on solution *pH*. Impedance data were interpreted on the basis of the general expression of the faradaic

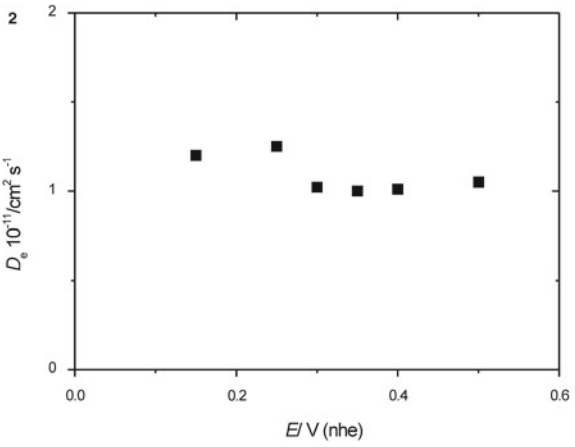

Fig. 2.8 Potential dependence of D_e calculated from Eq. (2.16) [13]

impedance of redox polymers with the diffusion–migration transport of two mobile species derived by Mathias and Haas [16]. The low-frequency capacitance, C_L was written as:

$$C_L = \left(F^2 Ad/RT\right)\left\{\beta\left[n^2 x(1-x)c\right]^{-1} + \left(z_i^2\, c_i\right)^{-1}\right\}^{-1} \tag{2.17}$$

where $\beta = 1 - Gx(1-x)$, G is an interaction parameter, x is equals the proportion of oxidized sites to the total electroactive sites, c is the total redox-site concentration, c_i is the concentration of ions with a charge number z_i, n is the number of electrons exchanged in a homogeneous reaction, d is the film thickness and A, the electrode area. The other symbols have their usual meanings. As according to the Mathias and Haas theory [16], Eq. (2.17) can be transformed into:

$$C_L = Ad\,\kappa\, t_e\, t_i\, D^{-1} \tag{2.18}$$

where κ is the film conductivity, $D(= D_i t_e + D_e t_i)$ is the coupled diffusion coefficient, which is expressed in terms of the electron (D_e) and mobile ions (D_i) diffusion coefficients and the transference numbers for electrons (t_e) and ions (t_i), respectively, then, the resistance of the bulk films, R_p, was written as:

$$R_p = d(A\kappa)^{-1} = d^2(DC_L)^{-1} t_e t_i \tag{2.19}$$

The low-frequency resistance, R_L, was also expressed in terms of the coupled diffusion coefficient D:

$$R_L = d^2(3DC_L)^{-1}(1 - 3t_e t_i) \tag{2.20}$$

The high-frequency charge-transfer resistance R_c, was related to the exchange current (i_0) of the redox couple at the metal/film interface by means of Eq. (2.21):

$$R_c^{-1} = nF(RT)^{-1} i_o = (nF)^2 (RT)^{-1} A\, k_s\, c_o^{(1-\alpha)} c_R^{\alpha} \tag{2.21}$$

where k_s is apparent standard heterogeneous rate constant, α is the transfer coefficient, c_o and c_R are the concentrations of the oxidized and reduced species, respectively. Equation (2.21) predicts that R_c reaches a minimum at nearly equal concentrations of the oxidized and reduced species in case of $\alpha = 0.5$ (Fig. 2.9). As the experimental dependence of the low-frequency resistance, R_L, on potential (Fig. 2.10) was basically similar to that of the charge-transfer resistance, R_c (Fig. 2.9) authors of Ref. [15] conclude that charge transport in the polymer occurs by a diffusion-like process due to molecular electron exchange, as suggested by Gabrielli et al. [4]. On the basis of relationships between R_L and the polymer resistance, R_p, the rate-determining step in charge transport through POAP films was discussed in [15]. Table 2.3 shows the two combinations of transport parameters in the extreme cases of ion-transport control, electron-transport control and mixed control. With regard to experimental data extracted from impedance plots showed in Ref. [15], R_p/R_L was very low (see Table 2.3), since R_L values were within the range 0.2–2 kΩ at a thickness film of $d = 0.1$ μm and R_p resulted very small (less than 2 ohm).

It was concluded in Ref. [15] from parameters listed in Table 2.3, that $t_e \gg t_i$ or $t_e \ll t_i$. Then, one of the two carriers moves much faster than the other at POAP. In order to shed light on this point, the authors of Ref. [14] calculated the D versus E dependence from experimental R_L (Fig. 2.10) and C_L values (Fig. 2.11). In spite of the error in the D values (near 50 %), it was found that D depends on E, that is, on the oxidation level of the polymer. The calculated D versus E dependence shows a maximum near the formal potential of POAP (Fig. 2.12).

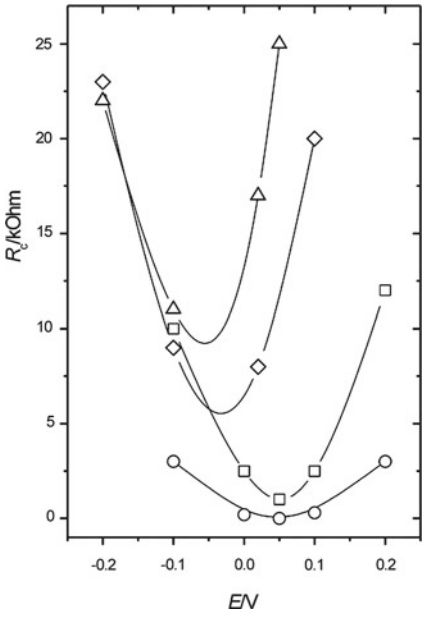

Fig. 2.9 Changes of the charge-transfer resistance with applied potential at different *pH* values: 0.5 (○); 1.3 (□); 2.5 (◇); 3.5 (△). Electrode area, $A = 0.071$ cm^2 [15]

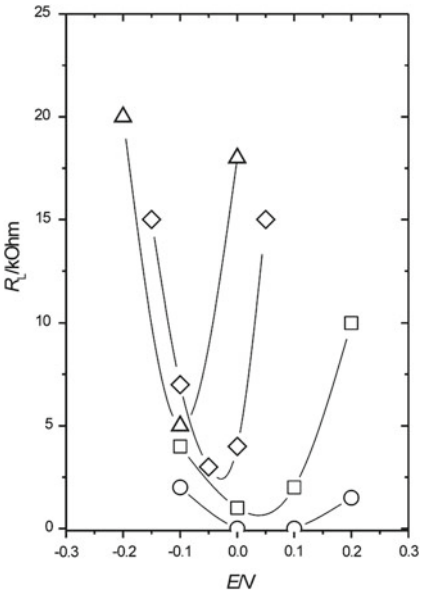

Fig. 2.10 Changes in the width of the Warburg region with applied potential at different *pH* values: 0.5 (o); 1.3 (□); 2.5 (◇); 3.5 (△). Electrode area, $A = 0.071$ cm^2 [15]

Table 2.3 Values of two combinations of transport parameters in the extreme cases of ion-transport control, electron- transport control and mixed control [15]

	Ion-transport control $t_e = 1$, $t_i = 0$	Electrón-transport control $t_e = 0$, $t_i = 1$	Mixed control $t_e = t_i = 0.5$
R_p/R_L	0	0	3
C_L/R_L	$d^2(3D)^{-1}$	$d^2(3D)^{-1}$	$d^2(12D)^{-1}$

Relationships extracted from the impedance model described in Ref. [15].

By comparing the D versus E dependence extracted from experimental R_L and C_L values with the D versus E dependence extracted from theoretical models [17], the existence of an electron-transport control in POAP was established. In this regard, authors of Ref. [15] consider the interaction between electroactive sites employing the coupled diffusion coefficient in electron-hopping conductive materials derived in [16], that is,

$$D = D_i t_e + \beta D_e t_i \tag{2.22}$$

where D_e and D_i are the diffusion coefficients of electrons and ions, respectively. At the extreme of ion-control ($t_e = 1$, $t_i = 0$), D becomes equal to D_i, which is potential independent. On the other hand, for electron-transport control ($t_e = 0$, $t_i = 1$), authors of Ref. [15] consider the expression,

$$D = D_e[1 - Gx(1 - x)] \tag{2.23}$$

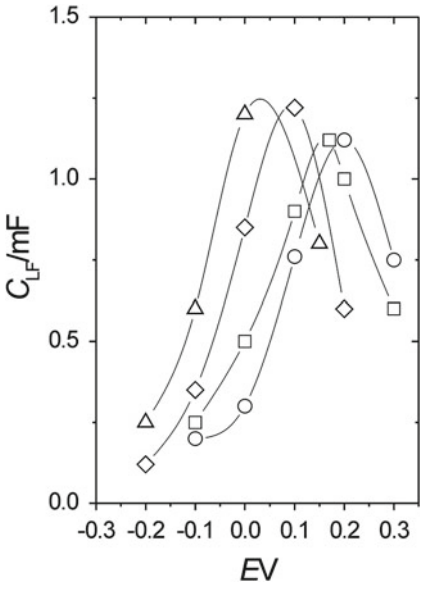

Fig. 2.11 Changes in the low-frequency capacitance with E at different pH values. 0.5 (o); 1.3 (□); 2.5 (◇); 3.5 (Δ). Electrode area, $A = 0.071$ cm^2 [15]

where if D is independent of the oxidation level, D will show a maximum of $D_e(1 - G/4)$ at $x = 0.5$. This expectation corresponds to experimental results shown in Ref. [15] (Fig. 2.12) with a G value of -10 and $D_e = 3.7 \times 10^{-9}$ cm^2 s^{-1}.

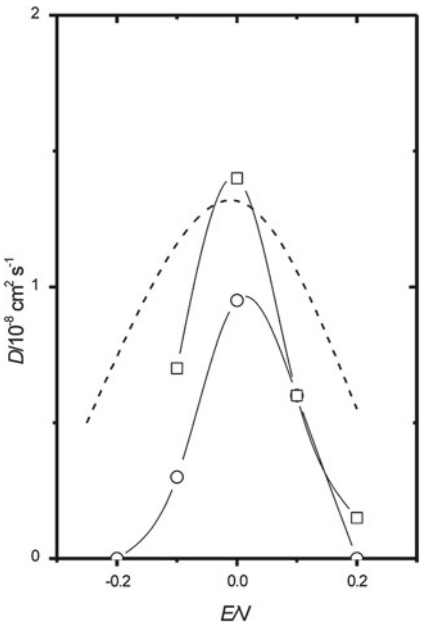

Fig. 2.12 Changes in coupled diffusion coefficients with applied potential in HCl–KCl solution (pH 1.3). (□) obtained from R_L and C_L; (o) estimated from method of Armstrong [17]; (- - -) calculated from the expression of the high-frequency capacitance, $C = F(RT)^{-1} Q_m x(1 - x)[1 - Gx(1 - x)]^{-1}$ and $D_e = k\lambda^2 c/6$, where k is the intermolecular electron-transfer rate constant and λ is the mean distance between two adjacent redox sites. $E^{o'} = 0$ V and $G = -10$ [15]

In the case of electron-transport control, the D_e value was found to be $D_e = 6 \times 10^{-9}$ cm^2 s^{-1} in 0.2 M HCl, from the estimated D maximum and a G value of -10. The D_e value obtained in Ref. [15] was very small in comparison with a D_i value of (0.9–5 6×10^{-6} cm^2 s^{-1}) reported for PANI films.

EIS was also employed in Ref. [18] to study the effect of the electrolyte solution on the transport properties of POAP. Different 0.1 M $HClO_4 + x$ M $NaClO_4$ solutions were employed, where x was varied between 0.4 and 2. The dependence of the characteristic impedance quantities at low frequency on the electrolyte concentration was interpreted on the basis of two models: a transmission line [19, 20] and a modified electron-hopping model described in Ref. [21]. Figure 2.13a, b shows the low-frequency capacitance (C_{LF}) and the low-frequency resistance (R_{LF}) vs potential dependences, respectively, for solutions of different ionic strengths. With regard to the transmission line model, impedance quantities obtained in Ref. [18] from experimental impedance spectra were employed in the Albery's Model [19, 20] to obtain different transport parameters of POAP films. Two separate distributed resistances are used in this model to represent the transport of electrons (R_e) and counter-ions (R_i) within the polymer [19, 20]:

$$R_e = RTc\phi_p / F^2 abAD_e(1/p + 1) \tag{2.24}$$

$$R_i = RT\phi_p(1 + p) / F^2 bAD_i \tag{2.25}$$

D_e and D_i are the diffusion coefficients for electronic species and ions, respectively; c is the total concentration of redox sites in the polymer; a, is the concentration of the reduced sites; and b the concentration of the oxidized ones ($a + b = c$). The parameter p represents the ratio of the volume of the polymer film to that of the aqueous pores; ϕ_p is the polymer film thickness; and A the geometric electrode area. The other constants have their usual meanings. The parameter p changes between 1 for a completely compact film and 0 for a completely porous one.

At low frequency the impedance expression given by the transmission line model, allowed to authors [18] to calculate $R_\Sigma (= 3R_{LF})$ from:

$$Z_{LF} = R_\Sigma / 3 - i/\omega C_\Sigma \tag{2.26}$$

where R_Σ is the sum:

$$R_\Sigma = R_e + R_i \tag{2.27}$$

and C_Σ is related to D_e through:

$$C_\Sigma^{-1} = C^{-1} + (D_e/\phi_p^2)\Psi \tag{2.28}$$

where C^{-1} describes the Feldberg capacitance and Ψ is:

$$\Psi = R_e[1 + (1 + \theta^{ox})]/[1 + (2s/\theta^{ox}pc)^2]^{1/2} \tag{2.29}$$

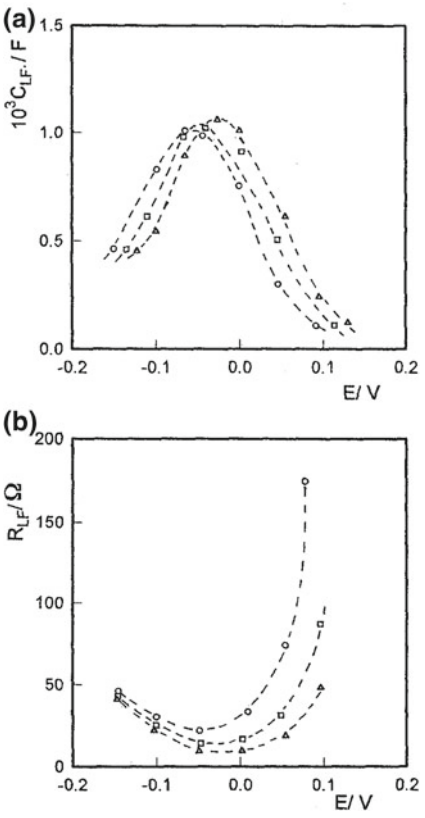

Fig. 2.13 **a** C_{LF} versus E for a 30 nm thick POAP film at different ionic strength: (o) $\mu = 0.1$ M, $\mu = 0.5$ M, $\Delta\mu = 2$ M **b** R_{LF} versus E for the same film and μ values [18]

In this last equation s is the salt concentration of the external electrolyte phase and $\theta^{ox} = b/c$ is the degree of oxidation of the polymer. When the polymer is completely oxidized authors [18] estimated p from:

$$Q_T^o = FAc\phi_p[p/(1+p)] \tag{2.30}$$

Q_T^o in Eq. (2.30) is the voltammetric charge for the oxidation process of POAP. With values of c, $\theta^{ox}(=\ b/c)$ and ϕ_p; D_i and D_e and p were employed as fitting parameters in order to obtain the best fit of Eq. (2.27) to experimental R_Σ versus θ^{ox} curves (continuous lines in Fig. 2.14). Despite p was estimated from Eq. (2.30), it was also employed as a fitting parameter in Eq. (2.27). The parameter p was considered as representative of the polymer porosity in this simple impedance model. In this regard, while D_i and D_e were considered to depend on film thickness and electrolyte composition, p was only considered to vary with the film thickness. Application of the electron-hopping model developed in [21] only gave an effective diffusion coefficient, D_{eff}. Figure 2.15 shows the D_{eff} versus θ_{ox} dependence for different ionic strengths of the electrolyte solution. At the different electrolyte concentrations, D_e obtained from the transmission line model was

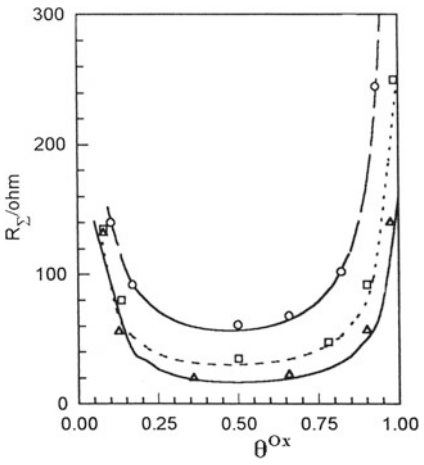

Fig. 2.14 Plots of the low-frequency resistance (R_Σ *vs.* θ_{ox}) for a 30 nm thick POAP film in 0.1 M $HClO_4$ + x M $NaClO_4$ solutions: (Δ) $x = 1.9$ M, ionic strength, $\mu = 2$ M; (□) $x = 0.4$ M, ionic strength, $\mu = 0.5$ M; (o) $x = 0$ M, ionic strength, $\mu = 0.1$ M. Symbols represent experimental values and *dashed lines* theoretical fit using the transmission line model [19, 20]

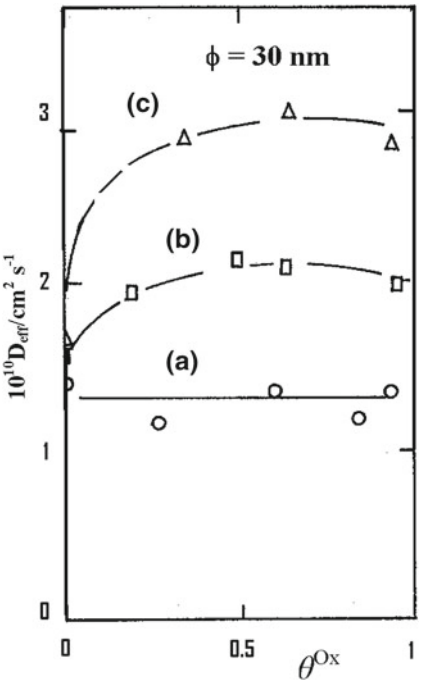

Fig. 2.15 D_{eff} versus θ_{ox} dependence for a 30 nm thick POAP film at different μ values: (o) 0.1 M, (□) 0.5 M, (Δ) 2 M. D_{eff} values were obtained from the model given in [21]

always two orders of magnitude lower than D_i. Also, as D_{eff} was very close to D_e, this was considered as indicative of a conduction mechanism at POAP films dominated by electron transport.

2.2.1 Conducting Potential Range of Poly(o-aminophenol)

POAP shows a relatively low conductivity as compared with other conjugated polymers. Table 2.4 lists the conductivity of some typical electroactive polymers.

On the basis of "polaron–bipolaron" model [29] of charging processes at polymer films, Ortega [30] investigated POAP by cyclic voltammetry and ESR measurements to determine the conducting potential range of the polymer. POAP films deposited on a Pt electrode were studied at *pH* 0.9, where spectra were recorded at different potentials, scanning forwards and backwards from −0.250 to 0.55 V (vs. SCE). The maximum in ESR spectra occurs in the potential range from −0.24 to approximately 0.0 V (see Fig. 1.16, Chap. 1). The decrease and further absence of a detectable ESR signal at potentials higher than 0.55 V suggests a combination of radicals to give rise to dication species, which are not ESR active because of their paired spin. The determined *g* value was 2.00710 for the spectra recorded from −0.2 to 0.05 V and 2.0076 for the one at 0.15 V. The slight change in *g*, due to the change in the nature of the electrostatic interactions between the charges in the polymer, was attributed to the combination of polarons at positive potentials to give rise to dications. Thus, it was concluded that at high positive potential values, the creation of bipolarons by a combination of polarons is possible at POAP films [30]. This conclusion is supported by other spectroscopic studies. Raman spectroscopy and voltammetry were coupled in [31] to identify structural changes in POAP during its redox process. Raman spectra of POAP contacting a 1 M $HClO_4$ solution exhibit bands whose intensities depend on the applied potential. For instance, the band associated with quinoid groups (1474 cm^{-1}) and the band assigned to –C=N– in quinoneimine units (1638 cm^{-1}) depend on the potential (Fig. 2.16).

The behaviour of these bands with the potential shows that when the potential increases, the band at 1474 cm^{-1} increases and the band at 1638 cm^{-1} also increases until a potential of about 0.2 V and thereafter, it diminishes. The fitting of these bands by employing Lorentz curves allowed the authors of [31] to quantify the evolution with the potential of the species related to these bands. The integrated intensity of the band at 1638 cm^{-1} increases until a potential around 0.15 V and then decreases. However, the integrated intensity of the band at

Table 2.4 Conductivity of some typical electroactive polymers

Polymer	[a]Conductivity (S cm^{-1}) of the oxidized polymer	References
Poly(*o*-aminophenol)	10^{-7}–10^{-6}	[1, 13, 15, 21–24]
Polyacetylene	3–1000	[25]
Polyaniline	0.01–5	[25]
Polypyrrole	0.3–100	[26]
Polythiophene	2–150	[27]
Poly(*p*-phenylene)	10–500	[28]

[a] Significantly higher conductivity has been published for the polymers listed but not in the context of their practical applications

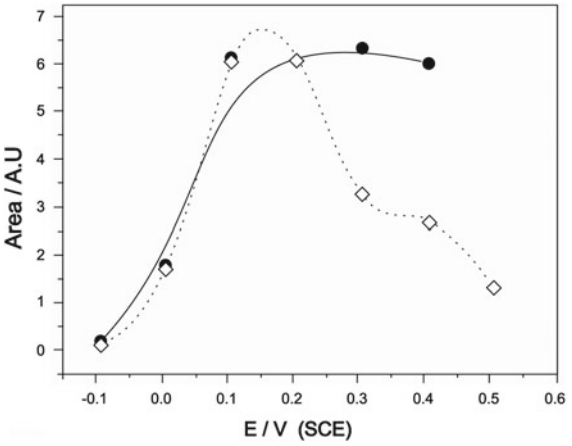

Fig. 2.16 Dependence of the relative area of 1474 cm^{-1} (•) and 1638 cm^{-1} (◇) Raman bands on the electrode potential for a POAP modified Au electrode in 1 M $HClO_4$ electrolyte solution [31]

1474 cm^{-1} increases until 0.15 V, and then it is maintained. Thus, the behaviour of the band at 1638 cm^{-1} corresponds to a typical intermediate species. Since POAP has a conductivity maximum at about 0.04 V versus SCE, the intermediate species was related to the polymer conductivity and then, it was assigned to a charged species. The authors of Ref. [31] indicate that the existence of an intermediate species suggests that the oxidation of POAP occurs through two consecutive reactions from the totally reduced phenoxazine form to the completely oxidised one, through a charged species, which could be a cation radical. Authors of Ref. [31] remark that the behaviour of the integrated Raman intensity of the band at 1638 cm^{-1} is similar to that of the band at 750 nm observed in the absorbance *versus* potential dependence in the UV-Vis region reported in [32]. Then, Raman and UV-Vis measurements suggest that the third species could be a cation radical, in agreement with the results obtained by EPR [30].

EIS was employed in Ref. [13] to obtain dependences of charge transfer and charge transport parameters of POAP films on the electrode potential within the range $0.125\ V < E < 0.7\ V$ (versus NHE). A conductivity value of $4.55 \pm 0.2) \times 10^{-7}$ ohm^{-1} cm^{-1} was obtained for POAP at $E = 0.3$ V (NHE). Authors of Ref. [13] remark that POAP exhibits a lower conductivity as compared with PANI. An electron-diffusion coefficient value D_e of about 1.3×10^{-1} cm^2 s^{-1} was also obtained.

Dynamic Monte-Carlo simulations were employed in order to find the morphological effect of the insulating–conducting (I–C) transition of a POAP film [33]. In these calculations it was assumed that the polymer has a random distribution of electroactive and electroinactive sites. The electrochemical switching potential (I–C) of the polymer and its percolative nature [34–36] under potential changes, was analyzed in Ref. [33]. The model of electrochemical system used in Ref. [33] consists in a conductive polymer film in a solution containing a large excess of supporting electrolyte and dopant ions. The film was considered to be conductive in the oxidized state and nonconductive in the reduced state. It was assumed that the

zone composed of only the conductive species is fully conductive and that the mass transfer of counter-or dopant ions associated with the charge transfer has only a minor effect on the propagation of the conductive zone. The conductive polymer film was simulated by means of a two-dimensional lattice of which each element was a regular rectangle. Each element was attributed to a conductive, a non-conductive or an electro-inactive site. A substrate electrode was allocated randomly on the lattice so that the ratio of the area of electroactive sites to that of the lattice was a given value, p (p is the percolation probability). On the basis of the cyclic voltammetry (CV) technique and the theory of propagation, the growth rate of the conductive zones was considered as an exponential function of the electrode potential. The dimensionless amount of interconverted conductive zones, X, was expressed in terms of the theoretical linear sweep voltammetry [37] as:

$$X = \int \kappa e^{\beta\xi} \left\{ [1 + \Phi(e^{\beta\xi} - \beta/\kappa)^{1/\beta}]^{-1} - (1 + e^{\xi})^{-1} \right\} d\xi \tag{2.31}$$

where, $\xi = (nF/RT)(E - E^{0r})$ is the dimensionless electrode potential, β is the chatodic transfer coefficient, κ is the dimensionless kinetic parameter given by $\kappa = k^{o}RT/nF\nu\delta$ and Φ is a function defined as:

$$\Phi(z) = z \text{ for } z \geq 0 \text{ and } 0 \text{ for } z < 0 \tag{2.32}$$

k^0 is the charge-transfer constant, δ is the thickness of the polymer film and v is the potential sweep rate. It was assumed that at the electrode/film interface, and under the Nernst boundary condition, $1/\left(1 + e^{-\xi}\right)$ fraction of the total electrode area is converted at any increment $\Delta\xi$. Therefore, the amount of conversion, $X(\xi + \Delta\xi) - X(\xi)$ was written as:

$$X(\xi + \Delta\xi) - X(\xi) = \Delta\lambda/(1 + e^{-\xi i}), \text{ for } i \in [1, \infty). \tag{2.33}$$

$\Delta\lambda$ is the side length of the square element and the value of ξ_i was obtained numerically for a given value of the initial potential, ξ_0 The initial potential, ξ_0 was estimated from Eq. (2.31) by taking $\Phi = 0$. Then, a series of $\{\xi_i\}$ was computed. Electroactive sites were assigned to the lattice by the Monte-Carlo method so that that the total area of the active sites was p-times the area of the lattice. The number n_i of the conductive sites converted at ξ_i was considered to be proportional to the faradaic charge at the step ξ_i to ξ_{i+1}. As the lattice consists of $N \times M$ rectangles, hence the dimensionless current was written as $n_i/[N \times M(\xi_{i+1} - \xi_i)]$ Various patterns of the conductive zones were observed in Ref. [33] at p ranging from 0.5 to 0.61. A two-dimensional patter of the conductive sites ($\xi = -4$ and $p = 0.50$) was observed when the current vanishes in linear sweep voltammetry. The sites have a very low electrical contact with the electrode under this condition. This effect was explained by assuming that under an insufficiently positive potential there are a few conductive sites on the electrode. The growth began at the sites on the first layer activated by the Nernst condition, (for $\xi = -2$, $p = 0.55$). In this case, the zones consist of a number of clusters, which are disconnected electrically from each other. Some of these patterns result

fractal. In this case, the zone grew not only in direction parallel to the electrode and toward the film/solution interface, but also in the direction toward the electrode. Further, growth yielded electrical percolation at $\xi = -0.50$ from the electrode to the top of the film. The fractal pattern occurs at percolation threshold ($p = 0.59$). The final converted pattern involved various sizes of islands after percolation threshold ($p = 0.61$) at $\xi = 0.5$. Since the islands consisted of not only electroinactive zones, but also nonconductive zones, the conversion ratio was less than p. Figure 2.17 shows the average linear sweep voltammogram corresponding to the patterns reported in Ref. [33]. From the peak current and the conversion ratio with p, the voltammogram was classified into the three controlled processes: Nernsian condition control ($0 < p < 0.55$), morphological control ($0.55 < p < 0.61$) and charge-transfer control at the interface between conductive and nonconductive sites ($p > 0.61$). The morphological effects are specific to the peak potential. The comparison of the simulated patters obtained in Ref. [36] with the corresponding linear sweep voltammogram shown in Fig. 2.17, reveals that the peak potential of linear sweep voltammetry could be considered as a first approximation of the percolation threshold potential of the electrochemically deposited conductive polymer film. In order to verify this assumption, authors of Ref. [33] performed an independent analysis to determine the percolation threshold potential of a conductive POAP film and compared it with the peak potential of a cyclic sweep voltammogram. Thus, POAP films in Ref. [33] were deposited on glassy carbon electrodes by multiple potential cycling between −0.2 and 0.9 V versus Ag/AgCl at a scan rate of 50 mV s^{-1} in a sulfuric acid solution (*pH* 5) containing *ortho*aminophenol at a concentration of 0.1 M. The POAP coated electrode was stepped in the positive potential direction and the growth of the conductive zone was investigated through examining the chronoamperometric behavior.

Figure 2.18 shows the chronoamperograms of the film/H_2SO_4 interface recorded at *pH* 5 at various potential steps in the range of 0.01–0.2 V/Ag/AgCl. The electrochemical activity of POAP begins at around 0.11 V, as indicated by the sharply rising initial current (I) and its relatively slow decay with time (t) (Fig. 2.18). Plots of I–$t^{-1/2}$ and I–t^{-1} were recorded at various potential step values. Below 0.15 V, linear dependency of I–$t^{-1/2}$ was observed indicating the dominance of the diffusion controlled processes giving rise to the development of the conducting conductive zone. Above 0.15 V, no linear dependency of I–$t^{-1/2}$ was observed over any appreciable period of time. On the other hand, good to fair linear plots of I–t^{-1} were obtained over a large time period. Interestingly, the slope of this dependency increases as the magnitude of the potential step increases to 0.17 V and decreases upon further increase of the size of the potential step.

An explanation of this behavior is given in Ref. [33]. It was considered that linear I–t^{-1} plots correspond to the production of finite quantities of material conducting form of the polymer under a potential step of finite height. The polymeric film is initially in the insulating mode, then, upon stepping the potential into the electrochemically active region, the polymer immediately in contact with the metallic surface is oxidized and converted to the conducting mode while the rest is still

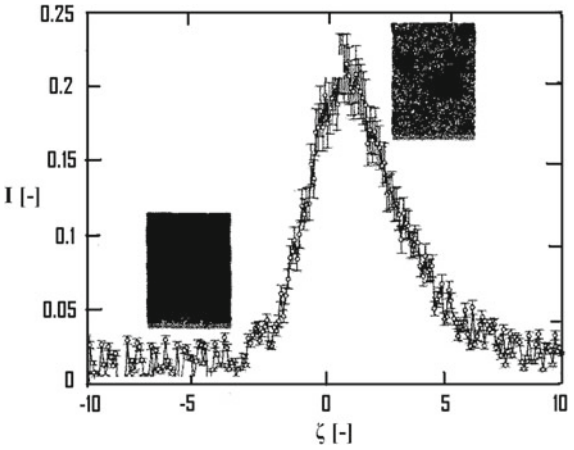

Fig. 2.17 Dimensionless voltammogram ($iRT/n^2F^2c^*\delta vp$ vs. ξ) simulated for distribution of the electroactive sites. Inset shows distribution for conductive zones at $\xi = -4$ (*lower*) and at $\xi = -0.59$ (*upper*), i is the current density, c^* is the concentration of the electroactive species, v is the potential sweep rate, p is the ratio of the area of electroactive sites to that of the lattice and δ is the thickness of the polymer film [33]

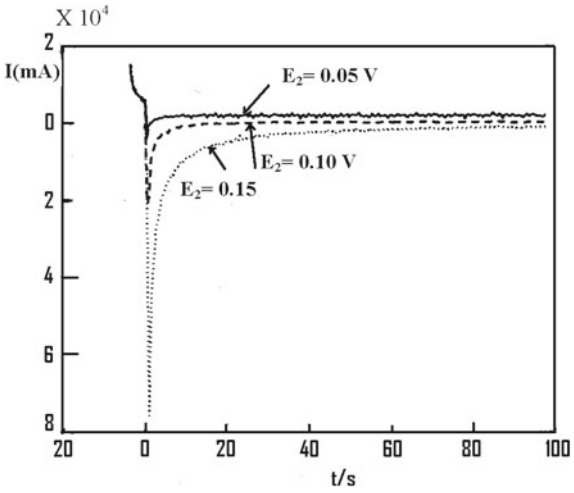

Fig. 2.18 Chronoamperograms of the POAP film/H_2SO_4 interface at various potential steps [33]

insulating. Further conversion has to continue at the partially metal-like progressive conducting zone. The size of the conducting zone (cluster) is certainly controlled by the charge delivered onto the electrode (film) at the specified potential step. The deposited film is converted into the conducting mode by repeating this process. Some of the conducting clusters keep growing and some are probably transported

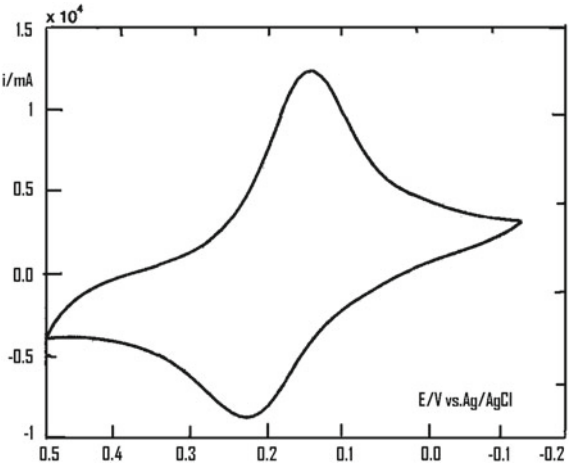

Fig. 2.19 Cyclic voltammogram of a POAP film in the presence of sulfate anions (*pH* 5). Scan rate: 50 mV/s [33]

trough the film by diffusion. It is believed that the rate of enlargement of the conducting cluster is slowed down by the depletion of the wandering (migrating off the metallic back contact) of the already existing small conducting clusters giving rise to the t^{-1} dependency of the current rate. However, the linearity was found to be limited to the potential range of $0.15\ \text{V} < E_c < 0.17\ \text{V}$. In the opinion of the author [33], E_c is definitely in the range of $0.15\ \text{V} < E_c < 0.17\ \text{V}$ near the peak potential of the corresponding voltammogram (Fig. 2.19).

This fact was confirmed by the Monte Carlo simulation results. Both the simulated linear sweep voltammetry and the potential step experiments show an extremely rapid drop in the current during C–I conversion. That is, the film changes from the conducting form to the insulating one, once the conversion yield reaches a threshold during the phase transition. Since, the transition is based on fractal formation, slight fluctuations, such as movement of the sites may change the cluster size. Therefore, the abrupt growth of the C zone and the onset of the current at E_c correspond to a rapid rise in the anodic voltammogram when the film is sufficiently reduced. Then, authors of Ref. [33] conclude that the percolation threshold during insulating/conducting transition of electrochemically deposited POAP films is in the range 0.15–0.17 V (Ag, AgCl).

2.2.2 *Effect of the Solution pH on the Charge-Transport Process at POAP Films*

The electrochemical response of POAP is highly dependent on the solution *pH*. The *pH* effects on the voltammetric response of POAP were described in Ref. [1] (see Eqs. (2.7) and (2.8), and Fig. 2.2). Also, a redox reaction of POAP was proposed in Ref. [1] (Fig. 2.4), which involves a process of addition/elimination of

protons coupled with a reversible electron transfer. The protonation of the oxidised form of POAP was considered as the coupled chemical reaction in the mechanism proposed in Ref. [1].

Electrochemical Impedance Spectroscopy was used in Ref. [21] to study the effect of the solution *pH* on the charge conduction at POAP films. An *a.c* impedance expression was derived on the basis of a model that considers a chemical reaction influencing the dynamics of the charge-transport process by electron hopping between redox sites. The model described in Ref. [21] considers a protonation reaction (Eq. (2.34)) coupled with a self-exchange process between oxidized and reduced sites (Eq. (2.35)):

$$\mathrm{O} + [\mathrm{H}^+]_{\mathrm{film}} \underset{k'_{-1}}{\overset{k'_1}{\leftrightarrow}} \mathrm{HO}^+ \tag{2.34}$$

$$\mathrm{OH}^+ + \mathrm{e}^- \underset{k_\mathrm{b}}{\overset{k_\mathrm{f}}{\leftrightarrow}} \mathrm{RH} \tag{2.35}$$

The analytical expression for the impedance derived in Ref. [21] is

$$Z(\omega) = R_{\mathrm{Qt}} + \left(RT/nF^2Ac\right)\left[k_\mathrm{f} + k_\mathrm{b}(K+1)/K\right]A(\omega, D_\mathrm{e}, k) \tag{2.36}$$

R_{Qt} in Eq. (2.36) is a charge-transfer resistance, which is given by the expression

$$R_{\mathrm{Qt}} = \left(RT/nF^2Ac\right)\left[(k_\mathrm{f} + k_\mathrm{b})\,(k_\mathrm{f}k_\mathrm{b})^{-1} + 1/K\,k_\mathrm{f}\right] \tag{2.37}$$

In Eqs. (2.36) and (2.37), A is the electrode area, c the volumetric redox site concentration, and K an equilibrium constant that can be explicitly written in terms of the solution *pH* as

$$K = \left(k'_1/k'_{-1}\right)K_\mathrm{p}10^{-\mathrm{pH}} \tag{2.38}$$

K also depends on the k'_1 and k'_{-1} constants involved in step (2.34) and a partition coefficient K_p, which determines the ratio between the proton concentration inside the film ($[\mathrm{H}^+]_{\mathrm{film}}$) and the actual proton concentration in solution ($[\mathrm{H}^+]_{\mathrm{sol}}$), i.e.,

$$[\mathrm{H}^+]_{\mathrm{film}} = K_\mathrm{p}[\mathrm{H}^+]_{\mathrm{sol}} \tag{2.39}$$

k_f and k_b in Eq. (2.36) are the forward and backward electrochemical rate constants involved in step (2.35), respectively, and $A(\omega, D_\mathrm{e}, k)$ is a function of the frequency, ω, which also contains an affective diffusion coefficient (D_e) to describe the charge-transport process within the polymer film and the constant $k = k'_{-1} + [\mathrm{H}^+]_{\mathrm{film}}\,k'_1$. OH^+ and RH (steps (2.34) and (2.35)) are the protonated oxidized and reduced forms of the polymer confined redox couple, respectively. Other chemical equilibria following the self-exchange (2.35) were ignored in Ref. [21]. Concerning step (2.35), the electroactive centres OH^+ and RH can exchange

electrons with the electrode at the metal/polymer interface following a Buttler–Volmer kinetics, with k_f and k_b given by the expressions

$$k_f = k_{sh} \exp\left[b_f\left(E - E^0\right)\right] \tag{2.40}$$

$$k_b = k_{sh} \exp\left[-b_b\left(E - E^0\right)\right] \tag{2.41}$$

E^0 in expressions (2.40) and (2.41) is the standard potential of the redox couple, b_f and b_b are the Tafel coefficients, $b_f = \alpha nF/RT$ and $b_b = (1 - \alpha)\, nF/RT$, and k_{sh} is the electrochemical standard rate constant. The other constants have their usual meanings. The redox centres are uniformly distributed throughout the polymer with a total concentration, c, given by

$$c = [O] + [HO^+] + [RH] \tag{2.42}$$

Eq. (2.36) was employed in [21] to fit experimental impedance diagrams of POAP films in solutions of different *pH*. In the model the equilibrium constant (K) (Eq. (2.38) for the protonation reaction appears in the different impedance quantities (Warburg coefficient (σ_{Qc}), low-frequency resistance ($R_{Q,\ LF}$), low-frequency capacitance ($C_{Q,\ LF}$), electron diffusion coefficient (D_e), etc.). Then, a comparison between experimental and theoretical impedance quantities at different *pH*s values was made in Ref. [21].

Figures 2.20 and 2.21 show some results of the fitting (continuous lines) of the theoretical impedance quantities derived in Ref. [21] to experimental (discrete points) data. It was found that the low-frequency capacitance and the conductivity decrease with *pH*. A conductivity value of about 3.2×10^{-6} S cm^{-1} at *pH* 0 was reported for POAP in Ref. [21]. Also, as the *pH* affects the dynamics of the electron-hopping process through reduction of the redox centre density, from the fitting it was possible to extract an electron-diffusion coefficient that decreases from 2.1×10^{-10} to 5×10^{-11} cm^2 s^{-1}as the *pH* increases from 0 to 2. Also, a *pKa* value about 2.3 for the proposed protonation reaction could be estimated from the model developed in Ref. [21].

Another *ac* impedance study of POAP-coated electrodes was performed in Ref. [15] to establish how the kinetic parameters of the charge-transport process are affected by the protonation levels and also by the degree of oxidation of the polymer. Impedance data were analysed on the basis of the electron-hopping transport accompanied with intermolecular proton exchange. The dependence of the charge-transfer resistance (R_c) on the potential (E vs. Ag/AgCl) at different *pH* values was evaluated from experimental impedance spectra (Fig. 2.9). R_c values obtained at a given *pH* reach a minimum at the formal potential of POAP, which was evaluated as the average of the voltammetric anodic and cathodic peak potentials. The minimum of R_c considerably increased with increasing *pH*. Also, the R_c *versus* E curve shifts to the negative potential with a rate of −0.06 V/*pH* as *pH* increases. This effect was considered as indicative of a proton participation in the redox reaction of POAP. With regard to low frequencies of impedance data, the capacitance (C_{LF}) was evaluated from the slope of Z'' versus ω^{-1} plot. C_{LF}

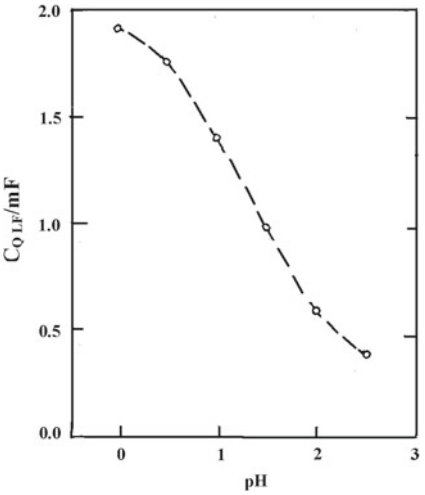

Fig. 2.20 Low-frequency capacitance $C_{Q,LF}$ versus *pH* at $(E - E^0) = -0.05$ V. (o) Experimental points extracted from the Nyquist diagrams obtained at different *pH* values. Thickness of the film 30 nm. Bathing electrolyte: $HClO_4 + NaClO_4$, ionic strength 1 M [21]

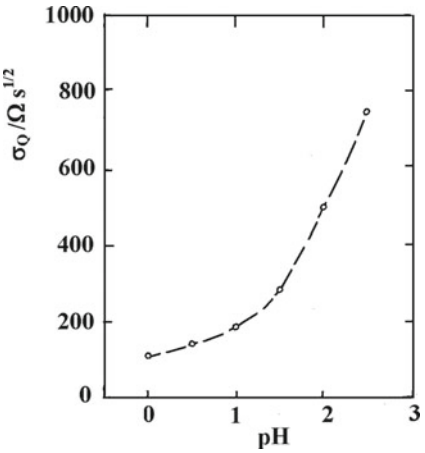

Fig. 2.21 Warburg coefficient σ_{Qc} versus *pH* at $(E - E^0) = -0.05$ V. (o) Experimental points extracted from the Nyquist diagrams obtained at different *pH* values. Thickness of the film 30 nm. Bathing electrolyte: $HClO_4 + NaClO_4$, ionic strength 1 M [21]

obtained at a given *pH* shows a maximum near the formal potential. The C_{LF} *versus E* curve shifts to the negative potential with increasing *pH*, whereas the maximum of C_{LF} was independent of *pH* (17 ± 1 mF cm^{-2} at a film thickness of 0.14 μm) (Fig. 2.11). As *pH* increases, it was also observed in Ref. [15] that the formal potential of POAP shifts to the negative direction with a rate of −0.06 V/*pH* in the *pH* range below 6. This shift was considered to indicate that one proton is released for each electron transferred in the oxidation process, thus electrochemical oxidation of the polymer was considered equal to its dehydrogenation. In this sense, it was considered in Ref. [15] that when the polymer including electroactive nitrogen atoms is oxidized, anions are inserted into the polymer (Eq. (2.43)), or else protons are released from the polymer (Eq. (2.44)) to maintain its electroneutrality:

$$P + Cl^{-}(s) \rightarrow P^{+}Cl^{-} + e\ (m) \tag{2.43}$$

$$PH \rightarrow P + H^{+}(s) + e(m) \tag{2.44}$$

where both P and PH denote the monomer unit in polymer chains, in disregard for its protonation. On the basis of the acid dissociation constant of phenazine, it was concluded in Ref. [15] that all species of the different oxidation states of POAP should be protonated in acid solutions. The redox reaction of the protonated POAP was expressed as indicated in Fig. 2.22.

The reduced form -NH_2^+– or –NH– (for the non-protonated polymer) has one hydrogen atom more than the oxidized form –$NH^{\bullet+}$– or –$N^{\bullet}$– (for the non-protonated polymer) where –NH_2^+–, –NH–, –$NH^{\bullet+}$– and –$N^{\bullet}$– represent hydrogen atoms in the heterocyclic rings. The adjacent two oxidized species combine to produce stable imines –NH^+= or –N= in the polymer chains (Fig. 2.22). From an electronic equilibrium at the metal/polymer interface and an ionic equilibrium at the polymer/solution interface, for reaction (2.44) the following relationship between the potential and the oxidation level was obtained in Ref. [15]:

$$E = E^0 - 2.3RTF^{-1}pH + RTF^{-1}\ln x(1-x)^{-1} \tag{2.45}$$

where x equals the proportion of oxidized sites to the total electroactive sites. Eq. (2.45) shows the formal potential shift with pH. Employing Eqs. (2.45) and (2.46) which defines the redox capacitance,

$$C_{LF} = dQ/dE = Q_m dx/dE \tag{2.46}$$

where Q is the charge required to oxidize the fully reduced polymer, Q_m is its maximum and x is the oxidation level evaluated as Q/Q_m, the low-frequency capacitance was written as:

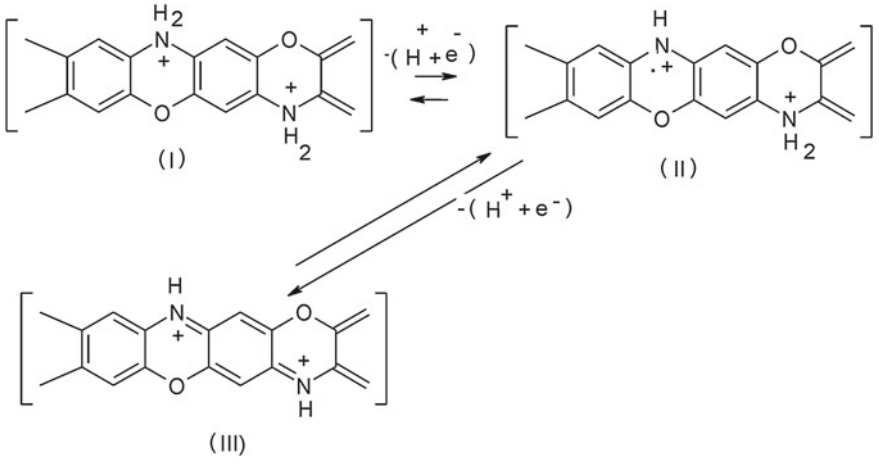

Fig. 2.22 Probable redox reaction of the protonated POAP proposed in [15]

$$C_{LF} = F(RT)^{-1} Q_m x(1-x) \tag{2.47}$$

Equations (2.45) and (2.47) predict that the capacitance is directly proportional to the film thickness through Q_m, and shows a maximum at a medium oxidation level and C_{LF} versus E curve shifts to the negative potential with increasing pH, as it experimentally observed. However, the calculated C_{LF} versus E curve has a smaller width of the capacitance peak as compared with the experimental data. The discrepancy was ascribed to activity effects involving an interaction between electroactive sites of the polymer. The theoretical curve was well fitted to experimental data by using a negative interaction parameter, which means a repulsive interaction between electroactive sites (see Eq. (2.23)). The charge-transport process in Ref. [15] was also expressed in terms of a coupled diffusion coefficient D (= $D_i\, t_e + D_e\, t_i$, where D_e and D_i are the electron and ion diffusion coefficients, and t_e and t_i are the transference numbers for electrons and ions, respectively). The D versus E dependence was calculated from experimental R_L and C_{LF} values (see Eq. (2.20)). It was observed that D decreases with pH (Fig. 2.23). In order to explain this dependence, it was considered that only protons are the ionic charge carriers in POAP. In this sense, the homogeneous electron transfer in the film should be accompanied with proton transfer from the reduced sites to the oxidised ones. This transport mechanism implies that electronic conductivities (κ_e) of the polymer probably decrease with its deprotonation. In this regard, authors of Ref. [15] measured κ_e of a POAP film at different oxidation levels with a symmetrical cell. It was effectively found that the electronic conductivity decreases with pH. As κ_e depends on D_e [16], authors of Ref. [15] attributed the κ_e decrease with increasing pH to the corresponding decrease of D_e. In this connection, in the electron hopping between adjacent redox sites in different oxidation states, D_e was expressed as a function of the intermolecular electron-transfer rate constant (k) and the mean distance (λ) between two adjacent redox sites [38]. Then, the D_e decrease with pH was attributed to a decrease of k with the polymer deprotonation.

EIS measurements were also performed in $LiClO_4$ and $HClO_4$ solutions at different pH values and constant ionic strength (1 M), to elucidate the role of protons in the conduction mechanism of POAP [11]. The simplified theory of polymer film impedances of Mathias and Haas [16] was applied in [11] to estimate an effective diffusion coefficient (D_{eff}) value of charge carriers inside POAP films. However, the estimation of D_{eff} was hardly possible, because of the absence of a well-defined Warburg region in the impedance spectra. Also, the low-frequency dependences of the imaginary component of POAP impedance spectra at different potentials exhibit curves that consist of two lines and an intermediate region in between. Only the first lines approximately satisfy the impedance theory, since their intercepts are near zero. The second intercepts are non-zero. Also, impedance measurements for POAP became very difficult for frequencies lower than 0.1 Hz due to the noise fluctuations observed in this frequency region. Thus, it was not possible in Ref. [11] to obtain real low-frequency capacity (C_{lf}) values of the POAP films and then, only estimations were obtained. Apparent capacities $C_{lf}^{(ap)}$

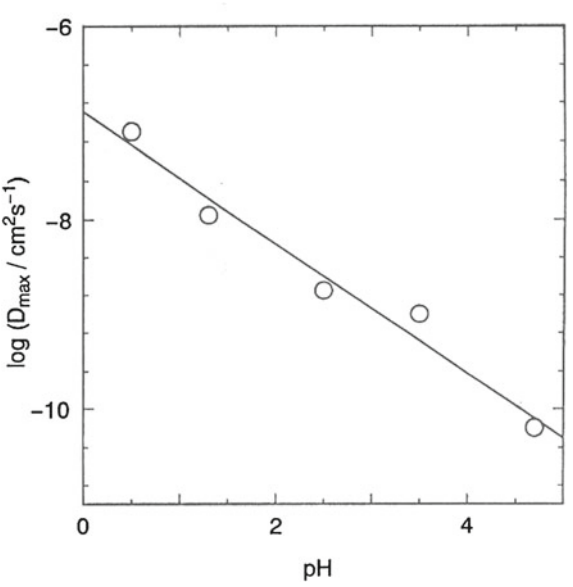

Fig. 2.23 The *pH* dependence of the *D* maximum obtained at a given *pH* [15]

were calculated from $\mathrm{d}(-\mathrm{Im}Z)/\mathrm{d}(f^{-1})$ slopes and they were compared with the C_{lf} values extracted from CV. The latter values are nearly three times higher than the former. Thus, impedance data presented in Ref. [11] demonstrate the capacity dispersion in the low-frequency region. Even when this phenomenon at the low-frequency region can be attributed to porosity effects of POAP films, the authors of Ref. [11] are rather disposed to explain the observed capacity dispersion as a consequence of the binding of hydrogen ions with polymer nitrogen-containing groups.

Interfacial resistance measurements [39] were also employed to study the redox mechanism of POAP and its dependence on the solution *pH* [40, 41]. The experimental arrangement in these investigations [39–41] was one in which a POAP film is supported on a thin gold film of thickness 30 nm. Interfacial resistance is not only sensitive to the presence of scattering centres but also to their distribution at the surface of a metal film. In this connection, it is demonstrated in Ref. [40] that the oxidation–reduction process of a POAP film, deposited on a thin gold film electrode, has a significant effect on the electronic transport of the base metal film. While Cyclic Voltammetry was used to quantitatively characterise the redox species transformation on the gold film surface contacting the polymer film, the resistance change $(\Delta R/R)$ was employed to investigate changes in the electronic properties at the gold|POAP interface during the redox conversion of the polymer [40]. Resistance changes with potential $(\Delta R/R - E)$ of a gold film free of and coated with a POAP film, both of them contacting a 0.1 M $HClO_4$ + 0.4 M $NaClO_4$ solution, were compared within the potential range –0.2 V $< E <$ 0.5 V (E vs. SCE) where POAP exhibits its maximal electroactivity (Fig. 2.24). As

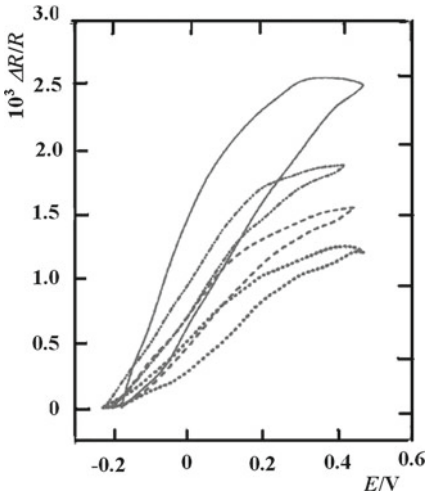

Fig. 2.24 $\Delta R/R$ versus E response for POAP coated gold film electrodes. POAP thickness: ϕ_p(—) 0 nm, (···)5 nm, (- - -) 10 nm, (-·-·-·) 60 nm. Scan rate: $v = 5 \times 10^{-3}$ V s^{-1}, $d = 30$ nm. Electrolyte: 0.1 M $HClO_4$ + 0.4 M $NaClO_4$ [39]

POAP becomes conductive at positive potentials (oxidized state) the $\Delta R/R$ versus E changes were referred to the potential value $E = -0.2$ V where POAP is its reduced state. The increase of the resistance of the naked gold film electrode (free of polymer) going from –0.2 V to 0.5 V was ascribed to ClO_4^- adsorption (Fig. 2.24). Also, within the same potential region a resistance increase was observed for the gold film modified with POAP.

However, the observed $\Delta R/R$ change appears attenuated respect to the gold film free of POAP and this attenuation becomes more pronounced as thicker is the polymer film. However, for high polymer thickness (thickness, $\phi_p > 60$ nm) the $\Delta R/R$ change becomes independent of ϕ_p. Furthermore, for $\phi_p > 60$ nm the resistance behaviour of the base gold film is independent not only of the polymer thickness but also of the external electrolyte composition (Fig. 2.25). The $\Delta R/R$ increase going from the reduced to the oxidized state of POAP (curves in Fig. 2.25b) was ascribed in Ref. [39] to the proper redox conversion of the POAP film.

Author of Ref. [39] explains the observed increase of resistance considering that during polymer oxidation generation of charged electronic entities at the polymer chains near the gold surface occurs by electron transfer across the polymer-metal interface. In this regard, the author remarks that the redox switching of POAP was interpreted in a previous work [32] in terms of the oxidation of the amino groups to imine. Thus, it should be expected that imine sites act themselves as different scattering centres compared with amine sites, increasing in this way the diffuse reflection (increase of ΔR) of conduction electrons on the gold film surface during POAP oxidation. With regard to Fig. 2.25 (b), the author of Ref. [40] indicates that it is possible that by means of resistance measurements on a gold film surface blocked with an enough thick POAP film the attention is paid to only one process, that is, the redox transformation of the

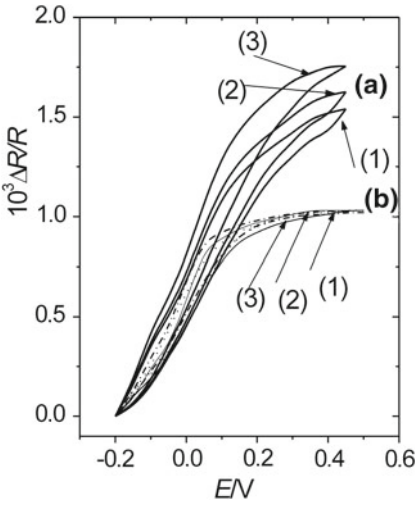

Fig. 2.25 $\Delta R/R$ versus E response for a gold film electrode ($d = 30$ nm) coated with **a** a 0.12 mC cm^{-2} and **b** a 2.8 mC cm^{-2}thick POAP film, in the presence of different electrolytes: (*1*) 0.1 M $HClO_4$ + 0.4 M $NaClO_4$, (*2*) 0.1 M H_2SO_4 + 0.4 M Na_2SO_4 and (*3*) 0.4 M sodium benzenesulphonate + 0.1 M benzenesulphonic acid. Scan rate: $v = 10^{-2}$ V s^{-1} [39]

polymer film due to its interfacial exchange with the metal surface. However, the same resistance measurements employed to study gold films coated with thinner POAP films ($Q_{red} = 0.2$ mC cm^{-2}) (Fig. 2.25a), which could not be sufficiently compact at the gold-POAP interface to prevent the interaction of species proceeding from the external electrolyte with the gold film surface, show some anion adsorption effects on the gold surface. Then, author of Ref. [39] concludes that for thin POAP films resistance changes could reflect interfacial effects (metal-polymer interface) due to a competition between the adsorption of different species proceeding from the external electrolyte and the own redox transformation at the metal-polymer interface. It is possible that at very low POAP thickness (<0.15 mC cm^{-2}) either polymer islands (a continuous film is formed by fusion of these islands) or polymer layers with imperfections exist on the gold surface. However, the resistance response of a gold film electrode coated with a thick POAP film becomes unique and independent of the type of external electrolyte contacting the polymer. Under these conditions, a linear increase of ΔR as a function of the degree of oxidation θ_{ox} of the POAP film was also observed in Ref. [40]. This ΔR change of the gold film coated with POAP was expressed in Ref. [40] as

$$\Delta R = -3/8G(\rho_b l_0/d^2)\Delta p \tag{2.48}$$

where ρ_b and l_0 represent the bulk resistivity of the massive gold and the mean free path of the conduction electrons of gold, respectively, G is a geometrical constant given by the ratio length/with for a rectangular film of thickness, d and Δp is the change of the specularity parameter, p [40]. On the assumption that the decrease of the specularity parameter $(-\Delta p)$ of the gold film surface going from the reduced to the oxidized state of POAP is proportional to the degree of oxidation (θ_{ox}) of the polymer film deposited on it, $\Delta p = -k\theta_{ox}$, Eq. (2.48) was written as:

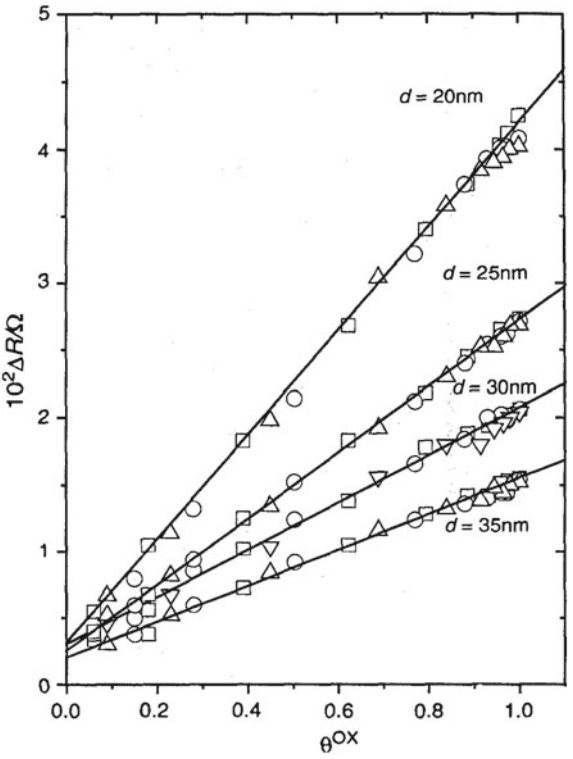

Fig. 2.26 ΔR versus θ^{Ox} dependences for different gold film thicknesses coated with the same POAP film. Film thickness, d, indicated on the figure. Different symbols represent different electrolytes: (O) 0.1 M $HClO_4$ + 0.4 M $NaClO_4$, (Δ) 0.1 M H_2SO_4 + 0.4 M Na_2SO_4 and (□) 0.4 M sodium benzenesulphonate + 0.1 M benzenesulphonic acid [39]

$$\Delta R = 3/8G(\rho_b l_0/d^2)k\theta_{ox} \tag{2.49}$$

Figure 2.26 shows $\Delta R - \theta_{ox}$ dependence for different film gold film thicknesses.

The observed linearity was explained in Ref. [40] in terms of an interfacial distribution of scatterers (imine sites) in the oxidized state with a spacing among them constant and larger than that corresponding to amine sites in the reduced state. In this connection, during POAP oxidation only one in every four or five amine sites are converted to the corresponding imine sites [32]. This gives rise to gaps which eventually would yield a distribution of oxidized sites less compact than the corresponding distribution of reduced ones. Another confirmation remarked by the author [39] about the different reflecting properties of the oxidized and reduced state of POAP is related to the different values of the site interaction parameters (r) obtained from the cathodic and anodic voltammetric responses of POAP in Ref. [1]. In this regard, the following values of anodic and cathodic site interaction parameters: $r_a = -0.55\ M^{-1}$ and $r_c = -0.18\ M^{-1}$, respectively, are reported in Ref. [1]. Both are negative, thus involving a repulsive energy of interaction. As a higher repulsion is observed between oxidized sites than reduced ones at POAP films, then a more extended configuration of oxidized sites should

be expected as compared with the corresponding distribution of reduced sites. Then, according to author of Ref. [40], it would also be expected that the distribution of oxidized sites reflects electrons more diffusely than the distribution of reduced sites.

A study about the distribution of redox sites of POAP as the solution *pH* increases employing CV and resistance measurements was carried out in Ref. [41]. The increasing difficulty in reduce the polymer from its oxidised state with increasing the *pH*, is shown in Fig. 2.27 and it was attributed to the fact that amine species become less protonated as the *pH* increases. The resistance response of the gold film coated with POAP is also affected as the solution *pH* increases (Fig. 2.28). Author of Ref. [41] also studied the ΔR versus θ_{ox} dependence as the solution *pH* is changed. However, the $\Delta R/R$ change was referred in Ref. [41] to the potential value $E = 0.5$ V, where POAP is assumed to be oxidised (imine groups not protonated) and the different *j–E* curves for the different *pH*s coincide (see Fig. 2.27). Consequently, starting at $E = 0.5$ V towards the negative potentials direction, that is, going from the oxidised to the reduced state of POAP, an attenuation in the $\Delta R/R$ response was observed with the increasing of the *pH* (Fig. 2.28) [41].

The resistance change going from the oxidised to the reduced state of POAP (Fig. 2.28) was correlated in [41] to the degree of reduction ω^{-1} of the polymer at each *pH* value. In this case, θ_{Red} was defined by the ratio $\theta_{Red} = Q_{Red}/Q_{T,Red}$. $Q_{T,Red}$ is the maximal voltammetric reduction charge, achieved at each *pH*. This is obtained by integration of the voltammetric current from $E = 0.5$ V to the lowest

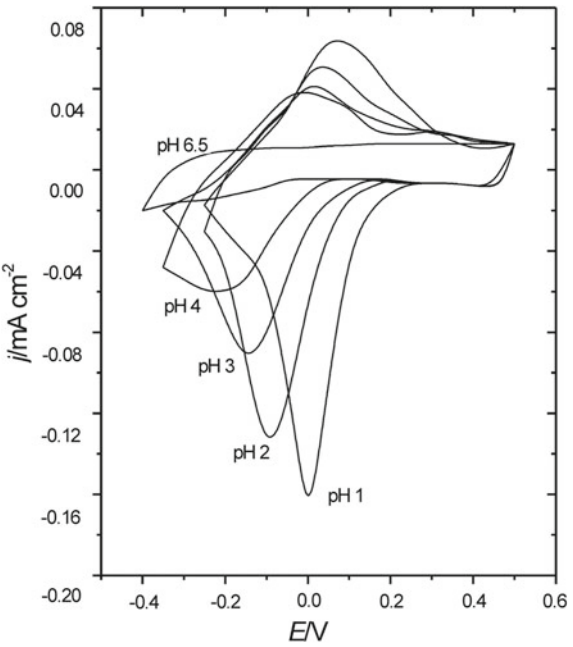

Fig. 2.27 *j* versus *E* responses for a gold film ($\phi_m = 30$ nm) coated with a 2.8 mC cm^{-2} thick POAP film contacting $HClO_4 + NaClO_4$ solutions of different *pH*'s. Constant ionic strength, *v pH* values indicated on the figure [41]

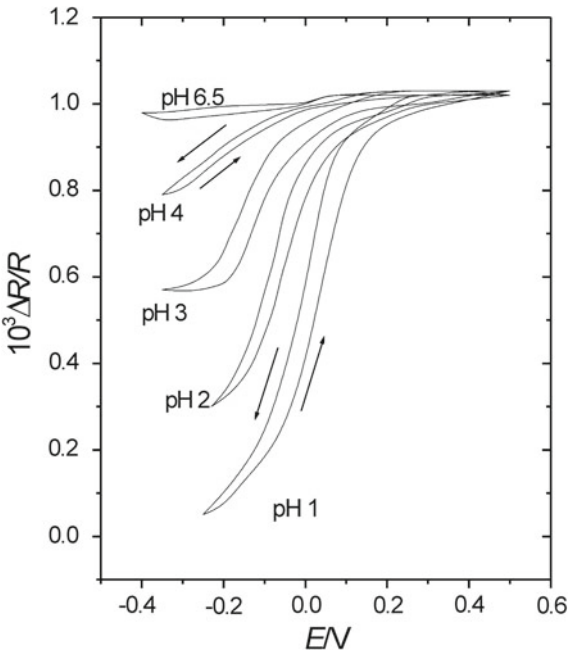

Fig. 2.28 $\Delta R/R$ versus E responses for the same POAP coated gold film and solutions indicated in Fig. 2.27 [41]

negative potential limit reached (see Fig. 2.27). Q_{Red} is the reduction charge at each E value, also assessed from $E = 0.5$ V toward the negative potential direction.

As can be seen from Fig. 2.27, $Q_{\text{T,Red}}$ decreases as the pH increases. It was assumed in Ref. [41] that at $pH = 1$ the polymer achieves its maximum degree of reduction ($\theta_{\text{Red}}^{\text{max}} = 1$ for $Q_{\text{T, Red}} = 2.8$ mC cm^{-2}), then, taking $Q_{\text{T, Red}} = 2.8$ mC cm^{-2} as the reference charge, lower $\theta_{\text{Red}}^{\text{max}}$ values are achieved with increasing the pH (Fig. 2.29). Thus, the $\theta_{\text{Red}} - E$ dependence (Fig. 2.29) was correlated with $\Delta R/R - E$ dependence (Fig. 2.28) going from the oxidised to the reduced state of POAP, at each pH value. This correlation leads to ΔR *vs.* θ_{red} dependences showed in Fig. 2.30. It is observed that the gold film resistance decreases nearly linearly during the POAP reduction. However, different slopes are observed depending on the solution pH.

Author of Ref. [41] considers as reference the $\Delta R/\theta_{\text{Red}}$ slope at pH 1, then, he remarks that as the higher is the solution pH the higher is the $\Delta R/\theta_{\text{Red}}$ slope. An explanation is given in Ref. [41] in relation to the change of the $\Delta R/\theta_{\text{Red}}$ slope with pH (Fig. 2.30). Author indicates that even when the reflection of conduction electrons on the gold film surface becomes more specular with increasing the degree of reduction of the polymer film at the different pH's, for a given θ_{Red} value (Fig. 2.30) the final reflection is more diffuse as pH increases. If only the amount of reduced sites decreases with increasing the pH, only one slope should be obtained. However, the effect of scattering centres on conduction electrons in

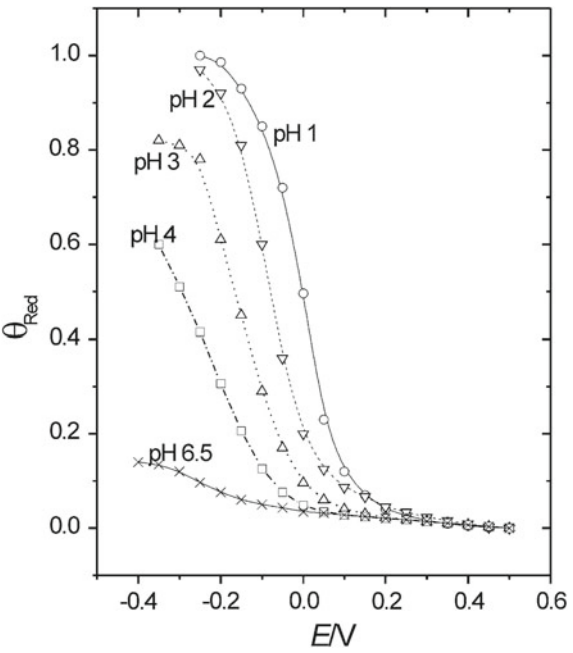

Fig. 2.29 θ_{red} versus E dependence for the same POAP coated gold film electrode and solutions indicated in Fig. 2.27. Different symbols correspond to different pH values [41]

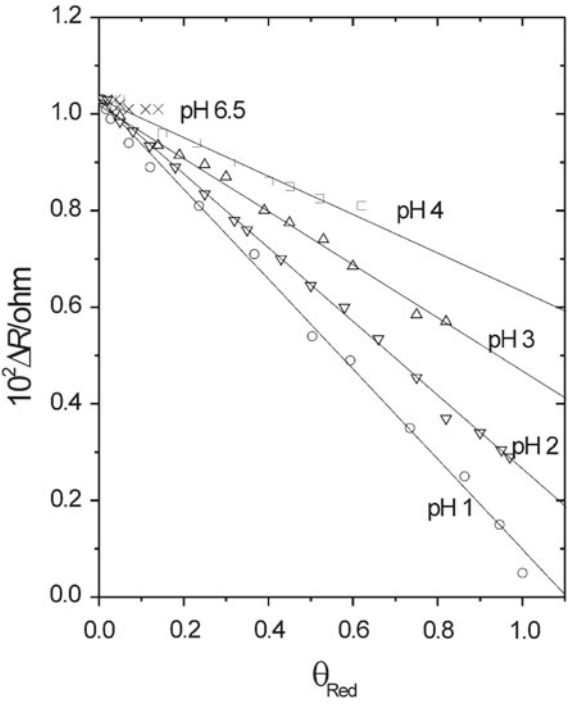

Fig. 2.30 ΔR *versus*. θ_{red} dependences for the same POAP coated gold film electrode and solutions indicated in Fig. 2.27. The same symbols as in Fig. 2.29

metal films is governed not only by the number of scatterers but also by its distribution over the metal surface [41]. In this sense, as mutual distances between scattering charges on a metal surface decreases towards the value corresponding to the wavelength of the conduction electrons of the metal ($\lambda_{Fermi} = 0.5$ nm in gold), the distribution of scatterers should reflect electrons more specularly [41]. Then, considering the increase of the slope in Fig. 2.30, it seems to be probable that as *pH* increases, the lower number of reduced sites at the polymer|metal interface forms surface distributions that scatter electrons more diffusely than that at *pH* 1. If the resulting surface structure of reduced sites at $pH > 1$ is thought as identical scatterers with a spacing that is equal to that at *pH* 1, again only one slope should be obtained. Then, the more immediate conclusion extracted by the author of Ref. [41] from resistance data at different *pH*'s is that the lower number of reduced sites formed as *pH* increases, also forms distributions with mutual distances between them that are larger as higher is the *pH* of the external solution. That is, reduced sites at the gold|POAP interface should form less compact distributions on the gold surface as *pH* increases, which reflect electrons not so specularly as the same amount of reduced sites at *pH* 1, does. According to author of Ref. [41], this effect could be attributed to a low degree of swelling of a polymer at high *pH* values. At high *pH* values the ability of the inner solution (incorporated into the polymer matrix) to reduce the electrostatic repulsion of the charged sites is limited. Under these conditions redox sites would adopt an extended configuration so as to minimise the coulombic repulsions.

2.2.3 *Effects of the Type and Concentration of Ions of the External Solution on the Charge-Transport Process at POAP Films*

Effects of the type and concentration of ions of the supporting electrolyte on the electrochemical response of POAP films were studied in several papers [1, 11, 18, 31, 42]. Some voltammetric experiments were performed in Ref. [1] by varying the ClO_4^- concentration between 0.1 and 1.7 M. While the anodic peak was not affected, the cathodic peak showed a positive variation. In this sense, a high concentration of perchlorate produces the same effect as a high proton concentration, making POAP more easily reducible. However, no noticeable changes were observed for anions such as SO_4^{2-}, PO_4^{3-} and Cl^- or cations such as Li^+, K^+ and Cs^+.

The participation of the supporting electrolyte anions in charge-transfer processes through POAP films was studied in $LiClO_4$ and $HClO_4$ solutions at different *pH* values and constant ionic strength (1 M) by employing CV and EQCM [11]. CV experiments with POAP-modified electrodes uncovered and covered with Nafion thin films were performed [11]. Nafion is known to hinder anionic permeability due to its own negative charge, so the films covered with this material

should significantly change their electrical properties, as compared to the uncovered ones, when supporting electrolyte anions participate in the redox activity of the films. No significant effect of Nafion on the redox response of POAP was observed. This finding allowed the authors [11] to conclude that no perchlorate anions are involved in the redox reactions of POAP. In order to confirm this conclusion, EQCM measurements on POAP films were carried out in Ref. [11]. The microbalance frequency change Δf_{cm} in the presence of the POAP films was measured simultaneously with their current responses under the electrode potential cycling. The $\Delta m/\Delta Q(E)$ ratio, where $\Delta m = \Delta f_{cm}/k$ (k is the constant of the Sauerbrey law) and $\Delta Q(E)$ is the charge consumed during the oxidation/reduction process, gave a mass number of about 3–5 in the main range of the cycling potential of 0.0–0.3 V (vs. Ag/AgCl). This mass number was considered very low, as compared with the molecular weight of ClO_4^- anion. Then, it was concluded that an insignificant insertion of the anions into the POAP films occurs during the redox reaction of the polymer.

The ionic exchange of POAP in the presence of perchlorate anions was studied by using Probe Bean Deflection (PBD) [31]. During the reduction scan only a positive deflection of the PBD signal was observed, which was indicative of a simultaneous expulsion of perchlorate and insertion of protons, the latter process being dominant. To check this conclusion, a PBD profile was simulated by convolution of the current response using parameters reported in the literature [43] and considering that only protons are exchanged between the solution and POAP. The simulated profile fits reasonably well the negative scan but differs significantly in the positive direction, suggesting that not only protons but also perchlorate anions are exchanged during the positive scan.

The effect of the ionic strength (μ) of the solution on the transport properties of POAP was studied employing EIE [18]. To this end 0.1 M $HClO_4$ + x M $NaClO_4$ solutions were employed, where the concentration of perchlorate anions, x, was varied in order to change the ionic strength.

Experimental complex impedance plots of POAP at constant potential and different ionic strengths were recorded (Figs. 2.31 and 2.32). It was observed that when POAP is in its oxidised state, impedance diagrams depend strongly on the electrolyte concentration (Fig. 2.31). However, when POAP is in its reduced state ($E = -0.1$ V vs. SCE), the impedance response does not exhibit a significant dependence on the bathing electrolyte concentration (Fig. 2.32).

Dependences of the characteristic impedance quantities, at low frequency, on μ were interpreted on the basis of two models: a transmission line model [19, 20] and a modified electron-hopping model [21]. From the former model it was possible to separately extract an electron (D_e) and an anion (D_x) diffusion coefficient. From the latter [21] only an effective diffusion coefficient, D_{eff}, was obtained. It was observed that the low-frequency capacitance C_{LF} does not depend much on the ionic strength (Fig. 2.13a). However, the low-frequency resistance, R_{LF}, depends markedly on μ at constant E value, for potential values higher than 0.0 V (SEC) (Fig. 2.13b). R_{LF} versus E curves pass through a minimum value, which depends on the electrolyte concentration. The fitting of experimental low-frequency

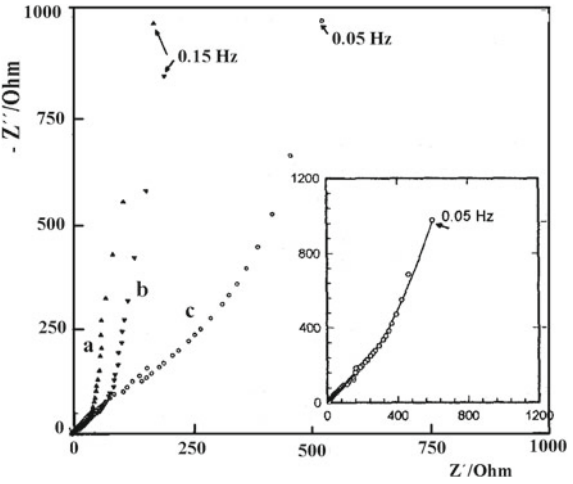

Fig. 2.31 Complex impedance plots for a 30 nm thick POAP film at $E = 0.1$ V (SCE) in 0.1 M $HClO_4$ + x M $NaClO_4$ solutions: (a) $x = 1.9$ M, ionic strength, $\mu = 2$ M; (b) $x = 0.4$ M, ionic strength, $\mu = 0.5$ M; (c) $x = 0$ M, ionic strength, $\mu = 0.1$ M. The inset is a comparison of the experimental (o) and calculated (—) points employing the model of the electron hopping reported in [18]

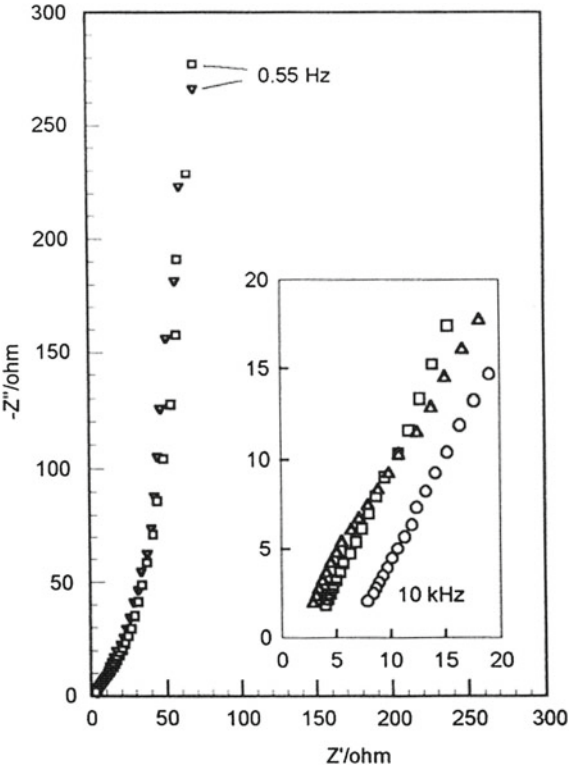

Fig. 2.32 Complex impedance plots for a 30 nm thick POAP film at $E = -0.1$ V (SCE) in 0.1 M $HClO_4$ + x M $NaClO_4$ solutions: (□) $x = 0.4$ M, ionic strength, $\mu = 0.5$ M; (Δ) $x = 0.9$ M, ionic strength, $\mu = 2$ M. The inset is a magnification of the low-frequency region [18]

resistance expressed as $R_\Sigma (= 3R_{LF})$ as a function of the degree of oxidation (θ_{ox}) by employing the transmission line model (Fig. 2.14), allowed the authors [18] to obtain D_e and D_x versus θ_{ox} dependences for different μ values. Also, application of the electron-hopping model described in Ref. [21] allowed the authors to obtain the (κ_e) dependence for different μ values (Fig. 2.15). Diffusion coefficient values for different ionic strengths obtained in Ref. [18] are shown in Table 2.5. Several explanations have been given to account for the dependence of the transport process at POAP films on external electrolyte concentration [18]. It has been suggested that an excess of supporting electrolyte can be incorporated into the polymer phase during the redox process. If the incorporated ions act as counterions, an increase in their concentrations within the film would cause a decrease in the resistance of charge transport through it or an equivalent increase in the diffusion coefficient. Another explanation invokes reduction of the electrostatic repulsion between redox centres as the electrolyte concentration increases, which allows a sufficiently facile ion transport. Another study about the effects of the electrolyte concentration and degree of oxidation on the conduction properties of POAP films by employing EIS is reported in Ref. [42].

The participation of different anions in the charge-transport process of POAP films was studied by employing fractal dimensions [44]. Fractal dimensions of POAP films doped with different anions were determined using CV and EIS experiments. The formalism developed by Stromme et al. [45] was employed in Ref. [44] to obtain the fractal dimensions. According to this formalism, α (called fractal parameter) is related to the fractal dimension, D_f, through Eq. (2.50):

$$\alpha = (D_f - 1)/2 \tag{2.50}$$

POAP films were deposited on glassy carbon in acidic media and in the presence of different anions. The film thickness was measured by assessing the voltammetric charge. Film thicknesses around 0.1 μm were employed in Ref. [44]. Voltammetric responses of POAP in the presence of different anions used in Ref. [44] are shown in Fig. 2.33. Correlations between the size of the anions, the length scales and the yardstick for scaling of the fractal surfaces with the fractal dimensions of the surfaces, were found in Ref. [44]. The fractal dimensions of the films in the presence different anions, ClO_4^-, SO_4^{2-}, NO_3^- and Cl^-, were 2.46, 2.46, 2.46 and 2.32, respectively. The fractal dimension in the presence of chloride

Table 2.5 Electronic D_e and ionic D_x, diffusion coefficients calculated from the transmission line model [19, 20] for a 30 nm thick POAP film at different ionic strengths. D_{eff} extracted from the model given in Ref. [21]. $pH = 1$, $c = 4.5$ M, $A = 0.081$ cm^2, $E = 0.1$ V, $p/(1+p) = 0.96$ [18] (*see* Eq. (2.28))

μ (Ionic strenght)/M	$10^{10}\ D_{eff}$/cm^2 s^{-1}	$10^{10}\ D_e$/cm^2 s^{-1}	$10^8\ D_x$/cm^2 s^{-1}
0.1	1.32	1.03[a] 1.2[b]	1.27
0.5	1.92	1.67[a] 2.20[b]	1.83
2	2.93	3.14[a] 3.18[b]	2.42

[a] Values extracted from the R_Σ versus θ_{ox} dependence

[b] Values extracted from the C_Σ^{-1} versus Ψ dependence

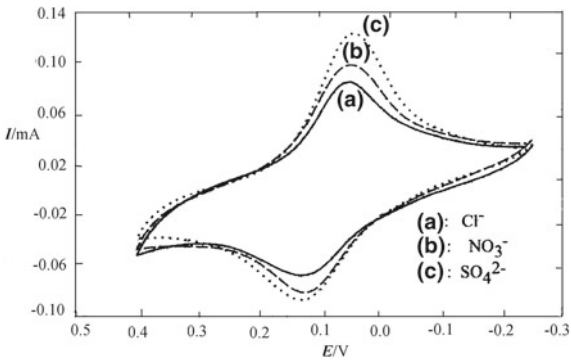

Fig. 2.33 Cyclic voltammograms of POAP films in the presence of different anions. *The inset* presents the voltammetric responses recorded at the indicated sweep rates for a POAP film in the presence of NO_3^- anions [44]

differs from the others. In order to shed light on the physical significance of the fractal dimension values, diffusion layer widths were employed as a yardstick to estimate the length scales traversed by anions on the surface at the condition of the maximum currents.

As according to the Fick's first law, the diffusion-limited current is proportional to the magnitude of the concentration gradient of the electroactive species, then, the width of the diffusion layer, ΔX, was expressed as:

$$\Delta X = z\,FAD\,C_b/i_{peak} \tag{2.51}$$

where C_b is the difference between bulk concentration of the anions inside the polymeric film and that of its surface at time τ (where the voltammetric peak current is reached). The diffusion coefficient value, D, was estimated using the Randles–Sevcik equation [2]. The width of the diffusion layer and the diffusion coefficient of selected anions are shown in Table 2.6. It was concluded from the results summarized in Table 2.6 that the distance sensed in the presence of different anion varies on the 11.7–2.98 Å range, and the possible cutoff of the fractal region investigated by employing the peak current method occurs at the length scales larger than 11.7 Å.

The fractal dimension of POAP was also obtained in [44] from EIE measurements. The impedance response of POAP films doped with different anions was obtained. An equivalent circuit compatible with the experimental impedance response was employed in [44]. The following Z versus ω dependence was used:

$$Z(\omega) \;= R + B(j\omega)^{-n} \tag{2.52}$$

The expression (2.52) corresponds to the electrical characteristics of a so called constant phase element (CPE) with $n < 1$ and B is a constant related to the capacitive nature of the interface. From the impedance response and equivalent circuits, the fractal dimensions were derived by using the Eq. (2.53):

$$D_f = \;(n+1)/n \tag{2.53}$$

Table 2.6 Diffusion coefficients and diffusion layer thickness for different anions [44]

Anion	$10^{13}\ D_a/cm^2\ s^{-1}$	$10^{13}\ D_b/cm^2\ s^{-1}$	[a]Diffusion layer thickness	[b]Diffusion layer thickness
SO_4^{2-}	2.4	8.1	3.18	2.98
ClO_4^-	6.5	7.4	10.70	3.02
NO_3^-	6.8	8.0	11.32	3.05
Cl^-	5.8	6.6	11.72	3.90

[a] Slow scan
[b] Fast scan

The D_f values obtained were 2.45, 2.43, 2.41 and 2.33, for ClO_4^-, SO_4^{2-}, NO_3^- and Cl^-, respectively. To determine the length scales used in the fractal scaling, Eq.(2.54), relating the electrode capacitance C_0, film resistance R and the frequency f of measurement, to the length scale λ, was employed:

$$\lambda = 1/(2\pi f C_0 R) \tag{2.54}$$

The capacitance C_0 at the frequency of f was obtained from C versus log f plots. Results are shown in Table 2.7. As can be seen from Table 2.7, the length scale in the 1.43–7.3 Å range was found. There is a partial overlap of the results obtained by employing both CV and EIE measurements. The smaller fractal dimension in the presence of chloride was attributed to its smaller size and has the consequence of providing larger yardstick for scaling of the surface.

The doping process of electrodeposited POAP films with different anions under the regime of CV was analyzed by the application of "Chaotic Logistic Map" [46]. Quadratic logistic map presentations of the current density versus charge for POAP films doped with different anions and under both, negative and positive potential scans were analyzed in Ref. [46]. The electrochemical data were fitted to a quadratic logistic map of the type [47, 48]:

$$x_{n+1} = r\,x_n(1 - x_n) \quad 0 < r < 4 \tag{2.55}$$

Eq. (2.55) describes the effect of feedback on the magnitude of some property x, as well as the effect of the parameter r that determine the occurrence of oscilatory and chaotic nature of the result. The magnitude x_n behaves chaotically for $3.45 < r < 4$, while for $3 < r < 3.45$, x_n gradually approaches a periodic motion of period 2. Only partial fittings were observed [46], then, authors conclude that the system is more complicated than a simple non-linear system with a feedback to

Table 2.7 Length scales and cutoff frequency region for the different anions [44]

Anion	Length scale/A	Frequency cutoff region
SO_4^{2-}	1.4–5.3	50 kHz–100 Hz
ClO_4^-	1.6–5.8	10 kHz–30 Hz
NO_3^-	1.8–6.1	100 kHz–1 Hz
Cl^-	2.3–7.3	1 kHz–100 Hz

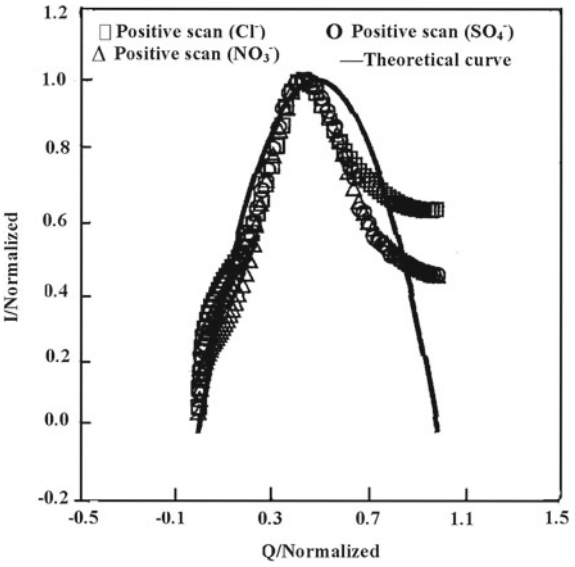

Fig. 2.34 *I* (Current density) versus *Q* (Voltammetric charge). The goodness of fit to the logistic map during positive potential cycles of POAP in the presence of different anions: (□) Cl^-, (o) NO_3^-, (Δ) SO_4^{2-}, (—) theoretical plot [46]

withstand a perfect fit to the quadratic logistic equation in the entire domain of *x*. Thus, other contributions, such as charge/discharge of the double layer capacitance (in general, any intervening phenomena other than the flux generated by diffusion), were considered as factors that complicate the behaviour of the doping process and cause deviation from a perfect fit.

A better fit was observed for the positive potential sweep, where participation of anions is the main phenomenon. However, it was observed that the increase of the positive potential sweep rate is accompanied by a decrease in anion-insertion in the polymer matrix (anion-insertion/movement cannot respond quickly enough to the increasing field). Thus, the doping process is no longer a dissipative one and a feedback-controlled phenomenon appears which is observed in the form of a more poor fit to the logistic map (Fig. 2.34). Furthermore, it was observed that the chloride/POAP system exhibits the least satisfactory fit. This fact was attributed to topological structural differences between a film doped with Cl^- and other one doped with other anions, as revealed by the differences of their fractal dimensions [44]. It is indicated that the Cl^- doped film possesses a self affine structure with less available regions in the film capable of participate in the transport process. Then, the dissipative processes occur less favourably in Cl^--doped films which cause the breakdown of the applicability of the logistic equation and a poorer fit, especially in the region of higher charges.

2.2.4 *Effect of the Film Thickness on the Charge Conduction Process of POAP*

While in some papers it is reported that only thin POAP films could be electrochemically synthesised [11, 13, 18, 21], in other ones thick films were manufactured [15]. POAP films synthesized in Ref. [11], for instance, did not exceed 50 nm due to the self-limiting effect caused by the low polymer film conductivity. Film thicknesses in the range 0.05–0.5 μm were examined in Ref. [15]. Also, while in some studies voltammetric charge values were employed for POAP film thickness estimation [11, 49], in other ones the ellipsometric thickness was considered [18].

Surface resistance was applied [49, 50] to study the interaction of different anions, such as perchlorate, sulphate and benzene sulphonate, and also a cation such as Cu(II), with a gold film surface when it is blocked with a POAP film. The dependence of the resistance change on the external electrolyte composition for POAP thickness lower than 0.25 mC cm^{-2} was attributed to a competition at the gold film surface, between the proper redox process of the polymer and the adsorption of the different species contained in the electrolyte solution on the gold surface. This result points to a discontinuous character of POAP for thicknesses lower than 0.25 mC cm^{-2}. For POAP thicknesses higher than 0.8 mC cm^{-2} the resistance response becomes independent of both the film thickness and electrolyte composition. This result is indicative of the presence of a compact polymer layer at film thicknesses higher than 0.8 mC cm^{-2}.

POAP films synthesized on ITO (In–Sn oxide conducting glass) electrodes seem to be continuous and have a fairly smooth surface and the thickness is almost uniform over the whole film [22]. Scanning electron micrographs of the POAP film surface revealed non-specific amorphous surface features. Morphology of POAP seems to be granular rather fibrous. The size of the nodules resulted about 0.1 μm. Plots of film thickness (d) and surface concentration of electroactive sites (Γ) versus the amount of charge (Q) passed to prepare the POAP films are shown in Figs. 2.35 and 2.36, respectively [22].

The film thickness, d, increases with increasing Q in the same way as the relation between Γ and Q does. The volume concentration of electroactive sites in the POAP films, with different thicknesses, was estimated as (Γ/d) from Γ and d given at a constant Q value [22]. The obtained volume concentration of electroactive sites value was $(5.0 \pm 0.5) \times 10^{-3}$ mol cm^{-3} irrespective of d. This result was indicative of a uniform distribution of electroactive sites in the films of different d values. Results reported in Ref. [22] indicate that POAP film thickness can be arbitrarily controlled by the charge passed during the film synthesis.

The effect of the film thickness on the POAP charge-transport process was treated in several papers [13, 15, 18]. EIS was employed in Ref. [13] to obtain transport parameters of thin POAP film electrodes. Impedance measurements were performed in the frequency range 0.01–10 kHz and at two different film

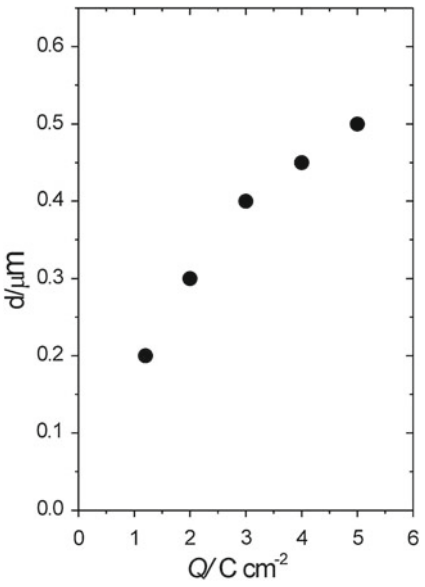

Fig. 2.35 Film thickness (d) versus the charge (Q) passed during the electrode potential scan [22]

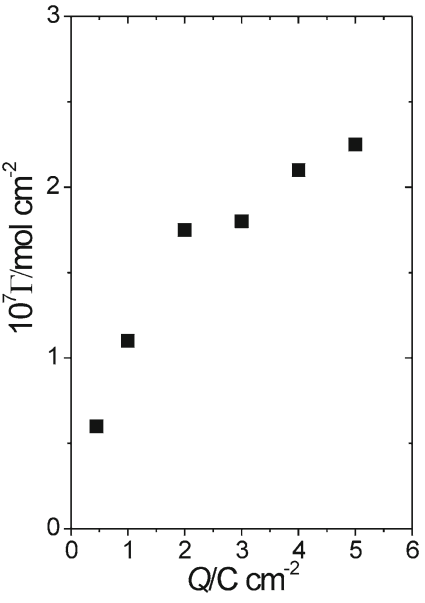

Fig. 2.36 Surface concentration (Γ) of electroactive sites in the film versus the charge (Q) passed during the electrode potential scan [22]

thicknesses ($d = 30$ and 300 nm). Nyquist diagrams at high frequency exhibit a depressed semicircle (Fig. 2.37) [13].

It was observed that the change of the film thickness does not affect the size of the semicircle. This fact was considered as indicative of the existence of an

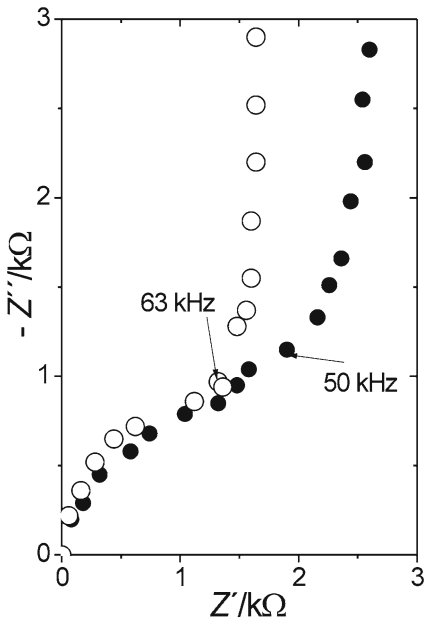

Fig. 2.37 Nyquist diagrams for POAP at different thickness: (O) 30 nm, (●) $d = 300$ nm. $E = 0.375$ V [13]

interfacial charge-transfer process at the metal|polymer interface (see Eq. (2.14) and Fig. 2.5). However, the pseudo-capacitive rise of Z'' at low frequencies occurs at larger Z' values for thicker films (Fig. 2.37). This effect means that the film resistance at low frequencies depends on the film thickness, d (see Eq. (2.15) and Fig. 2.7). The redox capacity was obtained from $-Z''$ *versus* ω^{-1} plots at sufficiently low frequencies. Despite the redox capacity increases with d, the dependence was not linear (Fig. 2.6). The low-frequency capacity for thick POAP films (0.05–0.5 μm), at a given potential and *pH*, was also found to be proportional to the film thickness [15].

Dependences of different characteristic impedance quantities on film thickness were also studied in Ref. [18]. Results were interpreted on the basis of two models, a modified electron-hopping model [21] and a transmission line one [19, 20]. While the former only allowed the authors [18] to obtain an effective diffusion coefficient, D_{eff}, the latter allowed the authors to obtain electron (D_{e}) and ion (D_{x}) diffusion coefficient values for different film thickness.

Table 2.8 shows the dependences of the respective diffusion coefficients on film thickness for POAP. The low conductivity of thin POAP films was explained in Ref. [18] in terms of a structure that changes as the film thickness increases. In this connection, during the synthesis of a polymer film, two or more stages of the polymerisation process have been distinguished: first, islands of the polymer are formed at the substrate surface, then a continuous film, compact (non-porous), is formed by fusion of these islands, and then, further growth takes place above this compact layer giving rise to the external, porous part of the film. In this regard, a

Table 2.8 Electronic D_e and ionic D_x, diffusion coefficients calculated from the transmission line model [19, 20] for different film thickness (ϕ). D_{eff} extracted from the model given in [21]. $\mu = 2$ M ($pH = 1$), $c = 4.5$ M, $A = 0.081$ cm^2, $E = 0.1$ V, $p/(1+p) = 0.96$ [18]

ϕ (thickness)/nm	10^{10} D_{eff}/cm^2 s^{-1}	10^{10} D_e/cm^2 s^{-1}	10^8 D_x/cm^2 s^{-1}
10	0.163	0.17	0.22
30	2.93	3.14	2.42
60	24.3	27.7	23.2

high permeability of thick films, as compared with thin ones, should allow the incorporation of electrolyte solution into the polymer matrix. Electrolyte incorporated into the film should affect the polymer conduction, increasing the rate of the charge-transport process.

2.3 The Charge Transport Process at Poly(o-aminophenol) (POAP) Film Electrodes in the Presence of Redox Active Solutions

The conduction properties of electroactive polymer films are often tested by analysing the electrochemical behaviour of the films contacting different redox active solutions. To this end, techniques such as CV, Rotating Disc Electrode Voltammetry and EIS have been employed. Redox mediation and redox solute permeabilities at film-coated rotated-disc electrodes are determined from the variations of limiting currents with the electrode rotation rate, film thickness and redox couple concentration. Complete mechanism diagnosis criteria from steady-state polarisation curves for redox mediation at electroactive polymers coated electrodes are discussed in Ref. [51]. Authors of Ref. [51], also present a review [52] about the theoretical basis for the electrochemical rectification in mediated redox reactions at redox polymer-modified electrodes.

Steady-state current–potential curves for the oxidation of $Fe(CN)_6^{4-}$ at bare and POAP film-coated rotating BPG (Basal-plane Pyrolytic Graphite) disk electrodes were compared in Ref. [12]. The comparison of the formal redox potential ($E^{0\prime}$) values of POAP (0.044 V vs. SSCE) with that of $FE(CN)_6^{4-/-3}$ couple (0.350 V vs. SSCE) in a 0.2 M $NaClO_4$ aqueous solution (pH 1) indicates that the oxidation of $Fe(CN)_6^{4-}$ is not thermodynamically mediated by POAP films. Then, the observed anodic currents in the presence of POAP were assigned to the oxidation of $Fe(CN)_6^{4-}$ ions that penetrate the POAP film to reach the electrode surface [12]. The quantitative analysis of the experiments reported in Ref. [12], were made employing the Koutecky–Levich equation [2]:

$$i_{lim}^{-1} = i_{Lev}^{-1} + i_s^{-1} \tag{2.56}$$

with

$$i_{\mathrm{Lev}} = 0.62nFAD_{\mathrm{sol}}^{2/3}v^{-1/6}C^{b}\Omega^{0.5} \tag{2.57}$$

$$i_{\mathrm{s}} = nFAC^{\mathrm{b}}D_{\mathrm{s}}\kappa\phi^{-1} \tag{2.58}$$

where i_{lim} is the limiting current, i_{Lev} is the Levich current, i_{s} is the "permeation current" of $Fe(CN)_6^{4-}$ through the POAP film, D_{sol} is the diffusion coefficient of $Fe(CN)_6^{4-}$ in the bulk solution, D_{s} is the diffusion coefficient of $Fe(CN)_6^{4-}$ into the POAP films, v is the kinematic viscosity of the solution, C^{b} is the bulk concentration of $Fe(CN)_6^{4-}$, κ is the partition coefficient of $Fe(CN)_6^{4-}$ between the film and the bulk of the solution and Ω is the rotation rate of the disk electrode. Experimental Koutecky–Levich plots i_{lim}^{-1} versus $\Omega^{-1/2}$ resulted linear, as expected from Eq. (2.56), and the slopes matched that at the bare electrode. Thus, D_{sol} and D_{s} were estimated: $D_{\mathrm{sol}} = (6.7 \pm 0.4) \times 10^{-6}$ cm^2 s^{-1} and $D_{\mathrm{s}}\kappa = (1.2 \pm 0.3) \times 10^{-9}$ cm^2 s^{-1}. It is remarked in [12] that for POAP, $D_{\mathrm{s}}\kappa > D_{\mathrm{app}}$ (see Table 2.2), that is, the overall charge-transport within the film is slower than the physical diffusion rate of a dissolved ion ($Fe(CN)_6^{4-}$) through the film.

Another study employing CV and RDEV about the electrochemistry of POAP-modified electrodes in the presence of different redox couples ($Fe(CN)_6^{4-/3-}$, hydroquinone/benzoquinone (HQ/Q), Sn^{2+}) was carried out in Ref. [53]. Different POAP film thicknesses between 10 and 70 nm were employed in Ref. [53] to study the diffusion process of electroactive species across POAP films. The diffusion process of the electroactive species through POAP was interpreted on the basis of the membrane-diffusion theory [54]. The electron hopping model was also employed in order to obtain the diffusion constant for the electron transport [4]. The effects of the electrode rotation rate (Ω) film thickness (ϕ), charge and concentration (c) of the electroactive species and acid concentration (x) of the solution, on the steady-state current–potential curves (I–E), were quantitatively analyzed in Ref. [53].

Steady-state current–potential (I–E) curves, at different Ω values, for a 60 nm thick POAP film contacting a x M $HClO_4$ + $(2 - x)$ M $NaClO_4$ + c (HQ/Q) solution where $x = 0.1$ and $c = 3 \times 10^{-3}$ M are shown in Fig. 2.38 [53]. Diffusion limited currents are observed at $E > 0.8$ V (vs. SCE) for HQ oxidation and at $E < 0.0$ V (vs. SCE) for the Q reduction. Besides, these main anodic and cathodic plateaux, the presence of a pre-plateau ($0.2\ \mathrm{V} < E < 0.4$ V) during Q reduction was also observed. At Ω and c fixed, I–E curves are film thickness (Fig. 2.39) and acid concentration (Fig. 2.40) dependent [53]. As HQ oxidation is not thermodynamically mediated on POAP, then, the observed anodic currents (Fig. 2.38) were assigned to the oxidation of HQ species that penetrate through the POAP films to reach the gold surface.

Benzoquinone (Q) is reduced in two waves (Fig. 2.38). The first one was attributed to the penetration of reactants into the film coupled with their subsequent discharge at the metal/polymer interface. The limiting current for the second wave ($E < 0.0$ V) is independent of ϕ and follows the Levich equation. This second wave was adjudicated to the rapid electron-transfer mediation at the POAP/redox active solution interface. Similar experiments were carried out in Ref.

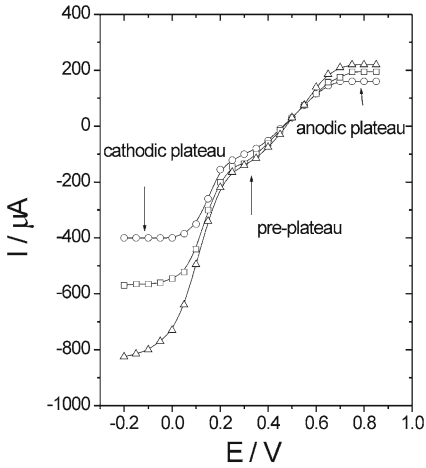

Fig. 2.38 *I–E* curves for different Ω values: $\Omega = 500$ (o), 1500 (□) and 3650 (Δ) rpm. $\phi = 60$ nm. Electrolyte: 0.1 M $HClO_4$ + 1.9 M $NaClO_4$ + 3 × 10^{-3} M (HQ/Q) [53]

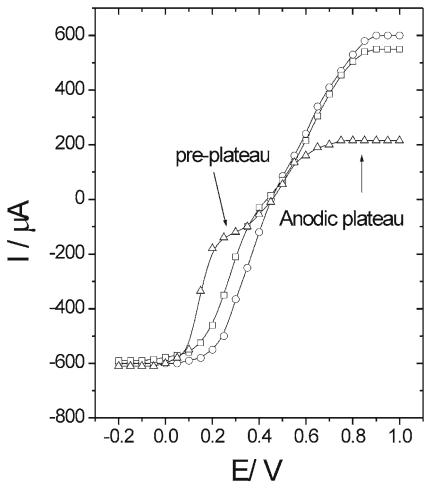

Fig. 2.39 *I–E* curves for different ϕ values: $\phi = 0$ (o), 13.7 (□) and 60 (Δ) nm. $\Omega = 1800$ rpm. Electrolyte: 0.1 M $HClO_4$ + 1.9 M $NaClO_4$ + 3 × 10^{-3} M (HQ/Q) [53]

[53] with POAP films contacting anionic $Fe(CN)_6^{4-/3-}$ and cationic Sn^{2+} redox active species. The permeation characteristics of POAP films at potential values $E > 0.8$ V (vs. SCE) were evaluated employing Eq. (2.59):

$$I_{\text{lim}}^{-1} = \phi(nFA\kappa D_s c)^{-1} + (0.62nFA\, D^{2/3} v^{-1/6} \Omega^{1/2} c)^{-1} \qquad (2.59)$$

In order to use Eq. (2.59) it was assumed that electroactive species dissolves into the polymer film with a partition equilibrium $\kappa = c_{\text{pol}}/c$ at the film/solution interface where c_{pol} and c are the respective concentrations of the species in the polymer and solution. D_s and D are the diffusion coefficients of the electroactive species in the polymer and solution, respectively. I_{lim} is the limiting current for the oxidation of electroactive species and the other terms have their usual meanings.

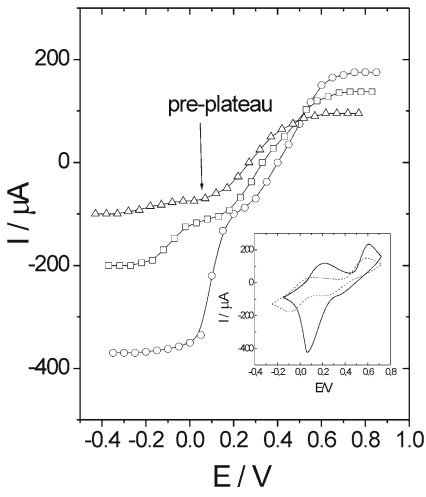

Fig. 2.40 *I–E* curves obtained in different x M $HClO_4 + (2 - x)$ M $NaClO_4 + 3 \times 10^{-3}$ M (HQ/Q) solutions. $x = 0.1$ (o), 0.01(□) and 0.001 (Δ). Electrode rotation rate: $\Omega = 800$ rpm. $\phi = 60$ nm. *Inset* cyclic voltammograms [53]

At constant c, x and ionic strength of the solutions, experimental I_{lim}^{-1} versus $\Omega^{-1/2}$ representations for different film thickness, give linear diagrams with nearly the same slope but different intercepts on the ordinate axis (Fig. 2.41) [53]. Thus, for the different oxidation processes studied in Ref. [53] and the Q reduction (first wave), κD_s values were extracted from the first term of Eq. (2.59). With regard to the film thickness, κD_s decreases as ϕ increases for the oxidation process of HQ.

The same behaviour was observed for the Q reduction (first wave) and oxidation of Sn^{2+} and $Fe(CN)_6^{4-}$ species at POAP films [53]. However, it was observed in Ref. [53] that in all cases, for film thickness higher than 60 nm, κD_s becomes independent of ϕ. Thus, extrapolated κD_s values for high film thickness

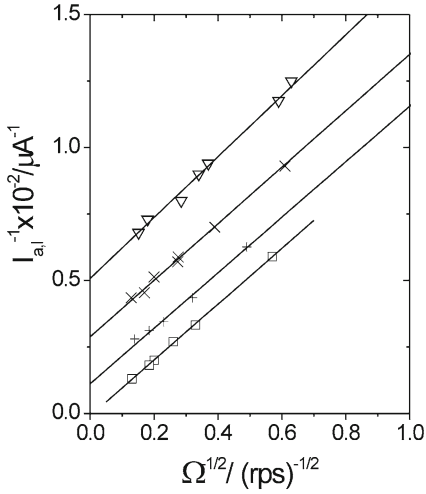

Fig. 2.41 Koutecky–Levich plots for different ϕ values: $\phi = 8$ (□), 41 (+), 60 (×) and 69 (Δ) nm. Electrolyte: a 0.1 M $HClO_4$ +1.9 M $NaClO_4 + 3 \times 10^{-3}$ M (HQ/Q) solution [53]

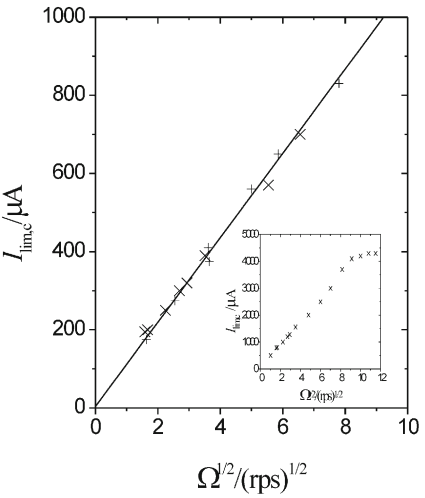

Fig. 2.42 Levich representations for the cathodic plateau $E < 0.0$ V. $\phi = 41$ nm(+) and 60 nm (X). Electrolyte: a 0.1 M $HClO_4$ + 1.9 M $NaClO_4$ + 3×10^{-3} M (HQ/Q) solution. *Inset* $I_{lim,c}$ versus $\Omega^{1/2}$ for a 60 thick POAP film [53]

were considered as true permeation rates for the different species studied [53]. The resultant extrapolated values were: $\kappa D_s(\mathrm{HQ}) = (0.92 \pm 0.2) \times 10^{-8}\,\mathrm{cm^2\,s^{-1}}$, $\kappa D_s(\mathrm{Fe(CN)_6^{4-}}) = (0.62 \pm 0.2) \times 10^{-9}\,\mathrm{cm^2\,s^{-1}}$ and $\kappa D_s(\mathrm{Sn^{2+}}) = (1.42 \pm 0.2) \times 10^{-10}\,\mathrm{cm^2\,s^{-1}}$ for the oxidation processes and $\kappa D_s(\mathrm{Q}) = (0.42 \pm 0.2) \times 10^{-8}\,\mathrm{cm^2\,s^{-1}}$ for the Q reduction.

A comparison of redox solutes permeabilities at POAP films with transport rate of electroinactive anions, such as perchlorate, was also made in Ref. [53]. It was observed that the electroinactive ions transport process within the POAP film is faster than the physical diffusion process of a dissolved electroactive species through the film. In the presence of HQ/Q species, the limiting current at $E < 0.0$ V depends linearly on $\Omega^{1/2}$ (Fig. 2.42). This wave was associated with the electron-transfer mediation at the POAP/solution interface where Q diffusion in solution limits the current [53]. However, it was observed in Ref. [53] that for thick POAP films contacting solutions of high concentration of HQ/Q ($c > 0.01$ mol $\mathrm{dm^{-3}}$), the limiting current at $E < 0.0$ V was independent of the electrode rotation rate for $\Omega > 7000$ rpm (see inset in Fig. 2.42).

Such a constant value of the current was attributed to a slow electron transport across the POAP film to mediate in the electron-transfer reaction at the polymer/solution interface. The limiting current at which $I_{lim,\,c}$ ($=I_e$) was independent of Ω, was considered as a representation of the maximum flux of redox species confined in the polymer. This fact was interpreted on the basis of Eq. (2.60) [53]:

$$I_e = nFAD_e c^*/\phi \tag{2.60}$$

where c^* is the concentration of redox species of the polymer and D_e represents a measure of the electron hopping rate. The n value expresses the number (fractions) of unit charges per monomer unit of the polymer. Equation (2.60) was employed in Ref. [53] to estimate the electron diffusion coefficient, D_e. The obtained value

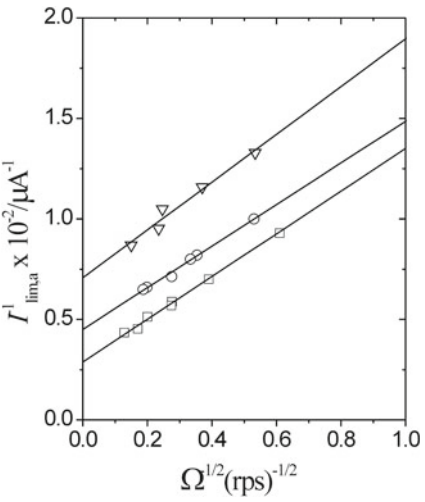

Fig. 2.43 Koutecky–Levich plots for different acid concentrations: x M $HClO_4 + (2 - x)$ M $NaClO_4 + 3 \times 10^{-3}$ M (HQ/Q) solutions, $x = 0.1$ (□), 0.01(o) and 0.001 (▽). $\phi = 60$ nm [53]

was $D_e = 2.4 \times 10^{-10}$ cm^2 s^{-1}. The effect of the acid concentration on the charge transport process of POAP films was also analyzed in Ref. [53].

Figure 2.43 shows that at c and ϕ fixed, experimental I_{lim}^{-1} versus $\Omega^{-1/2}$ dependences for HQ oxidation are linear plots with different intercepts at $\Omega \to \infty$ dependent on the acid concentration (x) in solution. The same behaviour was observed for Q reduction in the potential range corresponding to the pre-plateau (Fig. 2.38). Then, again by fitting of Eq. (2.59) to experimental data, κD_s values were obtained in Ref. [53] for both HQ oxidation and Q reduction at different x values.

Figure 2.44 shows $I_{lim,c}$ versus $\Omega^{-1/2}$ dependences corresponding to the main cathodic wave for a 60 nm thick POAP film contacting solution of different x values between 0.1 and 0.001. It was observed that after a certain Ω value, which depends on x, the liming current $I_{lim,c}$, becomes independent of Ω [53]. The values of Ω at which the limiting current becomes constant, is lower as x decreases. This effect was attributed to a slow electron transport across the polymer as x decreases [53]. By employing Eq. (2.60), values of D_e for different x values, were obtained (Table 2.9). This last result allowed the authors of Ref. [53] to conclude that POAP is less conductive as it becomes less protonated.

The redox mediation reaction of POAP films in the presence of the $Fe^{2+/3+}$ and $Fe(CN)_6^{3-/4-}$ redox couples was also studied employing RDEV in Ref. [52]. The i–E responses of the two external redox couples on both a naked Au and a POAP coated electrodes at an electrode rotation rate of 1200 rpm, are shown in Fig. 2.45. These i–E responses for POAP modified electrodes show no anodic currents, for both solutions. Authors of Ref. [52] remark that in the case of $Fe^{2+/3+}$ system (Fig. 2.45a), the cathodic limiting current is independent of the film thickness but it depends on the concentration of Fe^{3+}. However, for the case of $Fe(CN)_6^{3-/4-}$ solutions (Fig. 2.45b), the cathodic limiting current was independent of the

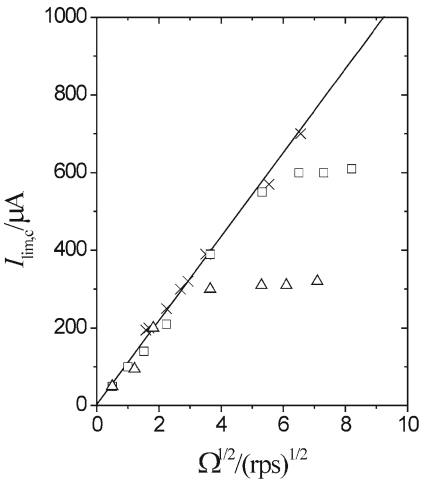

Fig. 2.44 I_{lim}^{-1} versus $\Omega^{1/2}$ for the 60 nm thick POAP film contacting a x M $HClO_4 + (2 - x)$ M $NaClO_4$ + 0.01 M (HQ/Q) solution, $x = 0.1$ (×), 0.01 (□) and 0.001 (Δ) [53]

Table 2.9 D_e values obtained for POAP films from Eq. (2.60) [a][53]

x	$10^{10}\ D_e/cm^2\ s^{-1}$
0.1	2.4
0.01	0.34
0.001	0.17

[a] Q reduction (second wave) xM $HClO_4 + (2 - x)$ M $NaClO_4$ $+10 \times 10^{-3}$M (HQ/Q) solutions. Electrode area, A = 0.23 cm^2, $n = 0.44$, $c^* = 4.7$ M, $\phi = 60$ nm

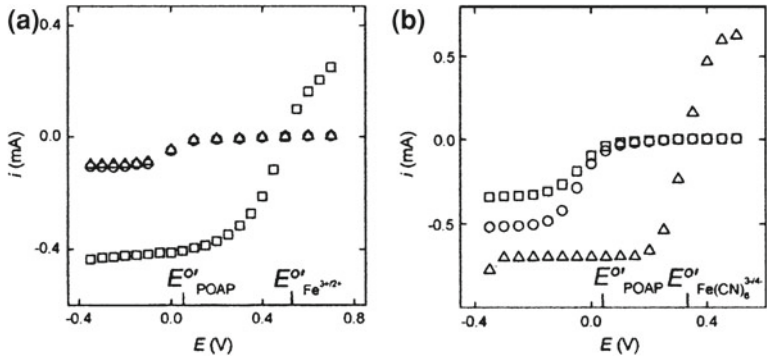

Fig. 2.45 Current–potential curves: **a** Naked Au electrode (□) and coated with a POAP film 88 nm thick (o) and 125 nm thick (Δ). Electrolyte: $HClO_4$ 0.1 M + $Fe^{2+/3+}$ 5 mM. **b** Naked Au electrode (Δ) and coated with a POAP film 88 nm thick (o) and 125 nm thick (□). Electrolyte: $HClO_4$ 0.1 M + $Fe(CN)_6^{3-/4-}$ 5 mM. The rotation rate was 1200 rpm [52]

concentration of $Fe(CN)_6^{3+}$ and increases with decreasing the film thickness. Furthermore, in this last case, for relatively high rotation speeds, the cathodic limiting current was independent of the rotation speed. This was considered as an indication of current control by charge transport in the film. The independence of the cathodic limiting current of the film thickness for the POAP/$Fe^{2+/3+}$system was considered as an indication that the electronic transport in the POAP film is not the rate-determining step of the transport process.

On the other hand, the permeation of Fe^{3+} in the film was ruled out in Ref. [52], because it is indicated that otherwise the half-wave potential for the coated electrode should be the same as that for the naked electrode. Then, authors of Ref. [52] conclude that according to the theoretical basis of the electrochemical rectification developed by themselves in a previous work [51], the cathodic limiting current must be controlled by the kinetic of the electron transfer between the redox species in solution and those from the polymer. Then, the observed *i-E* response was attributed to a slow kinetics for the mediated oxidation of Fe^{2+}. Concerning the POAP/$Fe(CN)_6^{3-/4-}$system, the electronic transport was considered to be the responsible for the observed cathodic limiting currents [52]. As the self-exchange in $Fe(CN)_6^{3-/4-}$ is much faster than in the $Fe^{2+/3+}$system, then authors of Ref. [50] conclude that the electron exchange reaction between $Fe(CN)_6^{3-/4-}$and POAP to be much faster than that between $Fe^{2+/3+}$ and POAP.

In order to analyze the conducting potential range of POAP, Ortega [30] carried out experiments with POAP films contacting different redox active solutions. The behavior of POAP-modified electrodes in contact with a 0.4 mol dm^{-3} $NaClO_4$ solution (*pH* 9) containing 10^{-3} mol dm^{-3} $Fe(CN)_6^{3-}$ was firstly studied. Ortega [30] attributed the strong dependence of the redox potential (E_0) of the $Fe(CN)_6^{3-} + e^- \Leftrightarrow Fe(CN)_6^{4-}$ reaction on the solution *pH* to the formation of $HFe(CN)_6^{3-}$. Ortega [30] remarks that E_0 for $Fe(CN)_6^{3-}$ is 0.36 V (vs. SCE), at *pH* 9, and then it is located in the region where the applied potential is more positive than the formal potential of the polymer $E_f = 0.05$ V (vs. SCE), which is defined as the average of cathodic and anodic peak potentials. The voltmmograms corresponding to the redox process of $Fe(CN)_6^{4-}$ at POAP-modified Pt electrode (Fig. 2.46) did not show peak ascribable to hexacyanoferrate ion in the region ranging from 0.0 to 0.75 V (vs. SCE).

Increasing concentrations of $Fe(CN)_6^{4-}$ were used in Ref. [30] as well as different thickness of films, but no peak was observed. However, a light increase in the cathodic peak current of polymer was observed as the concentration of $Fe(CN)_6^{4-}$increased. Ortega [30] attributes this effect to a very small amount of $Fe(CN)_6^{3-}$ that could be oxidized during the forward scan through pores formed from the swollen reduced form of the film, however, during the reverse scan, the polymer becomes more compact and the $Fe(CN)_6^{3-}$is reduced when the polymer becomes conducting. This assumption is consistent with a higher conductivity of POAP in the negative potential range comprised between −0.25 and 0.0 V (vs. SCE). $FeCl_2$ solutions were also employed by Ortega [30] to study the conduction potential range of POAP. Ortega [30] remarks that as the oxidation of Fe(II) to

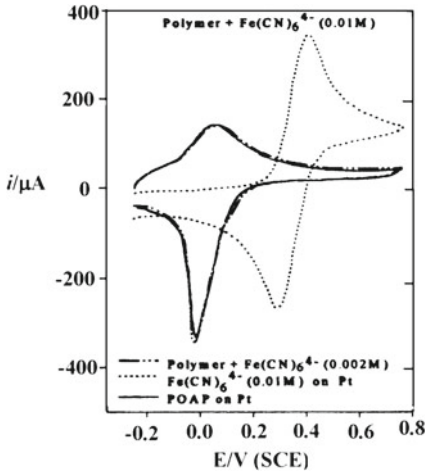

Fig. 2.46 Voltammograms corresponding to 60 nm thick POAP film in KCl (0.4 mol dm^{-3}) at *pH* 9 in presence and absence of $Fe(CN)_6^{4-}$ [30]

Fe(III) is reported to take place at the formal potential of 0.8 V (vs. NHE) in acid medium, and no peak ascribable to oxidation of Fe(II) is observed in the voltammetric response of POAP, then, he concludes that POAP is not conductive in the potential range more positive than the polymer formal potential.

Paraquat (1,1′-dimethyl-4,4′ bipyridylium or methyl viologen) was also employed by Ortega [30] to test the conductivity of POAP at negative potentials. Ortega remarks that paraquat was reported to exhibits two reversible peaks at –0.7 V (*vs*. Ag/AgCl) in aqueous solutions at *pH* 4 [55]. Then, reduced paraquat (0.5×10^{-3} mol dm^{-3}) was synthesized by Ortega and a voltammogram of this redox species on bare Pt was recorded in a neutral solution to avoid hydrogen evolution (Fig. 2.47). Ortega compared voltammograms of POAP in the presence and the absence of paraquat and he observed an additional current when POAP contacts paraquat within the negative potential range of POAP, exactly in the region where POAP is in a lower oxidation state (Fig. 2.47). Such additional current was not observed in absence of the radical methyl viologen, which was considered by Ortega as a signal of a higher conductivity of the film in that region as compared with more positive potential values.

Copper was also utilized by Ortega [30] to demonstrate the conductivity of POAP at negative potentials. The voltammograms corresponding to copper deposition from an acid solution containing $Cu(ClO_4)_2$ onto bare Pt and POAP-modified electrode are compared in Fig. 2.48.

The voltammogram of a POAP-modified electrode in contact with a Cu(II) solution clearly shows the oxidation and reduction peaks corresponding to the polymer and Cu(II)/Cu couple. The copper reduction peak appears at more negative potentials on POAP, probably due to the resistivity of the film while the cathodic current does not change significantly. However, the oxidation peak is not significantly affected by the presence of the POAP film. Voltammograms recorded at different scan rates showed that the reduction peak of copper depends on this

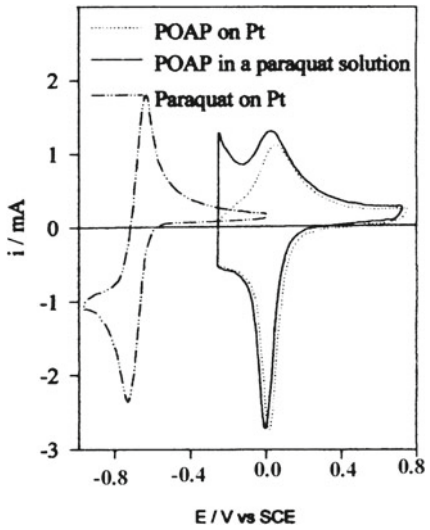

Fig. 2.47 Voltammograms of POAP in KCl (0.4 mol dm^{-3}) at *pH* 9 in presence and absence of paraquat. Area of working electrode 1.9×10^{-3} cm^2. Reduced paraquat was produced in situ on a mercury pool electrode (12 cm^2) [30]

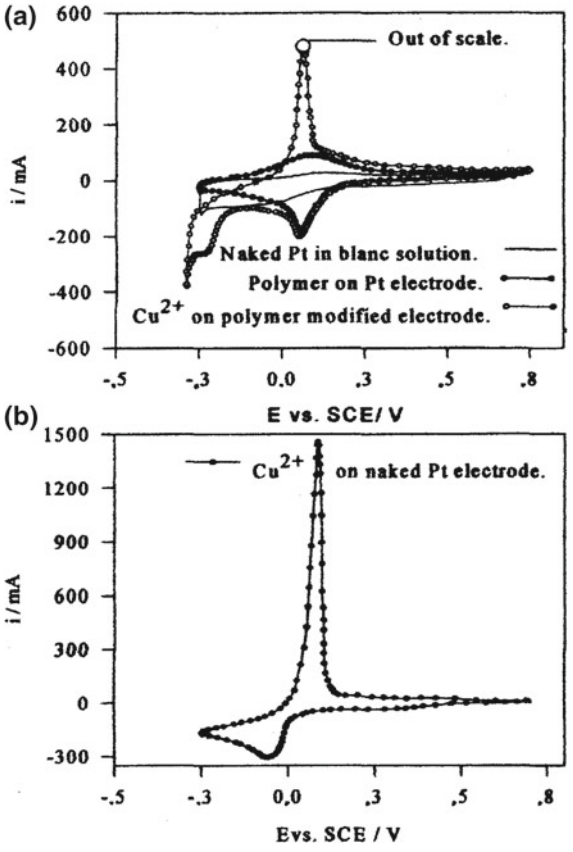

Fig. 2.48 Voltammograms of **a** 70 nm thick POAP film immersed in a 3.5×10^{-3} mol dm^{-3} in Cu(II) and 0.4 mol dm^{-3} $NaClO_4$ solution at *pH* 9. $v = 20$ mV s^{-1}. **b** Cu(II) on bare Pt in the same medium as **a** [30]

parameter in the same way as the POAP reduction peak. That is, it moves to more negative potential as the sweep rate increases. However, changes in the scan rates do not affect the oxidation peak potentials of the polymer and copper. According to Ortega [30], the more reasonable explanation for this behaviour is that the POAP film is conductive at negative potentials lower than −0.250 V (vs. SCE).

In this regard, Ortega [30] assumes that it is possible that the shift of the reduction peak of copper on POAP-modified electrode, with respect to the one observed from the naked Pt electrode originates from the different nature of the substrate, that is, from the potential-dependent resistance of the POAP film. Ortega also observed that reduction currents at the modified electrode were also very similar to those recorded when the bare Pt electrode is used. These features allow Ortega to conclude that the deposition of copper takes place on the polymer-solution interface, otherwise, an appreciable decrease in the current because of the diffusion of copper through the film would be observed. This assumption is supported by scanning electron micrographs of POAP films, where no pinholes were visible [30]. Then, the difference between current–potential profiles for the reduction of copper on POAP-modified electrode and naked Pt was attributed by Ortega to the resistance of the polymer film, expressed as:

$$R = \rho L/A \tag{2.61}$$

where R and L are the resistance and the thickness of the film, respectively, A is the area of the electrode and ρ is the resistivity of the film. Knowing that conductivity (σ) is $1/\rho$, and $R = \Delta E/i$, Eq. (2.61) becomes:

$$\sigma = iL/\Delta EA \tag{2.62}$$

where i is the current and ΔE is the difference of potential between points with the same magnitude of current for the reduction of copper curves on POAP-modified and naked Pt electrode.

RDEV was also employed by Ortega to study the copper deposition process [30]. Voltammograms of modified rotating disc electrode were recorded at different rotation rates. No change was observed in the voltammograms at a rotation rate lower that 50 rad/s because the process is controlled by charge transfer in the polymer matrix. The voltammograms were recorded at low scan rates (3 mV/s) so that steady-state conditions were kept during the experiments. Under such conditions, it was assumed by Ortega that the polymer should also have time to reach its equilibrium conductivity at each potential. The voltammograms corresponding to the reduction of copper on naked Pt and POAP-modified Pt electrodes are shown in Fig. 2.49. The smaller hump observed in the *i–E* curve for the reduction of copper on the modified electrode represents the reduction of the polymer while the larger one involves the reduction of the metal ion on the polymeric material.

Ortega remarks that small changes in the potential produce large changes in the current for the reduction of copper on naked Pt at 0.0 V. However, the curve corresponding to the POAP-modified electrode is less steep, which was attributed to the potential-dependent resistance of the film that controls the copper

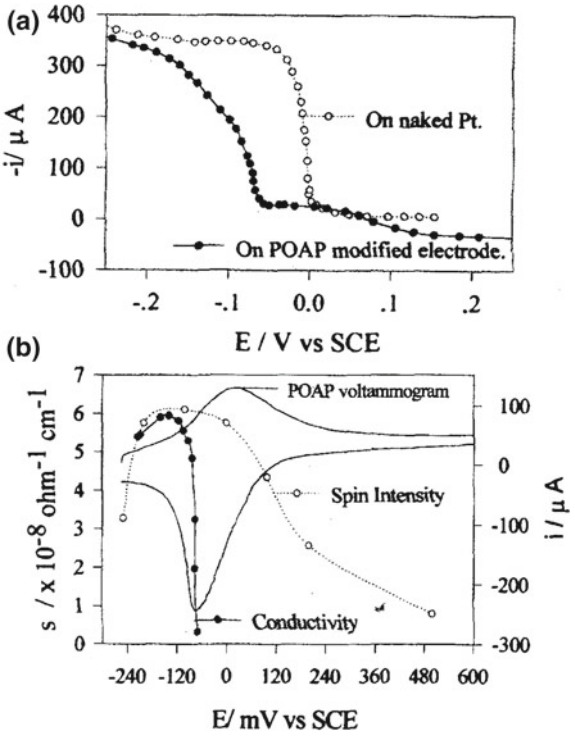

Fig. 2.49 **a** Voltammograms on the rotating Pt-POAP and Pt naked disc electrode in aqueous solution containing 3.5×10^{-3} mol dm^{-3} in Cu(II) at *pH* 9. Scan rate $v = 3$ mV/s and rotation rate 3 rad/s. **b** Changes in the conductivity of the film as a function of potential and its correlation with spin intensity (*see* Chap. 1) [30]

deposition. Ortega [30] determined the conductivity of the film as a function of polarization potential by using Eq. (2.62) and employing a surface area of the electrode of 0.33 cm^2 and a thickness of the film of 80 nm. The resulting $\sigma - E$ plot (Fig. 2.49 (b)), was compared with the spin intensity-E characteristic (see Fig. 1.16, Chap. 1). Ortega indicates that the conductivity increases very sharply at approximately -67 mV, peaks at approximately -120 mV and starts decreasing at more negative potentials. The conductivity and the spin intensity both exhibit maximum at -0.120 V, which according to Ortega shows the polaronic nature of the conductivity of the film at that potential range. At more positive potentials the number of polarons decreases, but no so steeply as the conductivity. This fact was explained by Ortega by assuming that when the concentration of polarons is high they start to combine to give rise to bipolarons, some of these bipolarons are converted to a higher oxidized state of the polymer, that is, the ones with opened structure, which decreases the conductivity in the polymer. Some polaron islands surrounded by fully oxidized units can still be present in segments of the chains so that the conductivity of the film is strongly reduced while ESR spectra still show

the presence of radicals. Values of conductivity for POAP calculated by Ortega are of the order 1.0×10^{-8} S/cm.

A voltammetric study about the conduction process through POAP-coated platinum electrodes employing neutral and charged species was carried out in Ref. [1]. With regard to positive charges species, it was observed in Ref. [1] that chemical substances, which are reduced on the bare electrode at potentials lower than the E_{pa} (anodic peak potential) of POAP, such as, Cr^{3+}, Cu^{2+} and Cd^{2+} could not be reduced above it with exception of protons. However, couples which have a formal potential value more positive than the E_{pa} of the POAP film could be easily oxidized [1]. With regard to neutral and negative charges species, three couples (ascorbic acid, hydroquinone and $K_4Fe(CN)_6$) were oxidized over POAP films Ascorbic acid suffers irreversible oxidation at a bare and a POAP electrode but the latter shows an increase of the total current, which was attributed to a catalytic effect of the film. Hydroquinone oxidizes reversibly at a modified electrode showing a negative catalytic effect, which was assigned to the film resistance. $K_4Fe(CN)_6$ oxidation shows, at low film thickness, a reversible behaviour. However, with a film thickness greater than 200 nm, quasi-reversible behaviour was observed. This effect was attributed to the film resistance [1]. A resistance value of POAP was calculated in Ref. [1]. The value obtained, with the assumption of fast charge transfer at the electrode/film and film/solution interfaces, was 15 ohms, which corresponds to a conductivity value of 1.34×10^{-4} S cm^{-1}. Authors of Ref. [1] conclude that POAP is conductive in the oxidized state and non-conductive in the reduced one.

2.4 POAP Deactivation and its Effect on the Charge-Transport Process

Partial oxidation of POAP films was studied by employing CV and EIS [56].

The voltammetric response of a fresh POAP film shows one peak at about 0.1 V (versus SCE) (Fig. 2.50a) and its impedance response for a potential corresponding to the peak potential shows a Warburg behaviour at high frequencies and a capacitive increase at low frequencies (Fig. 2.51a).

The early increase in the imaginary component of the impedance and the absence of a high-frequency semicircle in the impedance plots of POAP are indicative of fast interfacial charge transfer processes. POAP gives the same electrochemical response with potential cycling for more than 1 day provided that the positive potential does not exceed 0.5 V (versus SCE). However, after cycling the potential during several days POAP starts to show the characteristics of deactivation. Also, as the positive potential limit is increased beyond 0.5 V, the voltammetric response (Fig. 2.50b) and, more clearly, the impedance response (Fig. 2.51b) starts to change. In the latter case, a semicircle appears in the Nyquist plot, after deactivation (Fig. 2.51b). Deactivation is accompanied by a decrease in

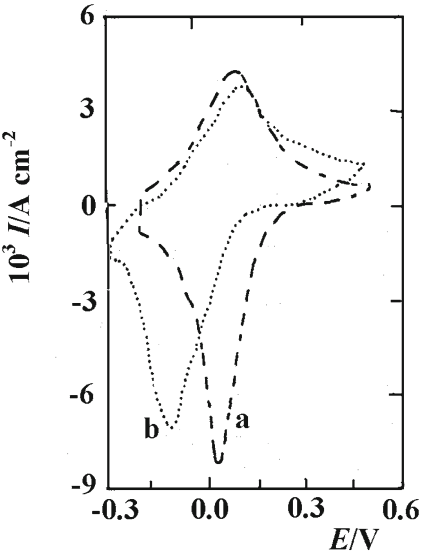

Fig. 2.50 Voltammetric response of POAP in a 0.1 M $HClO_4$ + 0.4 M $NaClO_4$ solution. $v = 0.1$ V s^{-1}. **a** Recently prepared and **b** after partial oxidation [56]

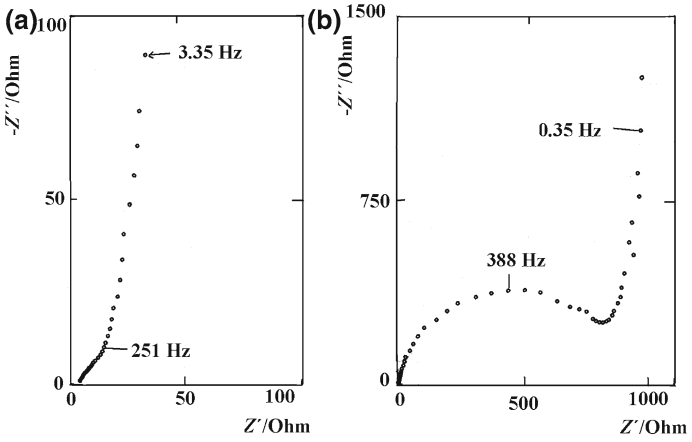

Fig. 2.51 Nyquist plots for POAP in a 0.1 M $HClO_4$ + 0.4 M $NaClO_4$ solution. $E = 0.1$ V versus SCE. **a** Recently prepared and **b** after partial oxidation [56]

the film conductivity. The total conductivity of the POAP films synthesized in Ref. [56] was calculated by extrapolating the pseudocapacitive behaviour to the real axis and subtracting the resistance of the electrolyte. The conductivity of an

immediately prepared POAP film decreased from 1×10^{-6} to 4×10^{-7} S cm^{-1} after its deactivation [56].

The irreversible deactivation of POAP films when the positive potential limit (E_{upl}) exceeds 0.5 V was also studied in the presence of a redox active solution employing CV, Rotating Disc Electrode Voltammetry (RDEV) and EIS in Ref. [57]. CV was employed to prepare and deactivate POAP films. Then, the electrochemical behaviours of the freshly prepared (nondeactivated) and deactivated POAP films were studied by RDEV and EIS in the presence of *p*-benzoquinone/hydroquinone, that is, when a redox mediation reaction is taking place at the polymer–solution interface. The reduced state of POAP (-0.2 V $< E <$ 0.0 V vs. SCE) was employed to compare the behaviour of nondeactivated and deactivated POAP films. The experimental impedance diagrams of POAP films contacting the *p*-benzoquinone/hydroquinone redox couple, were interpreted on the basis of the homogeneous impedance model described in Ref. [58]. Eleven POAP coated electrodes, all of the same polymer thickness, were consecutively manufactured in Ref. [57] to carry out the experiments. Each one of the 11 POAP coated electrodes was successively used as the working electrode in an individual experiment. The eleven POAP coated gold electrodes were split into three different groups. While the first group, including three samples, was subjected to a potential cycling where the positive potential limit E_{upl} was 1.0 V, the second and third ones, each involving four samples, were subjected to potential cycles where E_{upl} values were 0.8 and 0.65 V, respectively.

The different dependencies of the charge transfer and charge transport parameters on the degree of deactivation of the polymer films ($\theta_{Red,Max}$) were obtained in [57]. The parameter $\theta_{Red,Max}$ [57] was defined in such a way that $\theta_{Red,Max} = 1$ for a nondeactivted film, that is, for the film only subjected to potential cycles within the potential range -0.2 V $< E <$ 0.5 V (SCE). Then, $\theta_{Red,Max}$ values lower than 1 are representative of deactivated films and as the lower is $\theta_{Red,Max}$, the higher is the degree of deactivation of the polymer film. The different features of some of these dependencies (for instance, bulk electronic and ionic transport on $\theta_{Red,Max}$) were explained in terms of the different mechanisms of electron and ion transport in polymeric materials. The charge-transfer resistance at the metal-polymer interface, R_{mlf}, as a function of $\theta_{Red,Max}$ extracted from the fitting procedure employed in [57], is shown in Fig. 2.52.

R_{mlf} exhibits a strong increase from the beginning of the deactivation, that is, as (θ_{ox}) goes from 1 to 0. The ion-transfer resistance R_i^{fls} at the polymer-solution interface results almost one order of magnitude lower than R_{mlf}. Also, R_i^{fls} as a function of $\theta_{Red,Max}$ exhibits a different feature as compared with R_{mlf} (Fig. 2.53).

That is, while R_i^{fls} remains nearly constant ($R_i^{f|s} \sim 10\,\Omega\,cm^2$) within the range $0.6 < \theta_{Red,Max} < 1.0$, a marked increase in R_i^{fls} is observed from $\theta_{Red,Max} \sim 0.6$ towards $\theta_{Red,Max} \sim 0.2$ In the same way as R_{mlf}, a pronounced increase in the resistance related to the electron interfacial exchange R_e^{fls} at the polymer-solution interface, is observed from the beginning of the polymer deactivation (high $\theta_{Red,Max}$ values) (Fig. 2.54).

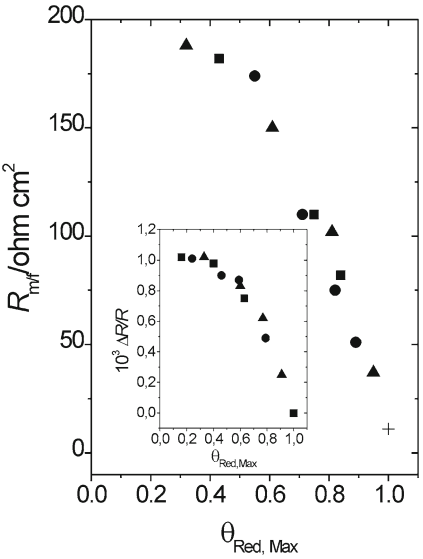

Fig. 2.52 Metal-polymer interfacial electron-transfer resistance ($R_{m/f}$) as a function of the degree of degradation, $\theta_{Red,\ Max}$ for eleven deactivated POAP films: (■) films of the first group; (▲) films of the second group; (●) films of the third group; (+) Value corresponding to the nondeactivated POAP film. Electrolyte: 0.1 M $HClO_4$ + 0.4 M $NaClO_4$ + 2 × 10^{-3} M (HQ/Q) solution. *Inset* Surface resistance change $\Delta R/R$ as a function of $\theta_{Red,Max}$ for same eleven deactivated POAP films indicated above [57]: (■) films of the first group; (▲) films of the second group; (●) films of the third group. The same electrolyte solution above indicated. Scan rate: $v = 0.01$ V s^{-1}[57]

However, R_e^{fls} values are nearly one order of magnitude lower than R_{mlf} values. Then, concerning the polymer-solution interface, a slow ion transfer process is observed for POAP as compared with the electron transfer process at this interface (compare Figs 2.53 and 2.54). With regard to the high-frequency capacity, C_H, starting at a value around 17 μF cm^{-2} for a nondeactivated film, C_H decreased with increasing the degree of degradation of the polymer, reaching a value about 5 μF cm^{-2} for a almost completely deactivated POAP film.

Diffusion coefficients for electron (D_e) and ion (D_i) transport as functions of $\theta_{Red,Max}$ are shown in Figs. 2.55 and 2.56, respectively. As can be seen, while D_e is strongly affected even at low degree of degradation $0.8 < \theta_{Red,Max} < 1.0$, D_i changes are more pronounced for $\theta_{Red,Max} < 0.6$ Authors indicate that taking into account that transfer and transport parameters obtained in Ref. [57] correspond to the reduced state of POAP ($E < 0.0$ V), it is possible that R_i^{fls} and D_i only reflect the proton movement through the polymer-electrolyte interface and inside the polymer film, respectively.

Authors [57] also remark that D_e values extracted from the Vorotyntsev's model [58] are near two orders of magnitude higher than D_i for POAP. Thus, these relative diffusion coefficient values contrast with those reported in other works,

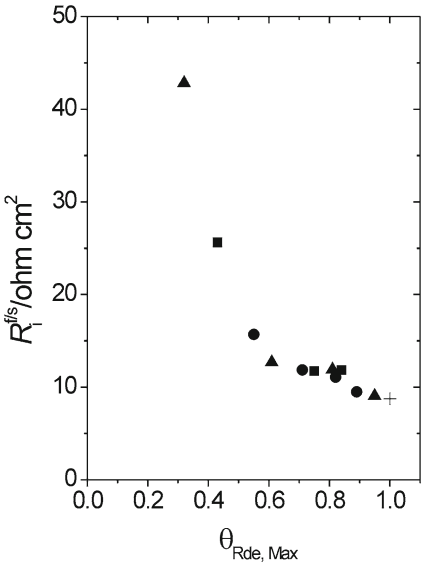

Fig. 2.53 Polymer-solution interfacial ion-transfer resistance ($R_i^{f/s}$) as a function of the degree of degradation, $\theta_{Red,\ Max}$ for the 11 deactivated POAP films synthesized in Ref. [57]: (■) films of the first group; (▲) films of the second group; (●) films of the third group. (+) value corresponding to a nondeactivated POAP film. Electrolyte: 0.1 M $HClO_4$ + 0.4 M $NaClO_4$ + 2 × 10^{-3} M (HQ/Q) solution [57]

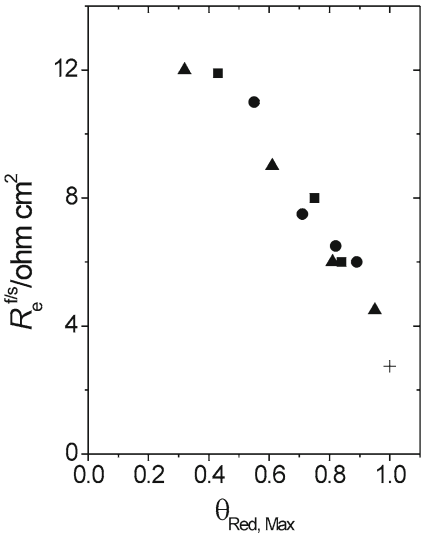

Fig. 2.54 Interfacial electron-transfer resistance ($R_e^{f/s}$) at the polymer-solution interface as a function of the degree of degradation, $\theta_{Red,Max}$ for the 11 deactivated POAP films described in Ref. [57]: (■) films of the first group; (▲) films of the second group.(●) films of the third group. (+) Value corresponding to the nondeactivated POAP film. Electrolyte: 0.1 M $HClO_4$ + 0.4 M $NaClO_4$ + 2 × 10^{-3} M (HQ/Q) solution [57]

where electron motion was considered slow relative to the ion motion [40]. An interesting comparison between the transversal charge transfer resistance at the metal–polymer interface R_{mlf} (obtained from EIE) and the lateral resistance $\Delta R/R$ along the electrode (obtained by Surface Resistance measurements [39, 40], as functions of $\theta_{Red,Max}$. (see inset in Fig. 2.52) was established in Ref. [57]. Similar features in R_{mlf} versus $\theta_{Red,Max}$ and $\Delta R/R$ versus $\theta_{Red,Max}$ dependencies were

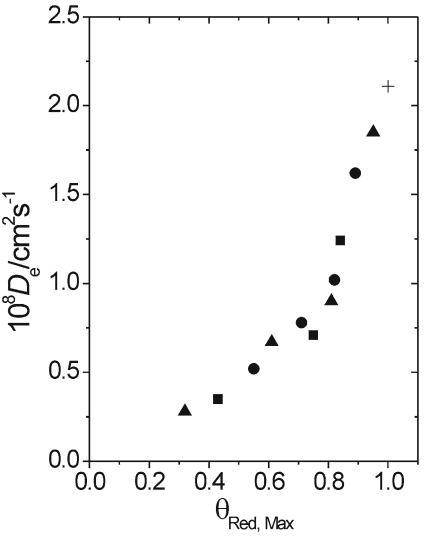

Fig. 2.55 The electron diffusion coefficient (D_e) as a function of the degree of deactivation, $\theta_{Red,Max}$ for the 11 deactivated POAP films described in Ref. [57]: (■) films of the first group; (▲) films of the second group; (●) films of the third group. (+) Value corresponding to the nondeactivated POAP film. Electrolyte: 0.1 M $HClO_4$ + 0.4 M $NaClO_4$ + 2×10^{-3} M (HQ/Q) solution [57]

observed, which was explained in terms of two different aspects of the electron motion at metal surfaces contacting a polymeric material. However, while R_{mlf} is a transversal resistance at the metal-polymer interface related to the electron transfer process during the redox reaction of the polymer, $\Delta R/R$ changes are attributed to the scattering of conduction electrons from the inside of the metal to the metal-polymer interface, caused by changes in the translational symmetry parallel to the interface due to the presence of different distributions of redox sites at this interface (a more expanded distribution of redox sites as more deactivated becomes the polymer) [39]. In this sense, $\Delta R/R$ changes are not considered as the direct result of the electron transfer between the species on the metal surface electrode and the electrode, but rather that they originate from the effect of foreign surface particles on the conduction electrons of the metal itself [39]. Thus, despite the different origins of these two electron resistances at the polymer-metal interface and the different type of measurements employed to obtain them (*ac* impedance measurements and potentiodynamic potential scans at low scan rates $v = 5 \times 10^{-3}\,V\,s^{-1}$), similar behaviours are observed as a function of the polymer deactivation. This observation is interesting because it seems that a given surface process on the electrode affects in a similar way both the electron transport along (parallel) the metal surface and the electron transfer across the electrode-polymer interface. Authors indicate that the results reported in Ref. [57] demonstrate that when POAP is subjected to rough conditions (excessive positive potential limits or prolonged potential cycling), as in some of its practical applications does (see Chap. 3), ion and electron diffusion inside the polymer and rates of interfacial charge transfer processes, are strongly affected, which should reduce drastically the efficiency of the material.

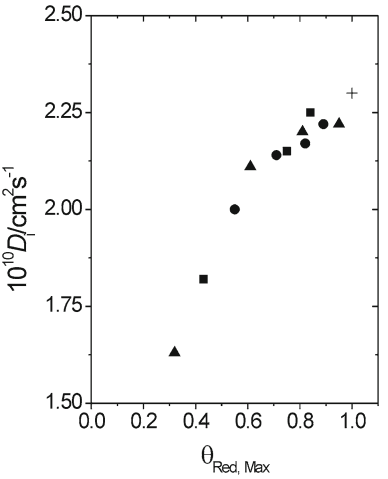

Fig. 2.56 The ion diffusion coefficient (D_i) as a function of the degree of deactivation, $\theta_{Red,Max}$ for the eleven deactivated POAP films synthesized in Ref. [57]: (■) films of the first group; (▲) films of the second group; (●) films of the third group. (+) Value corresponding to the nondeactivated POAP film. Electrolyte: 0.1 M $HClO_4$ + 0.4 M $NaClO_4$ + 2 × 10^{-3} M (HQ/Q) solution [57]

The electroactivity of a POAP film can be reduced by soaking in a 50 mM $Fe_2(SO_4)_3$ solution [59]. This deactivation was attributed to the interaction of iron ions with the redox sites of POAP, which impedes the protonation reaction of the polymer. A series of eight electrodes were prepared in [59] (see first column in Table 2.10) and each one of them was successively deactivated in an individual experiment by soaking in a ferric cation solution.

Each POAP film, after being equilibrated within the potential region $-0.2 < E < 0.5$ V in the supporting electrolyte solution (j–E response shown in dashed line in Fig. 2.57), was soaked in a 0.1 M H_2SO_4 + 0.05 M $Fe_2(SO_4)_3$ solution for different time periods (see second column in Table 2.10). Then, each

Table 2.10 Voltammetric reduction charge $Q_{Red,\ c}$ and degree of deactivation, θ_c^d, of different POAP films

POAP films[a]	[b]Soaking time/h	$Q_{Red,c}^c$/mC cm^{-2}	θ_c^d
1	2	2.44	0.13
2	4	2.04	0.27
3	5	1.87	0.33
4	10	1.57	0.44
5	16	1.32	0.53
6	21	1.15	0.59
7	24	1.12	0.60
8	33	1.06	0.62

[a] Numbers *1* to *8* represent different deactivated POAP films

[b] Different soaking times in a 0.1 M H_2SO_4 + 0.05 M $Fe_2(SO_4)_3$ solution

[c] Voltammetric reduction charge of the different deactivated POAP films after being subjected to the soaking process in the presence of the ferric cation solution

[d] Degree of deactivation of the different POAP films calculated from $\theta_c = 1 - \left(Q_{Red,c}/Q_{Red,T}\right).Q_{Red,T}(= 2.8\ mC\,cm^{-2})$ is the voltammetric reduction charge of a non-deactivated film [59]

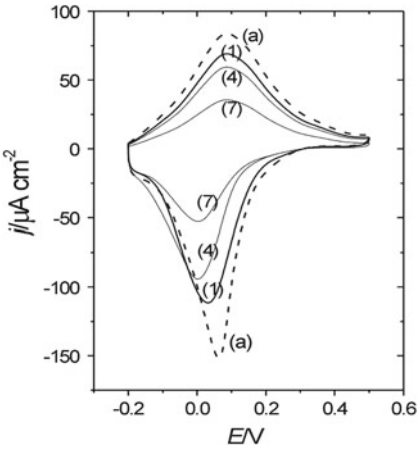

Fig. 2.57 Voltammetric (*j–E*) responses for 2.8 mC cm^{-2} thick POAP films: **a** (- - - -) a freshly prepared POAP film. Numbers (*1*), (*4*), (*7*) correspond to POAP films with different degrees of deactivation (θ_c): (*1*): $\theta_c = 0.13$; (*4*): $\theta_c = 0.44$; (*7*): $\theta_c = 0.60$. Electrolyte: 0.1 M $HClO_4$ + 0.4 M $NaClO_4$. Scan rate: $v = 0.01$ V s^{-1} [59]

one of these electrodes was extracted from the solution containing ferric ions and it was copiously washed with the supporting electrolyte solution, then the electrode was again transferred to the electrochemical cell containing the supporting electrolyte solution.

The corresponding *j–E* responses were again recorded for each one of the 8 POAP films. Figure 2.57 shows voltammetric responses corresponding to the films (1), (4) and (7) (see also Table 2.10), respectively, after being subjected to the soaking process previously described. With each one of these deactivated POAP films, RDEV experiments were performed in the presence of a solution containing equimolar concentrations of *p*-benzoquinone (Q) and hydroquinone (HQ) species (0.1 M $HClO_4$ + 0.4 M $NaClO_4$ + 2 × 10^{-3} M Q/HQ). Then, stationary current–potential curves (*I–E*) at different electrode rotation rates Ω were recorded. From these curves, cathodic and anodic limiting current *versus* electrode rotation rate (I_{lim} versus $\Omega^{1/2}$) dependences were obtained. Also, with some of these deactivated POAP films, *ac* impedance measurements, in the presence and in the absence of the HQ/Q redox couple in solution, were performed. In some experiments the HQ/Q redox couple concentration in solution was varied. In order to reactivate some deactivated POAP films, which had been initially treated with the ferric cation solution, they were treated with a 0.1 M NH_4OH solution [59]. The more attenuated voltammetric response of a POAP film with increasing soaking time in the ferric cation solution (Fig. 2.57) was considered as representative of a higher degree of deactivation of the polymer film [59]. In this regard, voltammetric reduction charge values corresponding to the completely reduced POAP films were compared for both non-deactivated films ($Q_{Red,T}$ = 2.8 mC cm^{-2}) and films subjected to the soaking process in the presence of the Fe(III) solution ($Q_{Red,c}$) (see column 3 in Table 2.10); then, a degree of deactivation (column 4 of Table 2.10) was defined in Ref. [59] as

$$\theta_c = 1 - \left(Q_{Red,c}/Q_{Red,T}\right) \tag{2.63}$$

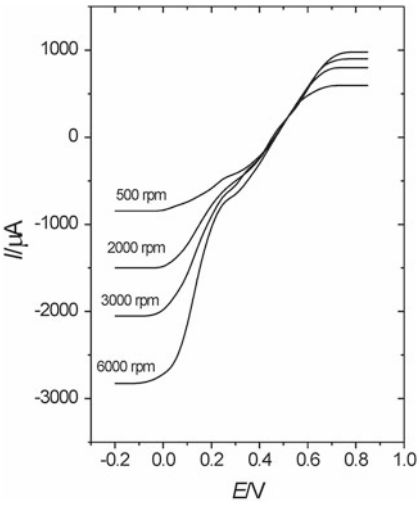

Fig. 2.58 Steady-state current–potential (*I–E*) curves for different rotation rates (Ω) of the rotating disc electrode. Non-deactivated POAP film (freshly prepared). Ω Values are indicated in the figure. Film thickness: 60 nm. Electrolyte: 0.1 M $HClO_4$ + 0.4 M $NaClO_4$ + 2×10^{-3} M(HQ/Q) [59]

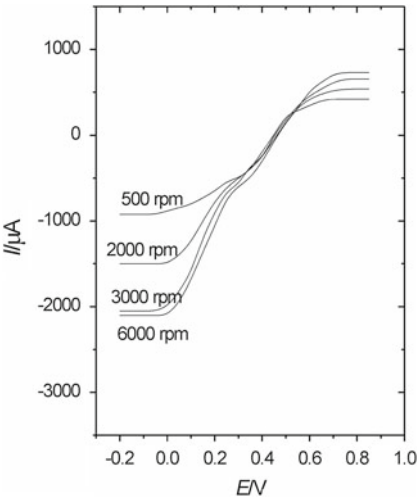

Fig. 2.59 Steady-state current–potential (*I–E*) curves for different rotation rates (Ω) of the rotating disc electrode. Deactivated POAP film ($\theta_c = 0.13$). Ω values are indicated in the figure. Film thickness: 60 nm. Electrolyte: 0.1 M $HClO_4$ + 0.4 M $NaClO_4$ + 2×10^{-3} M(HQ/Q) [59]

where $Q_{Red,c}$ is the total reduction charge assessed by integration of the corresponding *j-E* response from $E = 0.5$ V towards the negative potential direction for a deactivated film and $Q_{Red,\,T} = 2.8$ mC cm^{-2} is the total reduction charge for the non-deactivated film. In this way, for a non-deactivated POAP film (dashed curve in Fig. 2.57) the degree of deactivation was $\theta_c = 0$, taking $Q_{Red,\,T} = 2.8$ mC cm^{-2} as reference charge. However, values of $\theta_c > 0$ are indicative of POAP films that have been deactivated. Figure 2.58 shows stationary current–potential curves (*I–E*) at different electrode rotation rates Ω for a freshly prepared (nondeactivated) POAP film contacting a 0.1 M $HClO_4$ + 0.4 M $NaClO_4$ + 2×10^{-3}M Q/HQ solution. (*I–E*) curves at different Ω values were obtained for each one of the POAP films

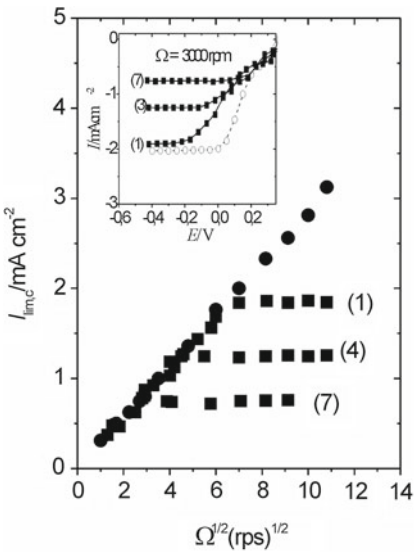

Fig. 2.60 Levich representations $I_{lim,c}$ versus $\Omega^{1/2}$ for POAP films contacting a 0.1 M $HClO_4$ + 0.4 M $NaClO_4$. + 2 × 10^{-3} M (HQ/Q) solution. (●) A non-deactivated POAP film. (*1*), (*4*) and (*7*) correspond to the three films indicated in Fig. 2.1. Inset: steady-state (*I*–*E*) curves for potential values $E < 0.2$ V at $\Omega = 3000$ rpm [59]

indicated in Table 2.10. Figure 2.59 shows this representation for a POAP film with $\theta_c = 0.13$. As can be seen by comparing Figs. 2.58 and 2.59, at each electrode rotation rate, the anodic limiting current for a deactivated POAP film is lower than that for a non-deactivated one. Also, after a given electrode rotation rate, which depends on the degree of deactivation, the cathodic limiting current for a deactivated film becomes independent of this variable.

Then, at potential values $E < 0.0$ V, $I_{lim,c}$ versus $\Omega^{1/2}$ dependences, for a non-deactivated film and also for each one of the deactivated POAP films indicated in Table 2.10, were extracted in Ref. [59]. For a non-deactivated POAP film a linear $I_{lim,c}$ versus $\Omega^{1/2}$ dependence, which follows the Levich equation, was obtained within a wide range of Ω values (Fig. 2.60). However, for POAP films that have been deactivated, after a certain Ω value, a constant cathodic limiting current value $I_{lim,c}$ independent of Ω is achieved.

Authors [59] remark that the transition, at which the cathodic limiting current becomes independent of Ω occurs at lower Ω values as the degree of deactivation increases. Interpretation of this effect was made on the basis of the electron-hopping model. Limiting current values at which $I_{lim,\,c}$ (=I_e) becomes constant were considered as a representation of the maximum flux of electrons confined in the polymer, according to Eq. (2.64)

$$I_e = n F A D_e c / \phi_p \tag{2.64}$$

In Eq. (2.64), c is the concentration of redox sites of the polymer and ϕ_p the polymer film thickness. D_e represents a measure of the electron hopping rate and n expresses the numbers (fractions) of unit charges per monomer unit of the polymer. A is the electrode area and F the Faraday's constant.

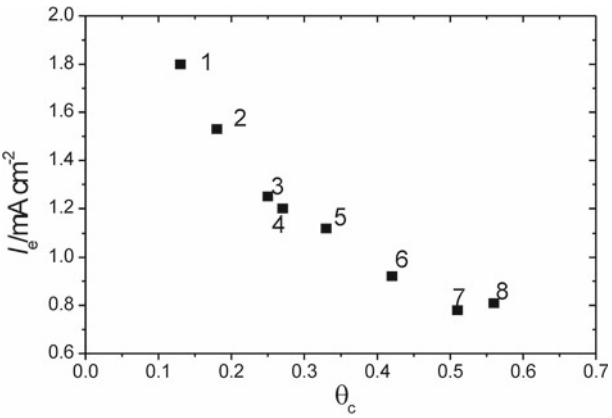

Fig. 2.61 Electron current I_e (Eq. (2.63)) as a function of θ_c. Numbers *1* to *8* correspond to each one of the POAP films indicated in Table 2.10 [59]

Experimental I_e values, corresponding to each one of the eight deactivated POAP films contacting a 2×10^{-3} M HQ/Q solution, were extracted from the cathodic plateau and they were represented as a function of θ_c (Fig. 2.61).

As can be seen, I_e decreases with increasing θ_c. In this regard, such a constant value of the current (I_e) at a given Ω value for deactivated POAP films was related to a slow electron transport across the POAP film to mediate in the electron-transfer reaction at the polymer|solution interface, as compared with a non-deactivated POAP film [59]. Author explains this effect indicating that as one increases the flux of Q (increase of Ω) from the bulk solution, then if the flux exceeds the supply of electrons from the electrode through the polymer to the electrolyte interface, the rate-limiting step will shift from the limiting transport of Q to the limiting transport of the charge through the polymer. In order to verify this limiting charge-transport process across the POAP film, the HQ/Q concentration in solution was increased in Ref. [59].

Figure 2.62 shows the $I_{lim,\,c}$ versus $\Omega^{1/2}$ dependence for the same films indicated in Fig. 2.60, but contacting a 3×10^{-3} M HQ/Q solution. The inset in Fig. 2.62 shows the same dependence for a 4×10^{-3} M HQ/Q solution. As can be seen by comparing Figs. 2.60 and 2.62, the constant current for a given deactivated film remains unchanged with increasing redox couple concentration in solution. However, this constant current is reached at a lower electrode rotation rate as the concentration of HQ/Q in solution is increased. On the basis of Eq. (2.64), the slower electron transport in deactivated films, as compared with non-deactivated ones, was attributed to a decrease of D_e. From data shown in Fig. 2.61 for I_e, and using the parameter values $c = 4.7$ M, $A = 1$ cm^2, $n = 0.44$ reported in other works, and $\phi_p = 60$ nm in Eq. (2.64), authors obtained a relative decrease of D_e from 5.4×10^{-11} to 2.4×10^{-11} cm^2 s^{-1} for a relative increase of θ_c from 0.13 to 0.62.

The decrease of D_e was attributed to an increase of the hopping distance between remnant active redox sites after deactivation. The increase of the hopping

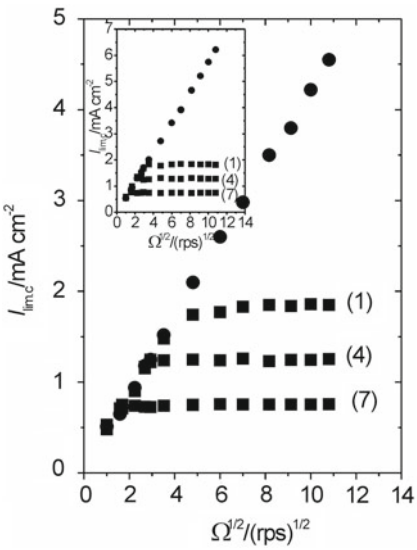

Fig. 2.62 Levich representations $I_{lim,c}$ versus $\Omega^{1/2}$ for POAP films contacting a 0.1 M $HClO_4$ + 0.4 M $NaClO_4$ + 3 × 10^{-3} M (HQ/Q) solution. (●) A non-deactivated POAP film. (*1*), (*4*) and (*7*) correspond to the three films indicated in Fig. 2.60. Inset: $I_{lim,c}$ versus $\Omega^{1/2}$ representations for the same films indicated in Fig. 2.60, but contacting a 0.1 M $HClO_4$ + 0.4 M $NaClO_4$ + 4 × 10^{-3} M (HQ/Q) solution [59]

distance with deactivation was explained assuming that the electronic interaction of iron ions with redox sites of POAP impedes the protonation of redox sites, and then they become inactive for the redox reaction of the polymer. This point was clarified in Ref. [59] by increasing the *pH* of the external solution contacting a nondeactivated POAP film. In this regard, when the concentration of perchloric acid was decreased from 0.1 to 10^{-4} M in a solution containing a constant HQ/Q concentration, the cathodic plateau on the *I–E* dependences at different electrode rotation rates was affected in a similar way as the increase of θ_c does. That is, after a certain Ω value, which depends on the acid concentration, a constant current (I_e) independent of the electrode rotation rate was observed [59].

Figure 2.63 shows $I_{lim,c}$ versus $\Omega^{1/2}$ dependences for a POAP film contacting an HQ/Q solution at different perchloric acid concentrations. Thus, the higher the solution *pH* is, the lower the electrode rotation rate value at which the current becomes constant. Then, the observed I_e decrease with increasing the solution *pH* allowed the authors to conclude that the effect of iron ions on the charge transport of POAP is similar to a deprotonation of the polymer. Another experiment was performed in [59] with POAP films that, after being deactivated by treatment with the ferric cation solution, were treated with an ammonium solution. Figure 2.64 compares the voltammetric response of a non-deactivated film with those of the same film, firstly deactivated by soaking in a ferric cation solution and then reactivated by treatment with a 0.1 M NH_4OH solution. An enhancement of the redox response was observed after reactivation. Figure 2.65 compares the $I_{lim,c}$ versus $\Omega^{1/2}$ dependence for the non-deactivated film (plot (a)) with those of the same film firstly deactivated (plot (b)) and then, reactivated (plot (c)) by alkaline treatment. As can be seen from Fig. 2.65 also, an enhancement of the constant

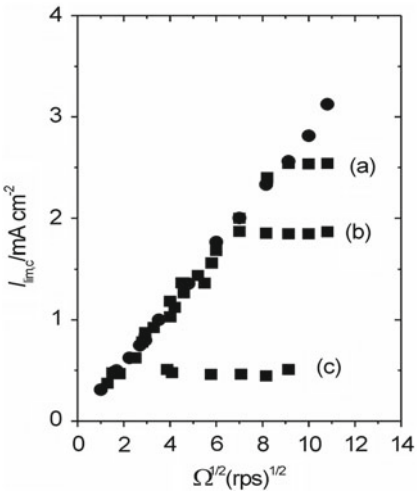

Fig. 2.63 Levich representations $I_{\text{lim,c}}$ versus $\Omega^{1/2}$ for a non-deactivated POAP film contacting x M $HClO_4 + (2 - x)$ $NaClO_4 + 2 \times 10^{-3}$ M HQ/Q solutions, (*a*) $x = 10^{-2}$ M; (*b*) $x = 10^{-3}$ M; (*c*) $x = 10^{-4}$ M. (●) $x = 0.1$. $E = -0.3$ V [59]

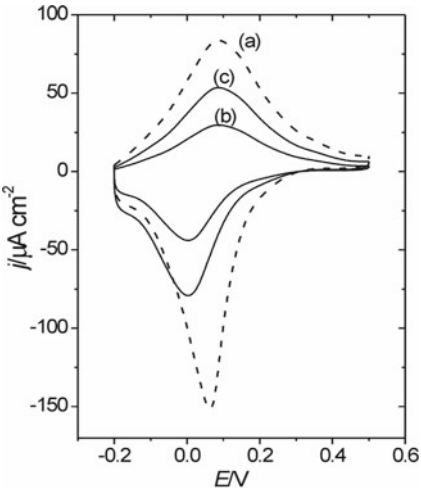

Fig. 2.64 Voltammetric (*j*–*E*) responses of: (*a*) A non-deactivated POAP film, $\theta_c = 0$; (*b*) the same film deactivated, $\theta_c = 0.62$; (*c*) the same film after reactivation, $\theta_c = 0.43$. Electrolyte: 0.1 M $HClO_4$ + 0.4 M $NaClO_4$. Scan rate: $v < 0.10$ V s^{-1} [59]

cathodic limiting current value is obtained with reactivation, but the Levich dependence corresponding to a non-deactivated film is not totally recovered. Then, authors conclude that the electron conduction of a deactivated POAP film can only be partially recovered with reactivation by treatment with an alkaline solution.

The HQ oxidation at potential values $E > 0.8$ V (vs. SCE) on both nondeactivated and deactivated POAP films was also studied in Ref. [59]. It was observed that at each electrode rotation rate, the anodic limiting current for a given deactivated film is lower than that corresponding to the same non-deactivated film (compare Figs. 2.58 and 2.59). Then, expression (2.65) was also employed in Ref. [59] to evaluate the blocking characteristics of the deactivated POAP films, during HQ oxidation. Equation (2.65) assumes that the electroactive species dissolves into

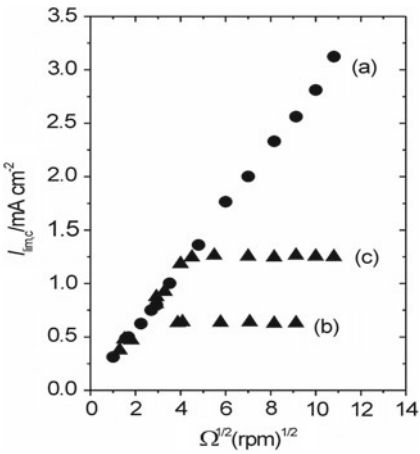

Fig. 2.65 Levich representations $I_{\text{lim,c}}$ versus $\Omega^{1/2}$ for the same POAP film indicated in Fig. 2.64 contacting a 0.1 M $HClO_4$ + 0.4 M $NaClO_4$ + 2×10^{-3} M (HQ/Q) solution. E = −0.2 V. (a) $\theta_c = 0$; (b) $\theta_c = 0.62$; (c) $\theta_c = 0.43$

the polymer film with a partition equilibrium $\kappa = c_{\text{pol}}/c_o$ at the film|solution interface, where c_{pol} and c_o are the concentrations of the species in the polymer and in the solution, respectively.

$$I_{a,l}^{-1} = \phi_p \left(nFA\,\kappa D_{\text{pol}} c_o\right)^{-1} + \left(0.62\,nFA\,D^{2/3} v^{-1/6} \Omega^{1/2} c_o\right)^{-1} \tag{2.65}$$

D_{pol} and D are the diffusion coefficients of the electroactive species in the polymer and in the solution, respectively, $I_{a,l}$ is the anodic limiting current for the oxidation of HQ species and the other terms have their usual meanings. Then, Eq. (2.65) was applied to POAP films with different degrees of deactivation in order to obtain the parameter κD_s, which represents a measure of the rate of diffusion of redox species incorporated into the deactivated film. It was observed in [59] that at constant c_o, experimental $I_{a,l}^{-1}$ versus $\Omega^{-1/2}$ representations for deactivated POAP films give linear diagrams with the same slope but different intercepts on the ordinate axis (Fig. 2.66).

By using a linear regression method authors determined the intercept at $\Omega \to \infty$ of these Koutecky–Levich plots at different θ_c values, and then κD_s was extracted from the first term of Eq. (2.65). Table 2.11 shows that the parameter κD_s decreases with the increase of the deactivation.

Authors were not able to separate κ from D_s. However, they attribute the κD_s decrease to the κ decrease. In this regard, authors assumed that the high degree of swelling, as a direct result of solvent ingress to compensate changes in the charge density within the film (proton inclusion and/or anion exclusion during reduction and the reverse during oxidation), are absent in a deactivated film. Then, as θ_c increases the poor electrolyte permeation would lead to low κ values, which would make the solute electroactive diffusion within the film difficult.

Besides RDEV experiments, *ac* impedance measurements were performed in Ref. [59] with nondeactivated POAP films and POAP films with different θ_c

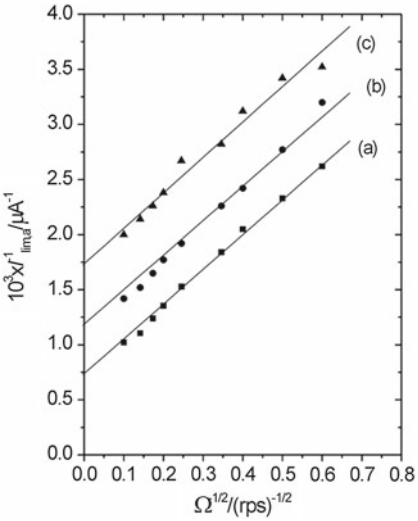

Fig. 2.66 Koutecky–Levich plots ($I_{a,l}$vs. $\Omega^{-1/2}$) for different deactivated POAP films. (a) $\theta_c = 0$; (b) $\theta_c = 0.13$; (c) $\theta_c = 0.27$. Film thickness: 60 nm. Electrolyte: 0.1 M $HClO_4 + 0.4$ M $NaClO_4 + 2 \times 10^{-3}$M (HQ/Q) solution. $E = 0.8$ V [59]

Table 2.11 Diffusion rate, κD_s, of hydroquinone species at different degrees of deactivation, θ_c

θ_c	$10^8\ \kappa D_s^a/cm^2\ s^{-1}$
0	2.0
0.13	1.24
0.42	0.88

[a] Diffusion rate values of hydroquinone species extracted from Koutecky–Levich plots

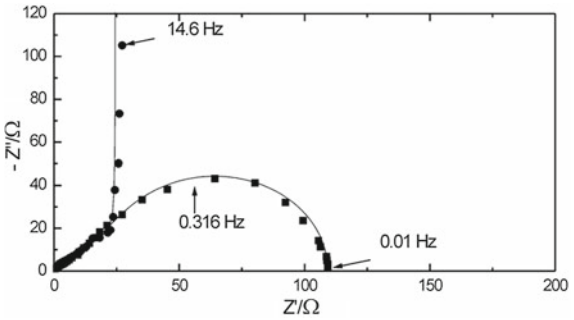

Fig. 2.67 *Ac* Impedance diagrams in the Nyquist co-ordinates ($-Z''$ vs. Z) obtained at $E = -0.3$ V for a non-deactivated POAP film (●) contacting a 0.1 M $HClO_4$ + 0.4 M $NaClO_4$ solution. The same POAP film (■) contacting a 0.1 M $HClO_4$ + 0.4 M $NaClO_4$ + 2×10^{-3} M (HQ/Q) solution. Rotation rate, $\Omega = 300$ rpm *Discrete points* are experimental data and *continuous lines* represent the fitting by using the theory given in Ref. [59]

values. The measurements were carried out, firstly, only in the presence of the supporting electrolyte solution, and then, in a solution of equimolar concentrations of *p*-benzoquinone (Q) and hydroquinone (HQ) species (0.1 M $HClO_4$ +

0.4 M $NaClO_4 + 2 \times 10^{-3}$M (Q/HQ). A potential value $E < 0.0$ V was selected to obtain impedance diagrams, where POAP acts as mediator in the reduction process of *p*-benzoquinone. In the supporting electrolyte, Nyquist diagrams of a nondeactivated POAP film show a Warburg region at high frequency followed by a pseudo-capacitive increase (Fig. 2.67).

However, for a deactivated POAP film, a high-frequency semicircle appears on the impedance diagram (Fig. 2.68). The presence of a high-frequency semicircle on the Nyquist diagram of deactivated POAP films was considered indicative of a lower value of the standard electrochemical rate constant k_{sh} (high charge-transfer resistance at the gold|POAP interface), as compared with the value corresponding to a nondeactivated film. Authors remark that this high charge-transfer resistance is consistent with the low reactivity of the redox sites in a deactivated film, as found by stationary current–potential measurements. In the presence of the HQ/Q redox couple, impedance diagrams of a deactivated POAP film exhibit two loops (Fig. 2.68). However, a nondeactivated POAP film only shows one loop at low frequency (Fig. 2.67).

For deactivated POAP films, it was found that while the loop at low frequency is Ω dependent (Fig. 2.69), the high-frequency semicircle is independent of this variable. However, the size of the high-frequency semicircle depends on the degree of deactivation (θ_c). In this regard, at a given Ω value, the higher the θ_c value is, the greater the high-frequency semicircle becomes. In Fig. 2.70, impedance diagrams of a non-deactivated POAP film are compared with those of the same film, firstly deactivated by soaking in a ferric cation solution to reach a θ_c value of 0.43 and then, reactivated by treatment with a 0.1 M NH_4OH solution, where θ_c was reduced to 0.27. A larger high-frequency semicircle is observed for $\theta_c = 0.43$ as compared with that for $\theta_c = 0.27$.

The impedance results reported in Ref. [59] were quantitatively interpreted in another work of the same author [60], on the basis of the general theory of *ac*

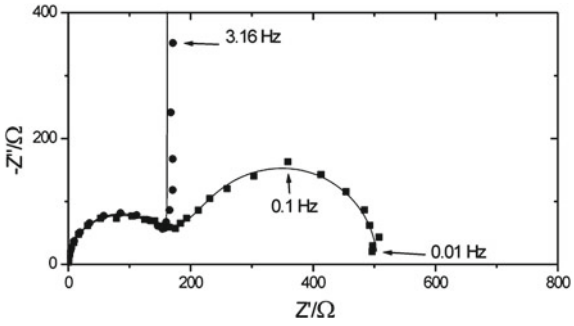

Fig. 2.68 *Ac* Impedance diagrams in the Nyquist co-ordinates ($-Z''$ vs. Z) obtained at $E = -0.3$ V for a deactivated POAP film (●) contacting a 0.1 M $HClO_4$ + 0.4 M $NaClO_4$ solution. The same POAP film (■) contacting a 0.1 M $HClO_4$ + 0.4 M $NaClO_4$ + 2×10^{-3} M (HQ/Q) solution. Rotation rate, $\Omega = 600$ rpm. $\theta_c = 0.27$ *Discrete points* are experimental data and *continuous lines* represent the fitting by using the theory given in Ref. [59]

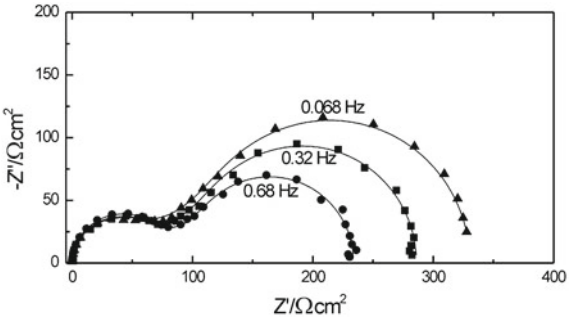

Fig. 2.69 *Ac* Impedance diagrams in the Nyquist co-ordinates ($-Z''$ vs. Z) obtained at $E = -0.3$ V for the film (*1*) of Table 2.1, $\theta_c = 0.13$. The different diagrams correspond to different electrode rotation rates, Ω : (▲) 1000 rpm; (■) 1500 rpm: (●) 2600 rpm. Electrolyte: 0.1 M $HClO_4 + 0.4$ M $NaClO_4 + 2 \times 10^{-3}$M (HQ/Q) solution. *Discrete points* are experimental data and *continuous lines* represent the fitting by using the theory given in Ref. [59]

impedance described in Ref. [58] (see continuous lines on impedance diagrams of Figs. 2.67, 2.68, 2.69 and 2.70). This theory was developed within the framework of the assumption that the redox active species are present in the solution phase and they participate in the interfacial electron exchange with the polymer at the film|solution boundary. In this way, a complete series of charge-transport parameters, electron and ion diffusion coefficients, interfacial resistances and capacitances as a function of the degree of deactivation were obtained in Ref. [60].

The theory described in Ref. [58] is based in Eq. (2.66):

$$Z_{m|film|es} = R_{m|f} + R_f + R_s + \left[Z_e^{f|s} R_i^{f|s} + W_f Z_{12}^m\right]\left(Z_e^{f|s} + R_i^{f|s} + 2W_f \coth 2v\right)^{-1} \quad (2.66)$$

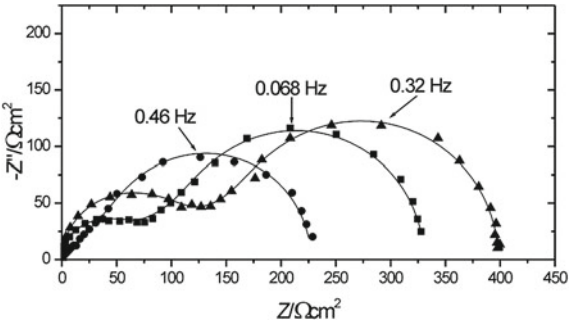

Fig. 2.70 *Ac* Impedance diagrams in the Nyquist co-ordinates ($-Z''$ vs. Z) obtained at $E = -0.3$ V and a constant electrode rotation rate, $\Omega = 1000$ rpm, for: (●) a non-deactivated POAP film ($\theta_c = 0$); (▲) the same film after deactivation ($\theta_c = 0.43$) and (■) the same film after reactivation ($\theta_c = 0.27$). Electrolyte: 0.1 M $HClO_4 + 0.4$ M $NaClO_4 + 2 \times 10^{-3}$M (HQ/Q) solution. *Discrete points* are experimental data and *continuous lines* represent the fitting by using the theory given in Ref. [58]

where

$$Z_{12}^{m} = Z_{e}^{f|s}[\coth\ v + (t_e - t_i)^2 \tanh v] + R_i^{f|s} 4t_i^2 \tanh v + W_f 4t_i^2 \quad (2.67)$$

In Eqs. (2.66) and (2.67):

$v = \left[\left(j\omega\phi_p^2\right)/4D\right]^{1/2}$ is a dimensionless function of the frequency ω, ϕ_p is the film thickness, D is the binary electron–ion diffusion coefficient, and t_i and t_e are the migration (high frequency) bulk-film transference numbers for anions and electrons, respectively. D is defined as $D = 2D_iD_e(D_e + D_i)^{-1}$ and $t_{i,e} = D_{i,\ e}(D_e + D_i)^{-1}$, where D_e and D_i are the diffusion coefficients for the electrons and ion species, respectively.

$W_f = \left[v/j\omega\phi_p C_p\right] = \Delta R_f/v$ is a Warburg impedance for the electron–ion transport inside the polymer film. $\Delta R_f\left(= \phi_p/4DC_p\right)$ is the amplitude of the Warburg impedance inside the film, and C_p is the redox capacitance per unit volume.

$R_f\left(= \phi_p/\kappa\right)$ is the high-frequency bulk-film resistance, R_s the ohmic resistance of the bulk solution (κ is the high-frequency bulk conductivity of the film), $R_{m|f}$ is the metal|film interfacial electron-transfer resistance, and $R_i^{f|s}$ is the film|solution interfacial ion-transfer resistance.

$Z_e^{f|s} = (R_e^{f|s} + W_s)$ is the electronic impedance, where $R_e^{f|s}$ is the interfacial electron-transfer resistance at the film|solution interface and W_s is the convective diffusion impedance of redox species in solution, which contains the bulk concentrations of ox(red) forms, $c_{ox}(c_{red})$, and their diffusion coefficients inside the solution, $D_{ox}(D_{red})$. Also, it contains the Nernst layer thickness, δ.

$R_e^{f|s}$ is defined as

$$R_e^{f|s} = RT\left(nF^2k_0c_{red}\right)^{-1} \quad (2.68)$$

where k_0 is the rate constant of the reaction between the film and the redox active forms in solution. Diffusion of the redox forms from the bulk solution to the film|solution interface can be regarded as stationary through the diffusion layer thickness, expressed in cm by

$$\delta = 4.98D_{ox,red}^{1/3}\eta^{1/6}\Omega^{-1/2} \quad (2.69)$$

where η is the kinematic viscosity of the solution in the same units as $D_{ox,red}$, and Ω the rotation rate of the disk electrode in rpm. The rest of the constants have their usual meaning. This model also includes the impedance behavior of the polymer contacting the inactive electrolyte (absence of the redox couple in solution) by considering $Z_e^{f|s} \to \infty$ in Eq. (2.66).

In the simulations used in Ref. [60], the number of transferred electrons, n, was assumed to be 0.44, and diffusion coefficient values of the redox species (Q and HQ) were considered equal, $D_{ox,red} = 1.5 \times 10^{-5}$ cm^2 s^{-1}. Also, the bulk concentrations of the redox substrate species were considered equal

($c_{ox} = c_{red} = 2 \times 10^{-6}$ mol cm^{-3}). The polymer thickness was considered as $\phi_p = 60$ nm. The value of the total redox site concentration of POAP was considered as $c_o = 4.7 \times 10^{-3}$ mol cm^{-3}. Then, the other parameters contained in Eq. (2.66) ($R_{m|f}$, R_i^{fls}, R_e^{fls}, C_p, D_e and D_i) were calculated from the experimental impedance data employing a fitting procedure based on the CNLS (Complex Nonlinear Squares) method. The first three parameters ($R_{m|f}$, R_i^{fls} and R_e^{fls}) were varied without restraints during the fitting. However, some reference values were considered for C_p, D_e and D_i. In this regard, for the film thickness used in Ref. [60] ($\phi_p = 60$ nm) and solution $pH = 1$, D_e and D_i values were allowed to vary within the range 10^{-7}–10^{-11} cm^2 s^{-1}, in such a way that diffusion coefficient values lower than 10^{-11} were considered not realistic. Concerning C_p, reference values were extracted from experimental $-Z''$ versus ω^{-1} slopes of impedance diagrams at sufficiently low frequency (in the absence of the redox substrate in solution). A contribution of the interfacial capacitance, C_H, also considered as a fitting parameter, was included in order to represent the actual impedance diagrams from the calculated ones.

The dependences of the different charge-transport and charge-transfer parameters on θ_c, extracted from the fitting procedure described in [60], are shown in Figs. 2.71, 2.72, 2.73, 2.74, 2.75, 2.76, and 2.77.

C_p versus θ_c dependence is shown in Fig. 2.71. Starting from a C_p value of about 27 F cm^{-3}, for a nondeactivated film, a decrease of C_p with increasing θ_c is observed.

The author of Ref. [60] remarks that C_p values correspond to the reduced state of POAP. $R_{m|f}$ exhibits an almost continuous increase from the beginning of the deactivation, that is, from $\theta_c = 0$ to $\theta_c = 0.6$ (Fig. 2.72). This increase was considered consistent with an increasing number of inactive sites at the metal|polymer interface, as the deactivation becomes more pronounced [59]. R_i^{fls} as a function of θ_c (Fig. 2.73) exhibits a different feature as compared with $R_{m|f}$.

While a strong R_i^{fls} increase is observed within the range $0 < \theta_c < 0.35$, a less pronounced increase is obtained at values of $\theta_c > 0.4$. Author [60] indicates that it is possible that the R_i^{fls} increase was related to the inhibition of the protonation reaction of surface redox sites during POAP deactivation. Also, the increase in the diameter of the HF loop of the impedance diagrams observed with increasing θ_c in [59] was assigned not only to a $R_{m|f}$ increase but also to a marked contribution of R_i^{fls}. R_e^{fls} values were extracted from Eq. (2.68) using k_o as fitting parameter ($0.1 < k_0 < 1$ cm s^{-1}). Within the whole range of θ_c values, the electron-transfer resistance R_e^{fls} at the polymer|solution interface (Fig. 2.74) shows a similar feature to that of $R_{m|f}$.

However, R_e^{fls} results almost one order of magnitude lower than both $R_{m|f}$ and R_i^{fls}. With regard to C_H values, starting at a value of around 17 μF cm^{-2} for a nondeactivated, it decreases in a nearly continuous way as the degree of deactivation increases, reaching a value of about 5 μF cm^{-2} for the maximum $\theta_c (\sim 0.6)$ value (Fig. 2.75). The C_H decrease, in the same way as the $R_{m|f}$ increase, was attributed to the creation of inactive gaps in the redox site configuration at the polymer|metal interface with deactivation.

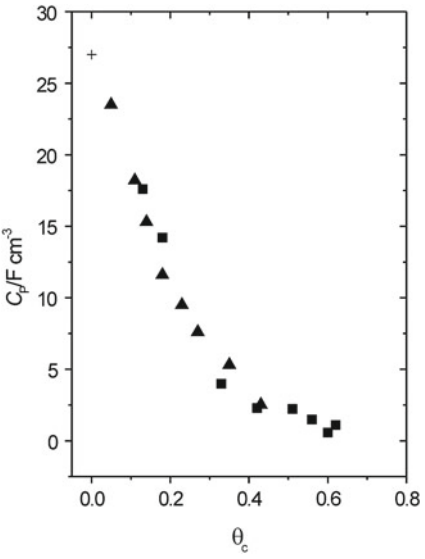

Fig. 2.71 Redox capacitance (C_p) as a function of θ_c: Deactivated (■) and reactivated (▲) films. (+) Value corresponding to the freshly prepared POAP film. Electrolyte: 0.1 M $HClO_4$ + 0.4 M $NaClO_4$ + 2 × 10^{-3}M (HQ/Q) solution [60]

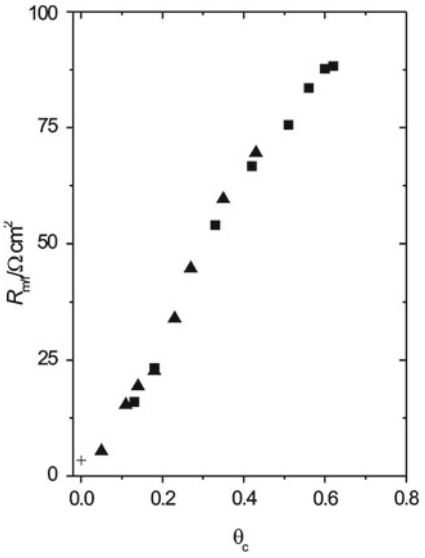

Fig. 2.72 Metal–polymer interfacial electron-transfer resistance ($R_{m/f}$) as a function of θ_c. The same symbols and conditions as indicated in Fig. 2.71

The author of Ref. [60] remarks that when deactivated POAP films are reactivated by alkaline treatment, all dependences ($C_p, R_{m|f}, R_e^{f|s}, R_i^{f|s}$ and C_H versus θ_c) (Figs. 2.71, 2.72, 2.73, 2.74 and 2.75) do not exhibit hysteresis within the whole θ_c range. All these dependences exhibit a univocal correspondence between deactivation and subsequent reactivation. However, this is not the case for

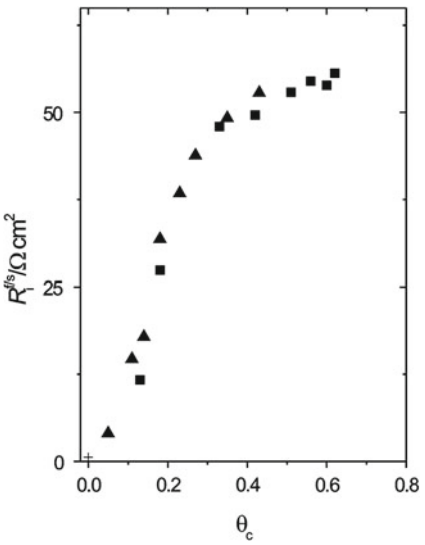

Fig. 2.73 Polymer–solution interfacial ion-transfer resistance ($R_i^{f/s}$) as a function of θ_c. The same symbols and conditions as indicated in Fig. 2.71

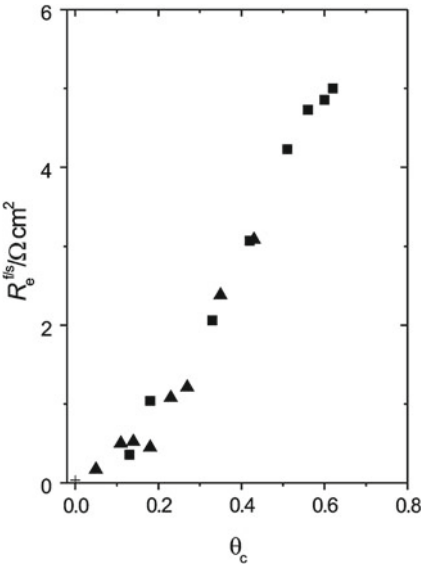

Fig. 2.74 Interfacial electron-transfer resistance ($R_e^{f/s}$) as a function of θ_c. The same symbols and conditions as indicated in Fig. 2.71

the dependences that involve diffusion coefficients for electron (D_e) and ion (D_i) transport. These dependences are shown in Figs. 2.76 and 2.77, respectively. Even though both dependences seem to show a univocal correspondence between deactivation and subsequent reactivation for θ_c values lower than 0.4, a hysteresis phenomenon is observed after the reactivation of films with θ_c values higher than 0.5.

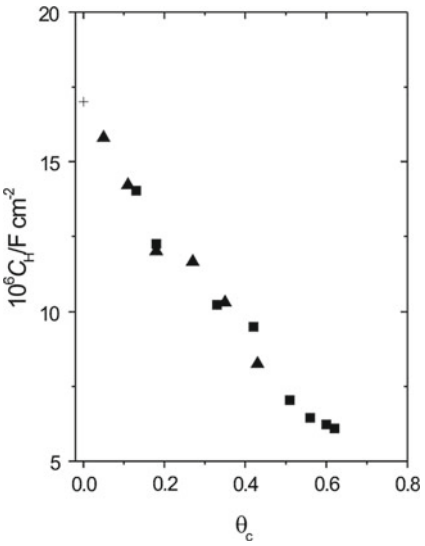

Fig. 2.75 Interfacial capacitance (C_H) at the metal–polymer interface as a function of θ_c. The same symbols and conditions as indicated in Fig. 2.71

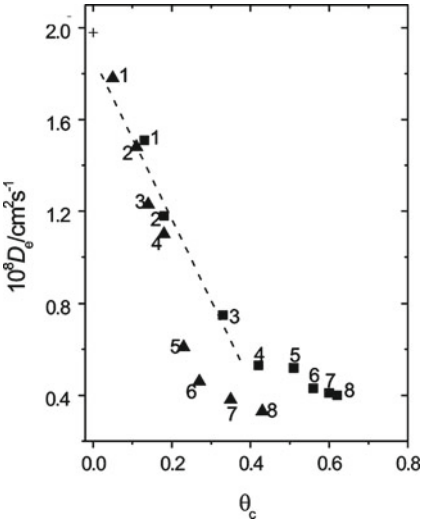

Fig. 2.76 Electron diffusion coefficient (D_e) as a function of θ_c. Numbers *1* to *8* represent each one of the eight films listed in Table 2.10. The same symbols and conditions as indicated in Fig. 2.71

The univocal D_e versus θ_c dependence within the deactivation range $0 < \theta_c < 0.4$ was linear with a slope $\Delta D_e/\Delta\theta_c = -1.6 \times 10^{-8}$ cm^2 s^{-1}. The decrease of D_e with the increase of θ_c shown in Fig. 2.76 was attributed to an increase of the hopping distance between remnant redox active sites after deactivation [60]. In order to explain the D_e decrease with θ_c, the author [60] invokes the expression of the electron diffusion coefficient, $D_e = a^2 k_0$, which is given in terms of the mean distance a, between adjacent redox sites and k_o is the

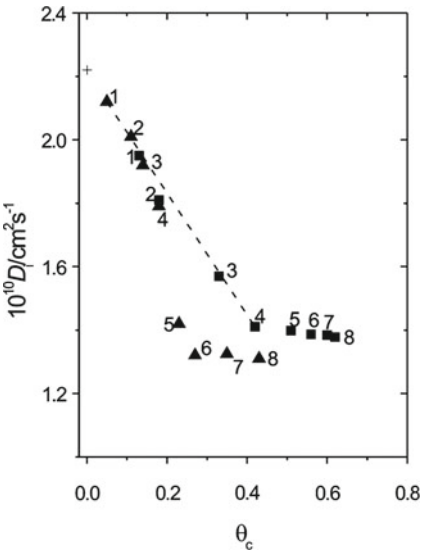

Fig. 2.77 Ion diffusion coefficient (D_i) as a function of θ_c. Numbers *1* to *8* represent each one of the eight films listed in Table 2.10. The same symbols and conditions as indicated in Fig. 2.71

intermolecular electron-transfer rate constant that exhibits an exponential dependence on a.

The hysteresis phenomenon during the reactivation process was attributed in Ref. [60] to a lack of relaxation of the configuration of redox sites of a film that was strongly deactivated ($\theta_c > 0.5$). This lack of relaxation was associated with the poor swelling effect at the reduced state of the polymer. With regard to ion transport, the D_i versus θ_c dependence (Fig. 2.77) exhibits the same characteristics as the D_e versus θ_c dependence.

A univocal correspondence was observed between deactivation and reactivation, for θ_c values lower than 0.4 with a slope value of $\Delta D_i/\Delta\theta_c = -2.0 \times 10^{-10}\,cm^2\,s^{-1}$. A change of slope was also observed at about $\theta_c \sim 0.5$. D_i was related to proton movements inside the polymer film rather than to anion transport.

2.5 Concluding Remarks About the Charge Conduction at POAP Films

Different electrochemical techniques applied to studying the charge conduction through POAP film electrodes indicate the existence of a charge-transport process that is diffusion-limited. It was suggested that this charge transport might be electron hopping with the necessarily charge-compensating counter-ion motion. In this regard, effective or apparent diffusion coefficient values were extracted from electrochemical measurements. Particularly, from impedance techniques it was possible to separate the charge transport process within POAP films in terms of ion

(D_i) and electron (D_e) contributions. D_e values are nearly two orders of magnitude lower than D_i values. This is indicative of a conduction mechanism dominated by electron transport. The conductivity of POAP was also interpreted on the basis of percolation theories. In this connection, a charge-transfer diffusion-controlled process within the potential range 0.11–0.15 V (Ag|Ag/Cl) was observed. Other kinetic parameters, such as the electrochemical standard rate constant, k^0, and the charge transfer coefficient, α, were also determined for POAP film electrodes. Values of k^0 within the range 10^4–10^6 cm s^{-1} have been reported. In some papers it was indicated that charge transfer through POAP films is complicated by irreversible injection processes at the film interfaces.

The conductivity potential range of POAP was explained on the basis of the polaron-bipolaron model. By employing ESR measurements, the existence of a conductivity maximum within the potential range −0.24 to 0.0 V (SCE) was established. The decrease and further absence of a detectable ESR signal, at potential values above 0.55 V (SCE), was attributed to a combination of radicals to give rise to dication species. EIS measurements also seem to indicate the existence of a conducting potential range between 0.1 and 0.6 V (NHE). On the basis of percolation theories, the percolation threshold during insulating-conducting transition was found to be in the range 0.15–0.17 V (Ag|Ag/Cl).

Effective diffusion coefficient values for POAP are two or three orders of magnitude lower than those determined for polyaniline. This was attributed to the different molecular structure and segment mobility of polymer chains. The presence of electron-donor substituents in the benzene rings of POAP should cause some loss of conductivity.

Voltammetric and *ac* impedance measurements show that the electrochemical response of POAP depends strongly on the solution *pH*. A redox mechanism was proposed for the polymer, in which the redox reaction involves a process of addition/elimination of protons coupled with a reversible electron transfer. The protonation of the oxidised form of POAP was considered as the coupled chemical reaction. Some impedance measurements seem to indicate that one proton is released for each electron transferred in the oxidation process, thus electrochemical oxidation of the polymer was considered equal to its dehydrogenation. It was suggested that the *pH* affects the dynamics of the electron-hopping process through reduction of the active redox centre density. In this connection, the decreasing electron conductivity observed for POAP as the *pH* increases was explained considering a decrease of the intermolecular electron-transfer rate constant between two adjacent redox sites with the polymer deprotonation.

The participation of supporting electrolyte anions in the charge-transport process of POAP was also studied. While some techniques, such as EQCM, seem to indicate that perchlorate anions do not participate in the redox reaction of the polymer, others, such as PBD, show that even when the insertion of protons is the dominant process during the reduction scan, during the positive direction not only protons but also perchlorate anions are exchanged between the solution and the polymer. By EIS it was observed that electron and ion coefficient values increase as the concentration of perchlorate anions increases.

With regard to the film thickness effect on the charge conduction process of POAP, it was observed that thin films exhibit a lower conductivity as compared with thick ones. This effect is clearly reflected in the ion and electron diffusion coefficient values extracted from EIS. Both parameters increase as the film thickness increases. This effect of the film thickness on the conduction properties was explained in terms of a polymer structure that changes when the film thickness increases. In this connection, while thin films are continuous, compact and non-porous, thick films are porous and more permeable to external electrolyte solution. Thus, electrolyte incorporated into a thick film should give rise to a higher rate of the charge-transport process as compared with that in a thin film.

The redox mediation of POAP on different redox couples in solution was analyzed by employing Cyclic Voltammetry and Rotating Disc Electrode Voltammetry. In some cases cathodic limiting currents, which are independent of the concentration of the redox couple in solution, are observed but they depend on the polymer film thickness. This was considered as an indication of current control by charge transfer across the polymer film. Conversely, in other cases limiting currents independent of the polymer thickness but dependent on the redox substrate concentration in solution were observed. In this latter case limiting currents must be controlled by the kinetics of the electron transfer at the polymer|solution interface. Anodic currents corresponding to oxidation of redox species that penetrate through POAP films to reach the metal surface were also observed. These anodic currents were employed to calculate physical diffusion rates of redox species across POAP films. It was observed that the electron transport through POAP is slower than the physical diffusion of redox species into the polymer. However, the physical diffusion rate of some redox active species across POAP films is comparable with the transport rate of electroinactive ions (perchlorate) into the polymer. The conducting potential range of POAP was analysed in the presence of redox active species. Some authors indicate that positive species that are reduced at potentials lower than the formal potential of POAP could not be reduced above such potential, with the exception of protons. However, species that have formal potential values more positive than the formal potential of POAP could be oxidised easily. Thus, it was concluded that the polymer is conductive in the oxidised state and non-conductive in the reduced one. Other authors have demonstrated that POAP is conductive at negative potentials. In this connection, it was reported that the conductivity of POAP as a function of potential increases sharply at approximately -0.067 V (SCE), peaks at approximately -0.120 V (SCE) and starts to decrease at more negative potential values.

With regard to the stability POAP film electrodes, they maintain their voltammetric response, at least for a day, provided that the positive potential limit does not exceed 0.5 V (SCE). However, after continuous cycling during several days, the polymer starts to show the characteristics of degradation. Also, if a freshly prepared film is subjected to a positive potential limit beyond 0.5 V (SCE), the voltammetric response, and more clearly the impedance response, shows a decrease in the film conductivity.

2.6 Some Critical Viewpoints About Charge Transport Parameter Values of Poly(o-aminophenol) Film Electrodes

It is evident that application of electrochemical models to interpret experimental results in the field of electroactive polymers is often complicated by concurrent difficulties that are not only theoretical but also experimental. In this connection, most of the impedance models employed to obtain transport parameters of POAP films assume the existence of a homogeneous (uniform) polymer layer on a smooth electrode surface. However, from the theory of porous electrodes and relevant electrochemical studies, it is known that their impedance behaviour differs from that of electrodes with a smooth surface. In some papers [39–41, 57, 59, 60] a thin gold film deposited under high vacuum conditions (10^{-7} Torr) was employed as base metal to deposit POAP films. In this way it was expected to reduce, at atomic scale, surface defects of the base electrode. On studying "size effects" [39] on thin gold films employed in Refs. [39–41] a value of the specularity parameter, $p \sim 0.91$, was estimated. The p value correlates with the roughness of the metal surface topography and the presence of surface defects. More precisely, this parameter represents the probability of an electron being reflected specularly or diffusely (due to the presence of defects) at the metal film surface. The p value ranges from 0, for complete diffuse scattering, to 1 for complete specular scattering. Thus, imperfections should lead to experimental p values much lower than 1. In this connection, p values of gold films employed in Refs. [36–41, 59, 60] are high enough ($p \sim 0.91$) to assume a low amount of surface defects on an atomic scale, as compared with the surface of a bulk electrode mechanically polished to deposit the polymer film.

With regard to the structure of the polymer layer, it was proved [49, 50] that when a 2.8 mC cm^{-2} thick POAP film covers a metal surface, ions from the electrolyte solution do not interact with the metal electrode, which should be indicative of the existence of a relatively compact polymer layer on the metal surface. Then, some papers as in Ref. [59, 60], where a thin gold film deposited by vacuum evaporation was employed as base electrode to deposit a thick POAP film on it, seem to justify the application of a homogeneous electrochemical impedance model to interpret experimental impedance diagrams. However, the thickness of the polymer film is always a critical parameter. In general, thickness is estimated from the charge consumed in reducing the polymer film [13, 15]. In some papers, the films were grown to approximately the desired thickness by employing a reduction charge versus ellipsometric thickness working curve [3, 21, 40–42]. In this connection, it was indicated that voltammetric responses of POAP result from two different processes. The former corresponds to a background film conduction, similar to that observed for the base electrode (unmodified electrode), while the latter is determined by the proper redox process of the film. Charge values corresponding to these different contributions are not always easy to separate in order to estimate film thickness values. It was suggested that the background conductance of the films most likely results from some residual charge in their bulk and their porosity.

There is evidence about the dependence of transport parameters of POAP on both film thickness and concentration of the external electrolyte solution [18]. This effect was explained considering that the polymer structure changes as the film thickness increases. In this regard, while thick POAP films seem to exhibit open structures that allow incorporation of the electrolyte into the polymer layer, thin films are compact enough to prevent the electrolyte incorporation. In this regard, the high permeability of some polymer films to transport redox species from the solution in contact with the polymer to the metal substrate was attributed to dispersed polymer structures with imperfections (*e.g.* pinholes and large channels) with large dimensions compared to those of species present in solution [54]. This effect should be taken into account when mechanism diagnosis criteria from steady-state polarisation curves for redox mediation at electroactive polymer-coated electrodes are considered, because redox species in solution could reach the metal surface by transport through pores in the polymer layer.

Complex impedance is one of the major techniques for the experimental study of electroactive polymer films. However, it should be taken into account that the estimation of transport parameters values of POAP, such as diffusion coefficient values, D, is often hardly possible on the basis of impedance spectra, because of the absence of a well-defined Warburg region for this polymer. In this connection, D values were obtained with an error of 50 % [15]. Besides, in some papers it is indicated that impedance measurements cannot be performed for frequencies lower than 0.1 Hz due to the noise fluctuations observed in this frequency region. In this regard, it was indicated that the estimated error in the values of the low-frequency resistance obtained from impedance spectra was around 30 % because of the overlap of the charge-transfer and the diffusion-controlled regions. The observed peculiarities at low-frequency impedance of POAP films were attributed to porosity effects [11].

With regard to impedance models, the general theory of *ac* impedance described by Vorotyntsev [58] was applied in Refs. [59, 60] to interpret experimental impedance spectra of POAP in the presence of active redox species in solution. However, this theory was developed within the framework of the assumption that the redox active species is only present in the solution phase but not inside the polymer film, and they participate in the interfacial electron exchange with the polymer at the film|solution boundary. However, it should be taken into account that this theory is strictly valid when charging of the interfacial double layers is negligible, that is, the theory does not account for charging the film|substrate and the film|solution layers in parallel with the process of injection of charge carriers. If this is not the case, a more complete model such as that developed by Vorotyntsev in Ref. [61] should be used. In Ref. [61], besides the traditional "double layer" capacitance and interfacial charge transfer resistances, two additional parameters for each boundary, "interfacial numbers" for each species and "asymmetry factors", are introduced. However, it should be indicated that even when the authors of Ref. [59] attempted to fit experimental impedance spectra by means of the *ac* impedance model presented in Ref. [61], the fitting was not much more precise than that obtained by applying the theory given in Ref.

[58]. Furthermore, the increasing mathematical difficulty of determining the numerous parameters of the model given in Ref. [61] from experimental data was remarked. Also, from the physical viewpoint, in some cases diffusion or incorporation of different species into polymer films could alter the molecular structure of the polymeric film, and then, its physical properties. Thus, application of models in these cases should only allow obtaining fitting parameters that do not represent the real physical properties of the system. Even when different authors do not expect a complete coincidence of the electrochemical properties of the polymer film with those predicted by theoretical models, qualitative agreements are often considered satisfactory enough to obtain information about electroactive polymers.

References

1. Barbero, C., Silber, J.J., Sereno, L.: Electrochemical properties of poly-*ortho*-aminophenol modified electrodes in aqueous acid solutions. J. Electroanal. Chem. **291**, 81 (1990)
2. Bard, A.J., Faulkner, L.R.: Electrochemical Methods. Fundamentals and Applications. Wiley, New York (1980)
3. Barbero, C., Zerbino, J., Sereno, L., Posadas, D.: Optical properties of electropolymerized orthoaminophenol. Electrochim. Acta **32**, 693 (1987)
4. Gabrielli, C., Takenouti, H., Haas, O., Tsukada, A.: Impedance investigation of the charge transport in film-modified electrodes. J. Electroanal. Chem. **302**, 59 (1991)
5. Nicholson, R.S.: Theory and application of cyclic voltammetry for measurements of electrode reaction kinetics. Anal. Chem. **37**, 1351 (1965)
6. Laviron, E.: Theoretical study of a reversible reaction followed by a chemical reaction in thin layer linear potential sweep voltammetry. J. Electroanal. Chem. **39**, 1 (1972)
7. Konopelnik, O.I., Aksimentyeva, O.I., Grytsiv, M.Ya.: Electrochromic transitions on polyaminoarene films on the transparent electrodes. Mater. Sci. **20**, 49–59 (2002)
8. Maksimov, Y.M., Khaldum, M., Podlovchenko, B.I.: Electrocatalysis on polymer-modified electrodes. Elektrokhimiya **27**, 739 (1991)
9. Dobosh, D.: Electochemical Constants. Ed. Mir., Moscow (1980)
10. Foot, P.J.S., Simon, R.: Electrochromic properties of conductiong polyanilines. J. Phys. D: Appl. Phys. **22**, 159 (1989)
11. Levin, O., Kondratiev, V., Malek, V.: Charge transfer processes at poly-o-phenylenediamine and poly-o-aminophenol films. Electrochim. Acta, **50**, 1573 (2005)
12. Ohsaka, T., Kunimura, S., Oyama, N.: Electrode kinetics of poly(o-aminophenol) film prepared by electro-oxidative polymerization of o-aminophenol and its electrochromic properties. Electrochim. Acta **33**, 639 (1988)
13. Barbero, C., Tucceri, R.I., Posadas, D., Silber, J.J., Sereno, L.: Impedance characteristics of poly(o-aminophenol) electrodes. Electrochim. Acta, **40**, 1037 (1995)
14. Chidsey, C.E.D., Murray, R.W.: Redox capacity and direct current electron conductivity in electroactive materials. J. Phys. Chem. **90**, 1479 (1986)
15. Komura, T., Ito, Y., Yamaguti, T., Takahasi, K.: Charge-transport processes at poly-o-aminophenol film electrodes: electron hopping accompanied by proton exchange. Electrochim. Acta **43**, 723 (1988)
16. Mathias, M.F., Haas, O.: An alternating current impedance model including migration and redox-site interactions at polymer-modified electrodes. J. Phys. Chem. **96**, 3174 (1992)
17. Armstrong, R.D.: Impedance plane display for an electrode with diffusion restricted to a thin layer. J. Electroanal. Chem. **198**, 177 (1986)

18. Rodríguez Nieto, F.J., Posadas, D., Tucceri, R.: Effect of the of the bathing Electrolyte Concentration on the Charge Transport Process at Poly(o-aminophenol) Modified Electrodes. An ac Impedance study. J. Electroanal. Chem. **434**, 83–91 (1997)
19. Albery, W.J., Elliot, C.M., Mount, A.R.: A transmission line model for modified and thin layer cells. J. Electroanal. Chem. **288**, 15 (1990)
20. Albery, W.J., Mount, A.R.: A further development of the use of transmission lines to describe the movement of charge in conducting polymers. J. Electroanal. Chem. **388**, 1 (1995)
21. Rodríguez Nieto, F.J., Tucceri, R.: The pH Effect on the Charge Transport at Redox Polymer-Modified Electrodes. An ac Impedance Study applied to Poly(o-aminophenol) Film Electrodes. J. Electroanal. Chem. **416**, 1–24 (1996)
22. Kunimura, S., Ohsaka, T., Oyama, N.: Preparation of thin polymeric films on electrode surfaces by electropolymerization of o-aminophenol. Macromolecules **21**, 894 (1988)
23. Tucceri, R.: A review about the charge conduction process at poly(o-aminopenol) film electrodes. Open Phys. Chem. J. **4**, 62 (2010)
24. MacDiarmid, A.G., Kaner, R.B.: In: Handbook of Conducting Polymers, T.A. Skotheim (ed.), vol. 1, p. 689. Marcel Dekker, New York (1986)
25. Huang, W.S., Hamphrey, B.D., MacDiarmid A.J.: Polyaniline, a novel conducting polymer. Morphology and chemistry of its oxidation and reduction in aqueous electrolytes. J. Chem. Soc. Faraday Trans. 1, **82**, 2385 (1986)
26. Chattaraj, A.P., Basumallik, I.N.: Improved conducting polymer cathodes for lithium batteries. J. Power Sources **45**, 237 (1993)
27. Tanaka, K., Shichiri, T., Yamabe, T.: Influence of polymerization temperature on the characteristics of polythiophene films. Synth. Met. **16**, 207 (1986)
28. Satoh, M., Kaneto, K., Yoshino, K.: Electrochemistry preparation of high quality poly(*p*-phenylene) film. J. Chem. Soc., Chem. Commun. **25**, 1629 (1985)
29. Chance, R.R., Boudreaux, D.S., Bredas, J.L., Silbey, R. In: T.A. Skotheim (ed.), Handbook of Conducting Polymers, vol. 2, p. 825. Marcel Dekker, New York (1986)
30. Ortega, M.: Conducting potential range of poly(o-aminophenol). Thin Solid Films **371**, 28 (2000)
31. Salvagione, H.J., Arias-Padilla, J., Pérez, J.M., Vázquez, J.L., Morallón, E., Miras, M.C., Barbero, C.: Study of the redox mechanism of poly(o-aminophenol) using in situ techniques: evidence of two redox processes. J. Electroanal. Chem. **576**, 139 (2005)
32. Tucceri, R.I., Barbero, C., Silber, J.J., Sereno, L., Posadas, D.: Spectroelectrochemical study of poly-o-aminophenol. Electrochim. Acta **42**, 919 (1997)
33. Malek, K.: Dynamic Monte-Carlo simulation of electrochemical switching of a conducting polymer film. Chem. Phys. Lett. **375**, 477 (2003)
34. Aoki, K.: Nernst equation complicated by electric random percolation at conducting polymer-coated electrodes. J. Electroanal. Chem. **310**, 1 (1991)
35. Aoki, K.: Simulation of electrochemical slow relaxation at electrically conducting polymer-coated electrodes based on the concept of percolation. J. Electroanal. Chem. **373**, 67 (1994)
36. Aoki, K., Teragashi, Y., Tokeida, M.: Light scattering of polyaniline films responding to electrochemical switching. J. Electroanal. Chem. **460**, 254 (1999)
37. Odin, C., Nachtschein, M.: Slow relaxation in conducting polymers. Phys. Rev. Lett. **67**, 1114 (1991)
38. Buck, R.P.: Electron hopping in one dimension: mixed conductor membranes. J. Phys. Chem. **92**, 4196 (1988)
39. Tucceri, R.: A review about the surface resistance technique in electrochemistry. Surf. Sci. Rep. **56**, 85 (2004)
40. Tucceri, R.I.: Surface resistance measurements on thin gold film electrodes coated with poly(o-aminophenol) films. J. Electroanal. Chem. **505**, 72 (2001)
41. Tucceri, R.I.: Specularity change of a thin gold film surface coated with poly(*o*-aminophenol) during the polymer redox conversion. The pH affect on the redox sites distribution at the metal||polymer interface. J. Electroanal. Chem. **543**, 61 (2003)

42. Rodríguez, F.J., Tucceri, R.: Influencia del grado de oxidación y de la concentración del electrolito soporte sobre el transporte de carga de un polímero electroactivo. Información Tecnológica **9**, 109 (1988)
43. Rudnicki, J.D., Brisard, G.M., Gasteiger, H.A., Russo, R.E., McLarnon, F.R., Cairns, E.J.: Effect of the supporting electrolyte and beam diameter on probe beam deflection experiments. J. Electroanal. Chem. **362**, 55 (1993)
44. Gobal, F., Malek, K., Mahjani, M.G., Jafarian, M., Safarnavadeh, V.: A study of the fractal dimension of the electrodeposited poly-*ortho*-aminophenol films in presence of different anions. Synth. Met. **108**, 15 (2000)
45. Stromme, M., Niklasson, G.A., Granqvist, C.G.: Determination of fractal dimension by cyclic *I-V* studies: The Laplace-transform method. Phys. Rev. B **52**, 14192 (1995)
46. Malek, K., Gobal, F.: Application of chaotic logistic map for the interpretation of anion-insertion on poly-*ortho*-aminophenol films. Synth. Met. **113**, 167 (2000)
47. González, E.R.: Interpretation of the Power Response of a Fuel Cell with a Quadratic Logistic Differential Equation. J. Electrochem. Soc., **143**, L 113 (1996)
48. Rasband, S.N.: Chaotic Dynamics of Nonlinear Systems. Wiley, New York (1990)
49. Tucceri, R.: Application of the Surface Resistance technique to detect the different interactions of ClO_4^-, SO_4^{2-} and $C_6H_5SO_3^-$ anions and Cu(II) cation with a gold surface partially blocked with poly(o-aminophenol). J. Argent. Chem. Soc. **94**, 55 (2006)
50. Tucceri, R.: The metal/electroactive polymer interface studied by surface resistance. J. Surf. Eng. Mater. Adv. Technol. **3**, 205 (2013)
51. Ybarra, G., Moina, C., Florit, M.I., Posadas, D.: Redox mediation at electroactive polymer coated electrodes: Mechanistic diagnosis criteria from steady state polarization curves. J. Electroanal. Chem. **609**, 129 (2007)
52. Ybarra, G., Moina, C., Florit, M.I., Posadas, D.: Current rectification by mediating electroactive polymers. Electrochim. Acta **53**, 3955 (2008)
53. Bonfranceschi, A., Pérez Córdoba, A., Keunchkarian, S., Zapata, S., Tucceri, R.: Transport across poly(o-aminophenol) modified electrodes in contact with media containing redox active couples. A study using rotating disc electrode voltammetry. J. Electroanal. Chem. **477**, 1 (1999)
54. Ikeda, T., Schmehl, R., Denisevich, P., Willman, K., Murray, R.W.: Permeation of electroactive solutes through ultrathin polymeric films on electrode surfaces. J. Am. Chem. Soc. **104**, 2683 (1982)
55. Pinilla Macías, J.M., Hernández Hernández, L., Moreno Sobrino, J.M., Sevella Escribano, M.T.: Determination of paraquat by cathodic stripping voltammetry after accumulation through the formation of an ion pair on a hanging mercury drop electrode. Electroanalysis **79**, 5 (1993)
56. Rodríguez Nieto, F.J., Tucceri, R., Posadas, D.: EIS Detection of the Partial Oxidation of Polymers derived from Aryl Amines. J. Electroanal. Chem. **403**, 241 (1996)
57. Tucceri, R.: The effect of high positive potentials on the different charge transport and charge transfer parameters of poly(o-aminophenol) modified electrodes. A study using cyclic voltammetry, rotating disc electrode voltammetry and ac impedance measurements. J. New Mater. Electrochem. Syst. **8**, 305 (2005)
58. Vorotyntsev, M.A., Deslouis, C., Musiani, M.M., Tribollet, B., Aoki, K.: Transport across an electroactive polymer film in contact with media allowing both ionic and electronic interfacial exchange. Electrochim. Acta **44**, 2105 (1999)
59. Tucceri, R.I.: Redox mediation and permeation processes at deactivated poly(*o*-aminophenol) films. A study applying rotating disc electrode voltammetry and electrochemical impedance spectroscopy. J. Electroanal. Chem. **633**, 198 (2009)
60. Tucceri, R.I.: Charge transfer and charge transport parameters at deactivated poly(o-aminophenol) film electrodes. A study applying Electrochemical Impedance Spectroscopy. J. Electroanal. Chem. **659**, 83 (2011)
61. Vorotyntsev, M.A.: Impedance of thin films with two mobile charge carriers. Interfacial exchange of both species with adjacent media. Effect of the double layer charges. Electrochim. Acta **47**, 2071 (2002)

http://www.springer.com/978-3-319-02113-3

Poly(o-aminophenol) Film Electrodes
Synthesis, Transport Properties and Practical Applications
Tucceri, R.
2013, VIII, 168 p. 111 illus., Hardcover
ISBN: 978-3-319-02113-3